ARTICLE

The electrical resistivity of Canada's lithosphere and correlation with other parameters: contributions from Lithoprobe and other programmes[1]

Alan G. Jones, Juanjo Ledo, Ian J. Ferguson, James A. Craven, Martyn J. Unsworth, Michel Chouteau, and Jessica E. Spratt

Abstract: Over the last 30 years, through Lithoprobe and other programmes, modern, high-quality magnetotelluric (MT) measurements probing deep into the lithosphere and underlying asthenosphere have been made at over 6000 sites across Canada in all provinces and territories, except Nova Scotia. Some regions are well covered, particularly Alberta, southern British Columbia, and western Ontario, whereas others remain poorly covered, such as Quebec and large swaths of Nunavut. Prior publications from individual studies have added significantly to the wealth of Canada's geoscience knowledge, and have demonstrated that MT can contribute significantly to understanding of the tectonic processes that have shaped Canada. However, to date no continent-scale maps of lithospheric electrical parameters have been constructed from the extensive MT database. Herein we review the contributions made by the MT components of Lithoprobe, and present new continental-scale maps of various electrical parameters at crustal and upper mantle depths for the whole of Canada. From those maps, combined with regional estimates of temperature, we develop derivative information on petrological–geophysical properties, including predictions of temperature and water content. We find that at 100 km depth the Canadian Shield is cold and dry, and the Cordillera is warmer but mostly dry, i.e., little water is present in the peridotite. Exceptions are beneath the Prairies, the Wopmay Orogen, and northeast Nunavut where there does appear to be water in the nominally anhydrous minerals. Also, southwest British Columbia appears colder than the rest of the Cordillera due to the subducting Juan de Fuca plate. In contrast, at 200 km depth almost all of Canada is dry.

Résumé : Au cours des trente dernières années, grâce à Lithoprobe et à d'autres programmes, des mesures magnétotelluriques (MT), modernes et de grande qualité, ont été prises à plus de 6000 sites à travers le Canada, dans toutes les provinces et territoires sauf en Nouvelle-Écosse; ces mesures sondaient profondément dans la lithosphère et l'asthénosphère sous-jacente. Certaines régions sont bien couvertes, surtout l'Alberta, le sud de la Colombie-Britannique et l'ouest de l'Ontario, alors que d'autres sont mal couvertes, par exemple le Québec et de grandes parties du Nunavut. Des publications antérieures, basées sur des études individuelles, ont grandement contribué à enrichir les connaissances géoscientifiques canadiennes et elles ont démontré que les mesures MT peuvent grandement contribuer à la compréhension des processus tectoniques qui ont formé le Canada. Toutefois, à ce jour, aucune carte des paramètres électriques lithosphériques, à l'échelle du continent, n'a été construite à partir de la vaste base de données MT. Dans le présent article, nous revoyons les contributions des composantes MT de Lithoprobe et nous présentons de nouvelles cartes à l'échelle du continent de divers paramètres électriques aux profondeurs de la croûte et du manteau supérieur pour l'ensemble du Canada. À partir de ces cartes, combinées à des estimés régionaux de température, nous dérivons de l'information sur les propriétés pétrologiques–géophysiques, incluant les prédictions de température et de teneur en eau. Nous avons trouvé qu'à une profondeur de 100 km, le Bouclier canadien est froid et sec et que la Cordillère est plus chaude mais surtout sèche, c.-à-d. la péridotite contient peu d'eau. Les exceptions sont sous les Prairies, l'orogène de Wopmay et le nord-est du Nunavut où il semble y avoir de l'eau dans les minéraux supposément anhydres. De plus, le sud-ouest de la Colombie-Britannique semble plus froid que le reste de la Cordillère en raison du plongement de la plaque Juan de Fuca. Par contre, à une profondeur de 200 km presque tout le Canada est sec. [Traduit par la Rédaction]

Introduction

During its five funded phases spanning two decades, the Lithoprobe project (Clowes 2010a) accomplished an astounding amount on its 10 transects (Fig. 1a), and generated geoscientific data that were and continue to be the envy of the rest of the world on an unparalleled spatial scale for much of road-accessible Canada. Much of the work undertaken under the auspices of Lithoprobe is presented in the two special volumes of the *Canadian*

A.G. Jones,* J. Ledo,† J.A. Craven, and J.E. Spratt.‡ Geological Survey of Canada, 615 Booth St., Ottawa, ON K1A 0E9, Canada.
I.J. Ferguson. Department of Geological Sciences, University of Manitoba, Winnipeg, MB R3T 2N2, Canada.
M.J. Unsworth. Department of Physics, University of Alberta, Edmonton, AB T6G 2J1, Canada.
M. Chouteau. Ecole Polytechnique, Génies Civil, Géologique et des Mines, C.P. 6079, succ. CV, Montréal, QC H3C 3A7, Canada.
Corresponding author: Alan G. Jones (e-mail: alan@cp.dias.ie).
*Present address: Dublin Institute for Advanced Studies, 5 Merrion Square, Dublin 2, Ireland.
†Present address: Departament de Geodinàmica i Geofísica, Facultat de Geologia, Universitat de Barcelona, Martí i Franques s/n, 08028 Barcelona, Spain.
‡Present address: Wakefield, QC, Canada.
[1]Lithoprobe Publication 1514.

Fig. 1. (*a*) Lithoprobe transect map of Canada with tectonic elements identified. Blue, Archean; green, Paleoproterozoic; brown, Mesoproterozoic; yellow–red, Phanerozoic. Lithoprobe transects: AB, Alberta Basement; AG, Abitibi–Grenville; EC, ECSOOT; GL, GLIMPCE; KS, Kapuskasing; LE, Lithoprobe East; SC, Southern Cordillera; SN, SNORCLE; WS, Western Superior: TH, Trans-Hudson Orogen Transect (THOT); (*b*) MT site locations (red points) on map of Canada with provinces and territories identified (blue boundaries): AB, Alberta; BC, British Columbia; MB, Manitoba; NB, New Brunswick; NL, Newfoundland and Labrador; NS, Nova Scotia; NT, Northwest Territories; NU, Nunavut; ON, Ontario; PE, Prince Edward Island; QC, Quebec; SK, Saskatchewan; YT, Yukon. Also shown on the map is the swath A–B (yellow); (*c*) MT site locations on simplified tectonic map of Canada based on tectonic age (from I. Artemieva, personal communication). JdF, Juan de Fuca.
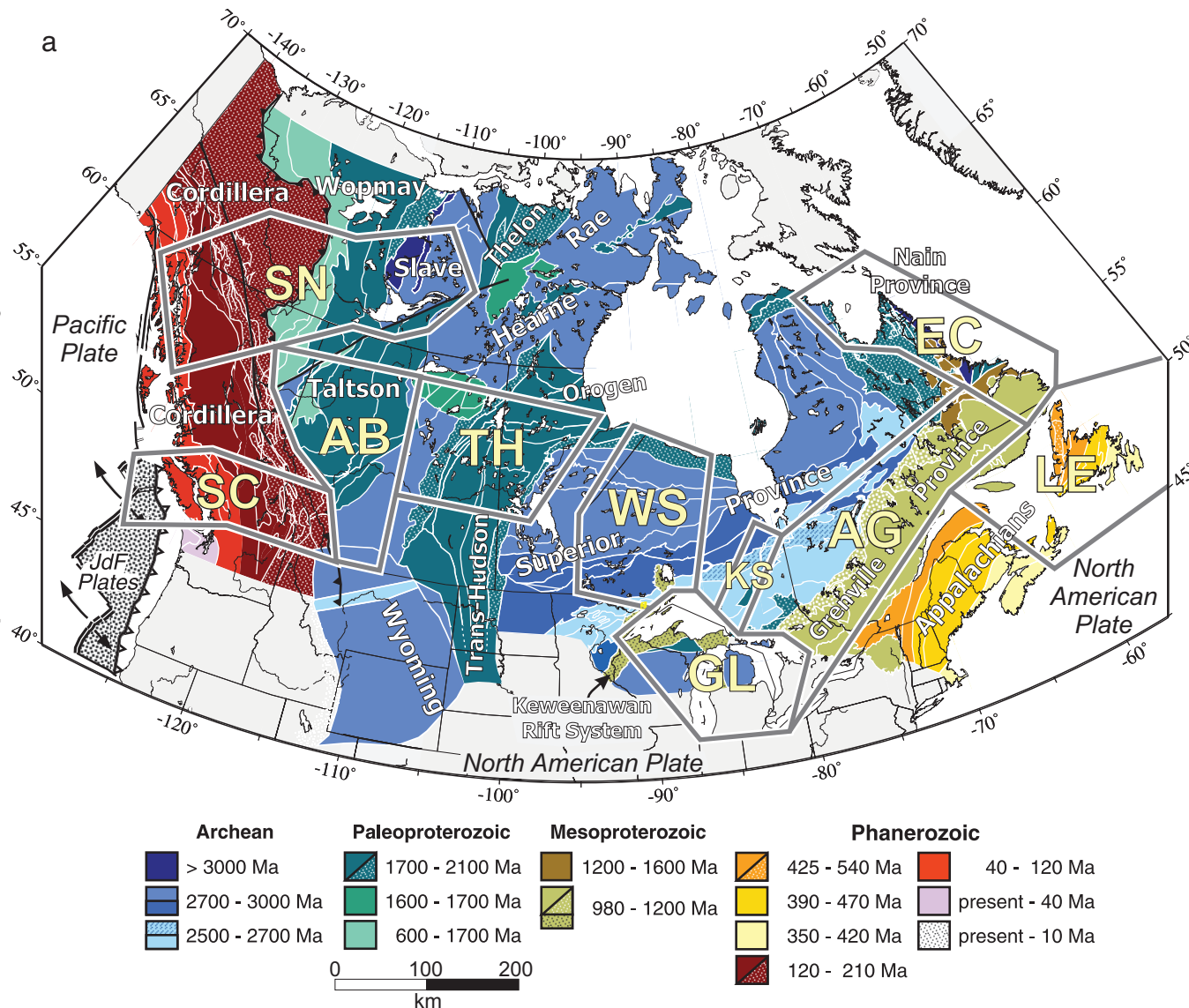
Journal of Earth Sciences published in 2010 (Clowes 2010*b*). These Lithoprobe data and their interpretations have given new constraints on the tectonic history of North America and have furthered our understanding of how our Earth has operated in the past and how it operates today. Further examination of the datasets will certainly yield fresh insights of global consequence for many years to come by scientists trained to think broadly and holistically, which is arguably Lithoprobe's greatest legacy.

Along with seismic reflection and seismic refraction studies, electromagnetic (EM) acquisition, particularly magnetotelluric data acquisition, was one of the three line item budgets for all Lithoprobe transects, with the exception of ECSOOT (Eastern Canadian Shield Onshore/Offshore Transect) and only a very minor contribution to GLIMPCE (Great Lakes International Multidisciplinary Program on Crustal Evolution), both of which were marine-based transects. This resulted in data from nearly 2000 sites,

predominantly in southern Canada where road access was possible but also in some remote localities in the Slave Craton with co-funding from the National Science Foundation and De Beers (Jones et al. 2001*c*; Jones et al. 2003). Regional controlled-source EM experiments were also conducted under Lithoprobe auspices across the Nelson Batholith and the Kapuskasing Uplift (Kurtz et al. 1989; Jones et al. 1994), as well as in targeted studies for mineral exploration in Buchans, Newfoundland, as part of Lithoprobe East (Boerner et al. 1993), the Sudbury Igneous Complex as part of Abitibi–Grenville (Boerner et al. 1994, 2000*a*), and the Thomson Nickel Belt (White et al. 2000) as part of THOT (Trans-Hudson Orogen Transect).

Other non-Lithoprobe geoscientific programmes running since the early 1980s yielded magnetotelluric (MT) data at a further 4000+ locations. Some of these locations in northern Canada are remote and required helicopter or float plane access. The total

Fig. 1 (*concluded*).

b

Canada MT station map

c

Canada MT station map
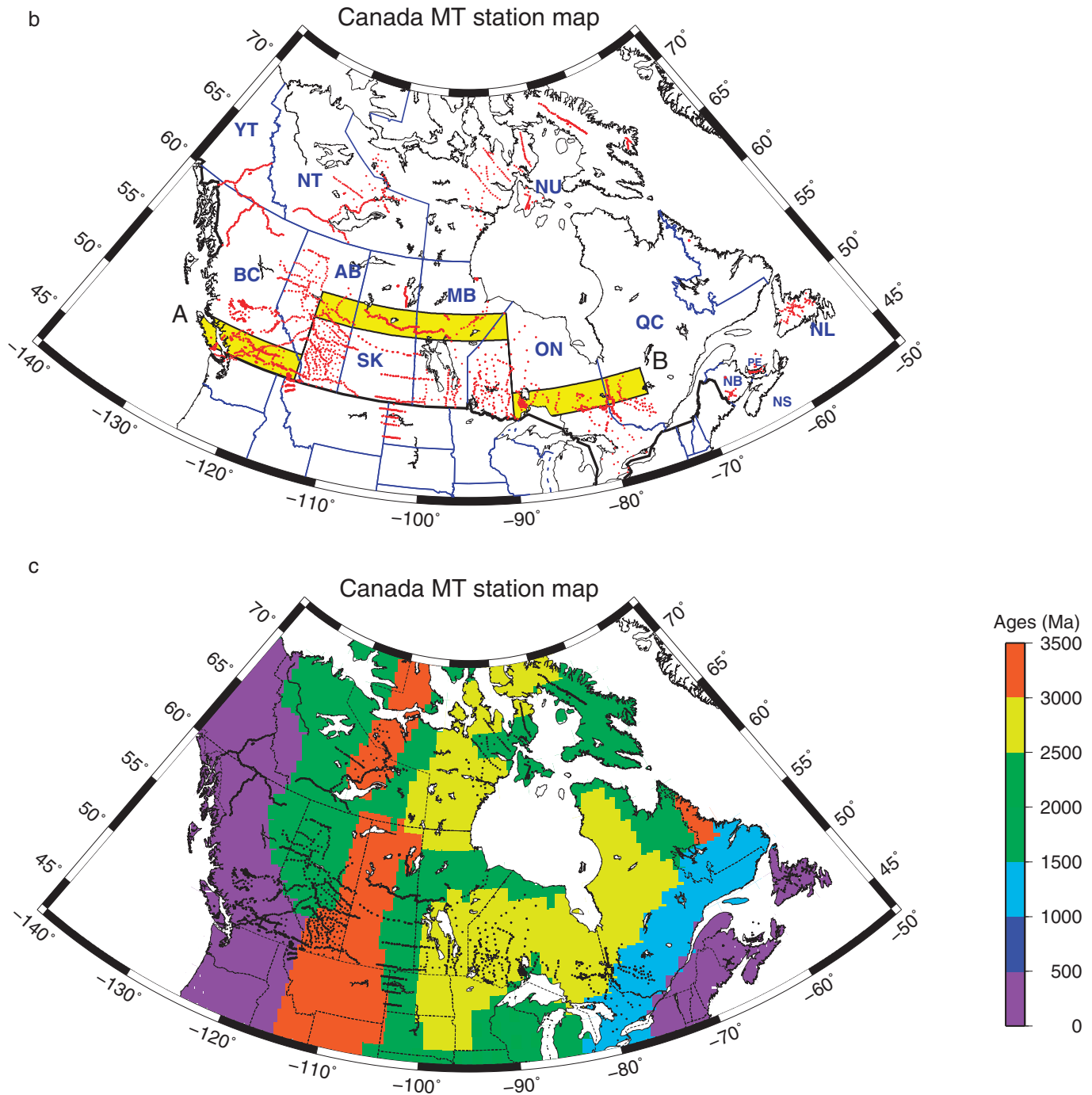
dataset is shown in Figs. 1*b* and 1*c*, and acquisition information is listed in Table 1. Conservatively, one can place a minimum figure of $1000 per site on the cost of acquisition, and for the remote locations $5000 per site or more. Hence, the MT dataset represents a 30 year investment by Canadian agencies of the order of $20 million, not counting the salaries of the scientists and students involved.

Herein we present, for the first time for any continent, continental-scale maps of lithospheric electrical information for as much of Canada as we have MT coverage. The electrical information includes approximate resistivity, anisotropy strength, and anisotropy direction. From the electrical information coupled with other geoscientific information, we draw conclusions on the

thermal state and water content of Canada's lithosphere. We subsequently review the contributions made by the Lithoprobe project, many of which are published in international journals but some of which are only to be found in Lithoprobe reports from the Transect Meetings.

The Canadian MT database

The Canadian MT database comprises high-quality broadband MT data acquired by modern systems as part of Lithoprobe activities plus other major programmes run over the last 30 years, such as the Federal Geothermal Energy Programme (GEP) in the early 1980s, the Federal Exploration TECHnology initiatives EXTECH-III

Table 1A. List of surveys in the Canadian MT database.

Survey	Year	Location	Equipment	Sites	Publications and theses
Southern/central BC: Jones and Gough (1995); Ledo and Jones (2001)					
GEP	1982	Mount Meager	MT-16	7	Flores et al. (1985); Ingham et al. (1987); Jones et al. (1988); Gupta and Jones (1990); Majorowicz and Gough (1991); Gough and Majorowicz (1992); Jones et al. (1992a), (1992b); Eisel and Bahr (1993); Jones (1993a); Jones and Dumas (1993); Jones et al. (1993b); Lilley (1993); Majorowicz et al. (1993a), (1993b); Majorowicz and Gough (1994); Cook and Jones (1995); deGroot-Hedlin (1995); Gupta and Jones (1995); Marquis et al. (1995); Chave and Jones (1997); Ritter and Ritter (1997); Soyer and Unsworth (2006); Rippe et al. (2013)
GEP	1982	Thomson Valley	MT-16	10	
GEP	1983	Cayley Mountain	MT-16	5	
UofA	1984	Rocky Mountain Trench	SPAM II	25	
GEP	1984	Anahim Lake	MT-16	5	
GSC/Lithoprobe	1984	Vancouver Island	MT-16	26	
GEP	1984	White Lake Basin	MT-16	15	
Phoenix Geophysics	1984	Purcell Anticlinorium	MT-16	90	
Duncan Exploration	1985	Purcell Anticlinorium	MT-16	100	
Shell	1985	Flathead Basin	MT1	12	*Ph.D. thesis:* Marquis (1992)
Shell	1985–1986	Purcell Anticlinorium	MT-16	57	
UofA	1986–1990	South-central BC	SPAM II	101	
GSC/Lithoprobe	1987	Southeastern BC	MT-16	27	
GSC/Lithoprobe	1988	Nelson Batholith	AET-EMAP	14	
GSC/Lithoprobe	1989–1990	Southern BC	V5	160	
UofA (POLARIS)	2003–2004, 2006, 2009	Southern BC	LiMS, NiMS	92	
Trans-Hudson Orogen/Willison Basin: Jones et al. (2005a)					
PanCanadian	1984–1985	Southern Saskatchewan	MT-16	37	Jones and Savage (1986); Jones (1988a), (1988b); Jones and Craven (1990); Agarwal and Weaver (1993); Ellis et al. (1993); Jones (1993b); Jones et al. (1993a); Takasugi et al. (1993); Uchida (1993); Wu et al. (1993); Zhao et al. (1993); Tournerie et al. (1995); Jones et al. (1997); Ferguson et al. (1999); Ferguson et al. (2005b); Garcia and Jones (2005a); White et al. (2005); Gowan et al. (2009)
GSC	1987	Central Saskatchewan	MT-16	34	
GSC/Lithoprobe	1992	Northern Saskatchewan and Manitoba	V5		
GSC/UW	1992	North Dakota	LiMS	64	
UofM	1992	Northern Saskatchewan	LiMS	15	*M.Sc. thesis:* Stevens (1999)
GSC/Lithoprobe	1994	Northern Saskatchewan	V5	30	*B.Sc. theses:* Cassels (1997); Norton (2000); Gowan (2005); Akaranta (2011)
Slave/SNORCLE: Jones et al. (2003), (2005c)					
GSC/Lithoprobe	1996	Southern Slave	V5	60	Jones and Ferguson (2001a); Jones et al. (2001c); Jones and Spratt (2002); Ledo et al. (2002); Wu et al. (2002); Eaton et al. (2004b); Ledo et al. (2004a); Ledo and Jones (2005); Wu et al. (2005); Lezaeta et al. (2007); Moorkamp et al. (2007); Spratt et al. (2009); Moorkamp et al. (2010)
			LiMS	58	
GSC/Lithoprobe	1998–2000	Slave Winter Road	MTU	43	
			LiMS	31	
GSC/Lithoprobe	1999	NWT and Yukon	ADU-06	151	*Ph.D. thesis:* Wu (2001)
			LiMS	75	*M.Sc. thesis:* Wennberg (2003)
GSC/NSF/Lithoprobe	1999–2001	Slave Lakes	WHOI	19	*B.Sc. thesis:* Wolynec (2000)
GSC	2000	Eastern Slave	LiMS	15	
GSC/NWT	2004	Slave to Bear	MTU	20	
			LiMS	6	
GSC/Ashton	2004	Northern Slave	MTU	6	
Alberta: Boerner et al. (2000b)					
GSC/UofA/Lithoprobe	1993–1995	Alberta	LiMS	320	Boerner et al. (1995); Kalvey and Jones (1995); Boerner et al. (1998), (1999); F.W. Jones et al. (2002c); Turkoglu et al. (2009)
UofA		Northern Alberta	NiMS	23	
Western Superior: Ferguson et al. (2005a)					
GSC/Lithoprobe	1997–1998	Western Superior	LiMS	158	*M.Sc. thesis:* Orellana (2006)
GSC	1999	Pickle Lake	MTU	8	*B.Sc. theses:* Wennberg (1999); Norton (2000); Tycholiz (2010); McLeod (2013)
GSC/Lithoprobe	2000	Northwestern Superior	ADU-06	38	
GSC/Lithoprobe/Falconbridge	2000	Fox River	ADU-06	13	

Table 1A (*concluded*).

Survey	Year	Location	Equipment	Sites	Publications and theses
Lithoprobe East					
GSC/Lithoprobe	1989	Buchans	V5 CSAMT	10	Boerner et al. (1993); Garcia et al. (2003) *M.Sc. thesis:* McNeice (1998)
Lithoprobe	1991	Newfoundland	V5	67	
Abitibi–Grenville: Boerner et al. (2000a)					
Lithoprobe			MTU	353	Chakridi et al. (1992); Kellett et al. (1992); Kurtz et al. (1993); Schultz et al. (1993); Mareschal et al. (1995); Zhang et al. (1995); Senechal et al. (1996a); Tournerie and Chouteau (1998); Langlois et al. (2000); Tournerie and Chouteau (2002); Adetunji et al. (2014)
Kapuskasing: Mareschal et al. (1994)					
GSC/Lithoprobe		Kapuskasing	MT-16	14 (pairs)	Chakridi et al. (1992); Mareschal et al. (1992); Kurtz et al. (1993); Schultz et al. (1993); Jones et al. (1994); Mareschal et al. (1994)
GSC/UW		Carty Lake	VLOP	1	
GSC		Kapuskasing	UTEM		
Other surveys					
GSC	1982	Miramichi, NB	MT-16	11	Kurtz and Gupta (1992)
RadWaste	1982–1983	East Bull Lake	MT-15	8	Kurtz et al. (1986b)
GEP	1983–1984	Prince Edward Island	MT-16	29 (pairs)	Jones and Garland (1986)
GEP	1985	Fredericton Basin, New Brunswick	MT-16	15 (pairs)	—
NSERC/EMR	1988	Charlevoix crater	Other	10	Mareschal and Chouteau (1990)
Lithoprobe/GLIMPCE	1989	Manitoulin Island and Bruce Peninsula	MT-16	11	Mareschal et al. (1991)
Gallery Resources	1997	Okak Bay, Labrador	V5 (AMT only)	46	Jones and Garcia (2003b)
GSC (NATMAP)	1998	Snowbird Tectonic Zone	LiMS	8	Jones et al. (2002a)
GSC	2001–2002	Baffin Island	MTU LiMS	45 15	Jones et al. (2002b); Evans et al. (2003), (2005b) *M.Sc. thesis:* Evans (2003)
GSC (FEDNOR)		Northern Ontario	MTU (AMT only)	845	—
POLARIS	2004	Manitoba	MTU	21	Gowan et al. (2009)
UofA	2002	Rocky Mountain Foothills	MTU	26	—
POLARIS	2002–2005	Southern Ontario	MTU/LiMS/NiMS	37	Frederiksen et al. (2006); Fernberg et al. (2007); Adetunji et al. (2014), Adetunji, A.Q., Ferguson, I.J., and Jones, A.G.: Magnetotelluric imaging of the lower Great Lakes region, Canada [manuscript in preparation] *Ph.D. theses:* Fernberg (2011); Adetunji (2014)
GSC	2005	Knee Lake	MTU	12	—
GSC (EXTECH-IV)	2006	McArthur River Mine	MTU (AMT only)	132	Tuncer et al. (2006); Farquharson and Craven (2009) *M.Sc. thesis:* Tuncer (2007)
GSC	2007–2008	Somerset Island	MTU LiMS	17 6	Spratt et al. (2013a)
GSC	2007	Nechako Basin, BC	MTU (AMT only)	732	Spratt and Craven (2011) *M.Sc. thesis:* Drew (2012)
GSC	2009	Cumberland Peninsula, Baffin Island	MTU	26	Craven et al. (2013)
GSC GEM	2010–2012	Central Rae Domain, Nunavut	MTU NiMS	—	Spratt et al. (2011), (2013b)

Note: The main review/overview references are given for each geographic/tectonic area. For a brief technical description of the MT systems, see Table 1B. GSC, Geological Survey of Canada; NSF, National Science Foundation; UofA, University of Albert; UofM, University of Manitoba; UW, University of Washington.

Table 1B. Description of MT systems.

Name	Manufacturer	Frequency/period range	Bits	Dates
MT-16	Phoenix Geophysics	384 Hz, 2000 s	16	1982–1990
V5	Phoenix Geophysics	BBMT: 384 Hz, 2000 s	24	1990–1998
		AMT: 10 000–10 Hz		
MTU	Phoenix Geophysics	BBMT: 384 Hz, 2000 s	24	From 1998
		AMT: 10 000–10 Hz		
LiMS	Geological Survey of Canada	20–10 000+ s	16	1992–2004
NiMS	Narod Geophysics	20–10 000+ s	24	From 1998
ADU-06	Metronix	20 kHz – DC (notional)	24	From 1998

Note: DC, direct current (0 Hz).

(Yellowknife) and EXTECH-IV (Athabasca) in the 1990s, the Federal Economic Development Initiative in Northern Ontario (FedNor) in the 1990s, the POLARIS project in 2002–2010 (Atkinson et al. 2003; Eaton et al. 2005), the Geological Survey of Canada's (GSC) Geo-Mapping for Energy and Minerals (GEM) project in the late 2000s, and other individual GSC and university-led experiments, the latter funded by the Natural Sciences and Engineering Research Council of Canada (NSERC). A list of all MT surveys that contributed data to the database, and the number of stations for each survey, with the type of recording instrumentation used, is given in Table 1. Also listed in Table 1 are the publications in international journals resulting from those surveys. Table 2 lists the Lithoprobe reports written by scientists using the Lithoprobe MT data, and Table 3 lists the students, post-docs, and visitors trained during Lithoprobe projects.

The total number of MT sites in the database is over 6000. The vast majority of those are from broadband MT (BBMT) studies, with acquisition in the period range of 0.01–1000 s (frequency range of 100–0.001 Hz), which gives information generally from about 5 km depth to 100+ km. Some 1000 of them are audio-MT (AMT), with acquisition at periods in the range of 0.0001–0.1 s (10 kHz to 10 Hz frequencies), which only gives information about upper crustal resistivity structure (top 5 km). Also, at some sites there was long-period MT (LMT) acquisition in the period range of 20-10,000+ s, in most places in tandem with BBMT acquisition, which gives information from the deep crust to the base of the lithosphere and beyond.

More than half of the sites are on the Canadian Shield, which is defined as the Precambrian regions of Canada identified in Fig. 1a. The Cordillera of western Canada is also reasonably well covered, but the Appalachians of eastern Canada less so. Clearly, northern Quebec and Nunavut need greater coverage.

Other measures of tectonic processes

We compare the electrical parameters we derive at various depths, in particular our anisotropy parameters (strength and direction), with other available measures of crustal and lithospheric tectonic processes from Canadian and global databases. These are surface heat flow data, stress data, SKS shear wave splitting observations, elastic thickness, and absolute plate motion. In addition, we compare our data with the Canadian data from a global model of temperature.

Surface heat flow

The surface heat flow (SHF) for Canada is taken from the continuously-updated North American database of Blackwell and Richards (2004) (Fig. 2a, dots), downloaded as of summer 2012, plus the recent compilation database of J.-C. Mareschal for the Canadian Shield (Perry et al. 2010, and personal communication, 2013) (Fig. 2a, squares). The SHF data were contoured using Generic Mapping Tools (GMT) (Wessel and Smith 1991, 1998) *surface* routine, with a 5 min contour interpolation and tension set to 0.95 internally and 0.05 on the boundary. Low SHF on the Canadian Shield and beneath Vancouver Island and high SHF in the Cordillera are obvious, and result from thickened compared to thinned

lithosphere (Fig. 2a), where for Vancouver Island this is a consequence of stacking of both continental lithosphere plus subducted oceanic lithosphere. Moderate SHF is apparent in the Maritimes, the western edge of the Canadian Shield, and central British Columbia (BC).

Stress data

We use the direction of maximum stress for Canada available in the 2005 release of the World Stress Map database (Reinecker et al. 2005) for comparison with our crustal anisotropy directions. The vast majority (>95%) of the 412 values in the stress compilation for Canada come from borehole breakout data in Alberta and in the Beaufort Sea (Fig. 2b). For comparison with our MT directions, we average these data using the GMT median filter routine *blockmedian* with an increment of 5° in longitude and 2.5° in latitude. Those averages are also plotted on Fig. 2b (red arrows). These stress data we take as indicative of upper crustal state, and thus compare them with our crustal resistivity maps.

SKS data

For lithospheric mantle depths, we compare shear wave splitting determinations using SKS phases (a shear wave on the source side that passes through the outer core as a compressional wave then as a shear wave on the receiver side) with our anisotropy directions. For SKS data for Canada and northern USA, we use the global compilation of the Upper Mantle Anisotropy Database maintained by Professor Matt Fouch (formerly Arizona State University, now DTM, Carnegie) (dark blue vectors in Fig. 2c), complemented by other Canadian sources as follows:

- Alberta (dark green vectors): Shragge et al. (2002);
- Slave (green and turquoise vectors): Bank et al. (2000); Snyder and Bruneton (2007);
- Churchill (dark blue vectors): Jones et al. (2002a);
- Superior (dark red vectors): Frederiksen et al. (2007);
- Baffin Island: Snyder (2003);
- Northern BC and southern Yukon (olive vectors), CANOE array: Courtier (2008); Courtier et al. (2010);
- Southern Ontario (dark red vectors): Eaton et al. (2004a);
- Rae Craton (red vectors): Bastow et al. (2011); Snyder et al. (2013).

For comparison with our MT geoelectric directions (see later in the text), as discussed earlier we average these data using the GMT median filter routine *blockmedian* with an increment of 5° in longitude and 2.5° in latitude. Those averages are also plotted on Fig. 2c (red arrows). We expect these data to be indicative of the fabric of the upper mantle, be it either lithospheric or asthenospheric mantle.

Elastic thickness

The elastic thickness of the Canadian Shield has been derived by Audet and Mareschal (2004, 2007) and for western Canada by Fluck et al. (2003). Thickest elastic thickness, >100 km, is found beneath Hudson Bay and to the west of Hudson Bay. Thinnest elastic thickness on the North American Craton, <40 km, is found beneath the Williston Basin in southern Saskatchewan correlative

Table 2. List of Lithoprobe reports presented using EM.

Year, Report	Transect Meeting	Reports
1986, 1	SC, Sidney, 18–19 September	Gough, I., 1986. Rationale for magnetotelluric sounding in the southern Cordillera Transect of LITHOPROBE. Proceedings of the Southern Cordillera Transect Workshop held in Sidney on 18th–19th September. Lithoprobe Report 1 and GSC Internal Report November 1986.
1988, 4	KS, Toronto, 16–17 February	(1) Bailey, R.C., and J.C. Macnae, 1988. A controlled source deep electromagnetic sounding across the Ivanhoe Lake Cataclastic Zone using the UTEM method. Proceedings of the Kapuskasing Transect Workshop held in Toronto on 16th–17th February. Lithoprobe Report 4, pp. 183–192.
		(2) Chouteau, M., M. Mareschal, R. Chakridi, and K. Bouchard, 1988. Preliminary results of a magnetotelluric survey across the Groundhog River block of the Kapuskasing Zone. Proceedings of the Kapuskasing Transect Workshop held in Toronto on 16th–17th February. Lithoprobe Report 4, pp. 177–182.
		(3) Kurtz, R.D., E.R. Niblett, J.A. Craven, R.A. Stevens, and J.C. Macnae, 1988. Electromagnetic studies over the Kapuskasing Structural Zone. Proceedings of the Kapuskasing Transect Workshop held in Toronto on 16th–17th February. Lithoprobe Report 4, pp. 169–176.
		(4) Mareschal, M., R. Chakridi, and M. Chouteau, M. 1988. A magnetotelluric survey across the Groundhog River block: progress report on the I-D interpretation. Proceedings of the Kapuskasing Transect Workshop held in Toronto on 16th–17th February. Lithoprobe Report 4, pp. 77–82.
1988, 5	LE, St. John's, 21–22 October	Wright, J.A., 1988. EM Modelling of structures on the Lithoprobe East Line. Proceedings of the Lithoprobe EAST Transect Workshop held in St. John's on 21st–22nd October. Lithoprobe Report 5, pp. 5–9.
1988, 6	KS, Toronto, 18 November	(1) Bailey, R.C., J.A. Craven, J.C. Macnae, and B.D. Polzer, 1988. Deep UTEM controlled source electromagnetic sounding across the Ivanhoe Lake Cataclastic Zone. Proceedings of the Kapuskasing Transect Workshop held in Toronto on 18th November. Lithoprobe Report 6, pp. 65–76.
		(2) Mareschal, M., R. Chakridi, and M. Chouteau, 1988. A magnetotelluric survey across the Groundhog River Block: Progress report on the pseudo 1-D interpretation. Proceedings of the Kapuskasing Transect Workshop held in Toronto on 18th November. Lithoprobe Report 6, pp. 77–81.
1989, 7	SC, Vancouver, 25–26 February	(1) Bailey, R.C., and J.C. Macnae, 1989. Shallow controlled source electromagnetic sounding in the Omineca crystalline belt. Proceedings of the LITHOPROBE Southern Cordilleran Transect Workshop held in Vancouver on 25th–26th February. Lithoprobe Report 7, pp. 134–138.
		(2) Dosso, H.W., and Kang, S., 1989. Dipole–dipole analogue modelling of subsea sedimentary basins. Proceedings of the LITHOPROBE Southern Cordilleran Transect Workshop held in Vancouver on 25th–26th February. Lithoprobe Report 7, pp. 165–168.
		(3) Gough, D.I., J.M., DeLaurier, and J.P. Whelan, 1989. Magnetotelluric soundings on the southern Cordillera transect. Proceedings of the LITHOPROBE Southern Cordilleran Transect Workshop held in Vancouver on 25th–26th February. Lithoprobe Report 7, pp. 112–122.
		(4) Hyndman, R.D. 1989. Water in the lower continental crust: Modelling magnetotelluric, seismic refraction and seismic reflection results. Proceedings of the LITHOPROBE Southern Cordilleran Transect Workshop held in Vancouver on 25th–26th February. Lithoprobe Report 7, pp. 176–179.
		(5) Jones, A.G., D.E. Boerner, R.D. Kurtz, R.D., D. Oldenburg, and R. Ellis, 1989. Electrical crustal structure at the edge of the North American craton. Proceedings of the Southern Cordilleran Transect Workshop held in Vancouver on 25th–26th February. Lithoprobe Report 7, pp. 123–126.
		(6) Paulson, K.V., 1989. A magnetotelluric study across the Purcell Trench. Proceedings of the LITHOPROBE Southern Cordilleran Transect Workshop held in Vancouver on 25th–26th February. Lithoprobe Report 7, pp. 127–133.
1989, 8	AG, Montreal, 8 June	Mareschal, M., A.G. Jones, and R.D. Kurtz, 1989, Electromagnetic sounding in the Abitibi belt, 1989. Proceedings of the Lithoprobe Abitibi–Grenville Workshop held in Montreal in June on 8th June. Lithoprobe Report 8, pp. 56–58.
1990, 11	SC, Calgary, 3–4 March	Jones, A.G., R.D. Kurtz, D.E. Boerner, J.A. Craven, G. McNeice, D.I. Gough and J.M. DeLaurier, 1990. Electromagnetic investigations over the southern Cordilleran Lithoprobe transect: 1990 status report. Proceedings of the Southern Cordilleran Transect Workshop held in Calgary on 3rd–4th March. Lithoprobe Report 11, pp. 64–74.

Table 2 (*continued*).

Year, Report	Transect Meeting	Reports
1990, 12	THOT, Saskatoon, 12–13 October	Jones, A.G., 1990. Current status of MT studies in Saskatchewan. Proceedings of the Trans-Hudson Transect Workshop held in Saskatoon on 12th–13th October. Lithoprobe Report 12, pp. 35–37.
1990, 19	AG, Montreal, 31 October – 1 November	(1) Kellett, R., R. Kurtz, M. Mareschal, R. Groom, F. Aucoin, and M. Chouteau, 1990. Preliminary magnetotelluric studies over the Cadillac Break and the Pontiac. Proceedings of the Abitibi–Grenville Transect Workshop held in Montreal on 31st October – 1st November. Lithoprobe Report 19, pp. 25–28.
		(2) Kurtz, R., M., Mareschal, R. Kellett, F. Richard, G. McNeice, and R. Bailey, 1990. Preliminary magnetotelluric studies over the Round Lake batholith. Proceedings of the Abitibi–Grenville Transect Workshop held in Montreal on 31st October – 1st November October. Lithoprobe Report 19, pp. 29–32.
1990, 13	LE, St. John's, 24–25 October	Jones, A.G., 1990*a*. Electromagnetic imaging of modern and ancient subduction zones and plans for EM studies in LITHOPROBE EAST. Proceedings of the LITHOPROBE EAST Transect Workshop held in St. John's on 24th–25th October. Lithoprobe Report 13, pp. 102–110.
1991, 16	SC, Calgary, 16–17 March	Jones, A.G., R.D. Kurtz, D.E. Boerner, J.A. Craven, G.W. McNeice, D.I. Gough, J.M. DeLaurier, and R.E. Ellis, 1991. Electromagnetic investigations over the Southern Cordilleran Lithoprobe transect: 1991 status report. Proceedings of the SC transect workshop held in Calgary on 16th–17th March. Lithoprobe Report 16, pp. 38–55.
1991, 18	KS, Toronto, 25–26 April	Mareschal, M., 1991. Summary of EM work in the Kapuskasing Uplift. Proceedings of the KSZ transect workshop held in Toronto on 25th–26th April. Lithoprobe Report 18, pp. 44–50.
1991, 25	AG, Montreal, 19–20 November	(1) Boerner, D.E., R. Kellett, and M. Mareschal, 1992. Inductive EM sounding of the Sudbury Structure. Proceedings of the Abitibi–Grenville Transect Workshop held in Montreal on 19th–20th November. Lithoprobe Report 25, pp. 165–168.
		(2) Kellett, R., M. Chouteau, R.D. Kurtz, and M. Mareschal, 1992. A magnetotelluric transect from the Grenville to the northern Abitibi. Proceedings of the Abitibi–Grenville Transect Workshop held in Montreal on 19th–20th November. Lithoprobe Report 25, pp. 55–58.
		(3) Kurtz, R., M. Mareschal, F. Richard, R. Kellett, and R.C. Bailey, 1992. Crustal structure from MT soundings along a profile from the Kapuskasing to the Pontiac. Proceedings of the Abitibi–Grenville Transect Workshop held in Montreal on 19th–20th November. Lithoprobe Report 25, pp. 59–63.
		(4) Zhang, P., R.D. Kurtz, M. Chouteau, and M. Mareschal, 1991. Audiomagnetotelluric (AMT) investigations in the Abitibi Subprovince. Proceedings of the Abitibi–Grenville Transect Workshop held in Montreal on 19th–20th November. Lithoprobe Report 25, pp. 65–68.
1991, 23	LE, St. John's, 29–30 November	Wright, J.A., G. McNeice, T. Korja, A.G. Jones, J. Craven, and R. Ellis. 1991. Electromagnetic studies in the Lithoprobe East Transect. Proceedings of the LITHOPROBE EAST Transect Workshop held in St. John's on 29th–30th November. Lithoprobe Report No. 23, pp. 45–48.
1992, 24	SC, Edmonton, 6–8 March	(1) Gough, D.I., and J.A. Majorowicz, 1992. Magnetotelluric soundings, structure and fluids in the Canadian Cordillera. Proceedings of the Southern Canadian Cordillera Transect Workshop and Cordilleran Tectonics Workshop held in Edmonton on 6th–8th March. Lithoprobe Report 24, pp. 43–50.
		(2) Majorowicz, J.A., D.I. Gough, and T.J. Lewis, 1992. Correlation between depth to the lower crustal high conductivity layer and heat flow in the Canadian Cordillera. Proceedings of the Southern Canadian Cordillera Transect Workshop and Cordilleran Tectonics Workshop held in Edmonton on 6th–8th March. Lithoprobe Report 24, pp. 51–60.
1992, 26	THOT, Saskatoon, 9–10 March	(1) Fowler, C.M.R., D. Stead, B.I. Pandit, B. Janser, and E.G., Nisbett, 1992. Physical properties of rocks from the Trans Hudson Orogen, Proceedings of the Trans Hudson Orogen Transect Workshop held in Saskatoon on 9th–10th March. Lithoprobe Report 26, 117–119.
		(2) Jones, F.W., and A. Correia, 1992. Magnetotelluric soundings in the frequency range 0.01–130 Hz in Northern Saskatchewan, Proceedings of the Trans-Hudson Orogen Transect Workshop held in Saskatoon on 9th–10th March. Lithoprobe Report 26, pp. 111–116.
1992, 33	AG, Montreal, 15–16 December	(1) Blais, E., M. Mareschal, and P. Zhang, P. 1992. An audiomagnetotelluric survey in western Sudbury: application to exploration. Proceedings of the Abitibi–Grenville Transect Workshop held in Montreal on 19th–20th November. Lithoprobe Report 33, pp. 83–90.
		(2) Dufour, R., Mareschal, M., Kellett, R., Heiligman, M., Desmon, B., Kurtz, R., and Bailey, R., 1992. Variations in azimuthal electrical anisotropy at lower crustal/upper mantle depths in the Canadian Shield. Proceedings of the Abitibi–Grenville Transect Workshop held in Montreal on 19th–20th November. Lithoprobe Report 33, pp. 91–96.

Table 2 (*continued*).

Year, Report	Transect Meeting	Reports
		(3) Kellett, R., 1992. A high frequency magnetotelluric survey across the Lac Bouchette gabbro–anorthosite intrusion Grenville Province. Proceedings of the Abitibi–Grenville Transect Workshop held in Montreal on 19th–20th November. Lithoprobe Report 33, pp. 109–112.
1993, 31	AB, Calgary, 1–2 March	(1) Kurtz, R.D., D.E. Boerner, J.A. Craven, F.W. Jones, and I. Ferguson, 1993. Electromagnetic studies along the Alberta Basement Transects. Proceedings of the Alberta Basement Transect Workshop held in Calgary on 1st–2nd March. Lithoprobe Report 31, pp. 50–52.
		(2) Kalvey, A., and F.W. Jones, 1993. Preliminary results form a magnetotelluric survey in west-central Alberta. Proceedings of the Alberta Basement Transect Workshop held in Calgary on 1st–2nd March. Lithoprobe Report 31, pp. 53–59.
1993, 34	THOT, Regina, 1–2 April	(1) Jones, A.G., Craven, J.A., McNeice, G.W., Ferguson, I.J., Boyce, T., Farquharson, C., and Ellis, R.G., 1993. The North American Central Plains conductivity anomaly within the Trans-Hudson Orogen in northern Saskatchewan. Proceedings of the THOT transect workshop held in Regina on 1st–2nd April. Lithoprobe Report 34, pp. 40–55.
		(2) Jones, F.W., and A. Kalvey, 1993. Magnetotelluric measurements between 106°–107° W and 55.5°–56.75° N in Northern Saskatchewan. Proceedings of the THOT transect workshop held in Regina on 1st–2nd April. Lithoprobe Report 34, pp. 56–63.
		(3) Stead, D., B.I. Pandit, B. Janser, and C.M.R. Fowler, 1993. Physical properties of rocks from the Trans Hudson Orogen — An update. Proceedings of the THOT transect workshop held in Regina on 1st–2nd April. Lithoprobe Report 34, pp. 213–218.
1993, 41	AG, Montreal, 14–15 April	Louis, P., M. Mareschal, D. Livelybrooks, and J. Martignole, 1993. A magnetotelluric survey in the Grenville Province: preliminary results. Proceedings of the Abitibi–Grenville Transect Workshop held in Montreal on 14th–15th April. Lithoprobe Report 41, pp. 93–98.
1994, 37	AB, Calgary, 14–15 February	(1) Kurtz, R.D., D.E. Boerner, J.A. Craven, S. Rondenay, and W. Qian, 1994. Deep electromagnetic results from the Alberta Basement Central Corridor. Proceedings of the Alberta Basement transect workshop held in Calgary on 14th–15th February. Lithoprobe Report 37, pp. 84–96.
		(2) Kalvey, A., and F.W. Jones, 1994. Magneto-telluric measurements in west-central Alberta. Proceedings of the Alberta Basement transect workshop held in Calgary on 14th–15th February. Lithoprobe Report 37, pp. 97–101.
1995, 48	THOT, Regina, 3–4 April	Ferguson, I.J., and Jones, A.G., 1995. 1994 Electromagnetic measurements on the Trans Hudson Orogen transect. Proceedings of the THOT transect held in Regina on 3rd–4th April. Lithoprobe Report 48, pp. 162–169.
1995, 47	AB, Calgary, 10–11 April	Boerner, D.E., Kurtz, R.D., Craven, J.A., and Jones, F.W. 1995. Electromagnetic results from the Alberta Basement Lithoprobe Transect. Proceedings of the Alberta Basement transect workshop held in Calgary on 10th–11th April. Lithoprobe Report 47, pp. 35–45.
1995, 53	WS, Kingston, 26–27 October	Boerner, D., J. Craven, R. Kurtz, R. Bailey, and I. Ferguson, 1995. Electromagnetic studies in the western Superior Transect. Proceedings of the WS transect workshop held in Kingston on 26th–27th October. Lithoprobe Report 53, p. 74.
1996, 51	AB, Calgary, 28 February – 1 March	Boerner, D.E., Kurtz, R.D., Craven, J.A., and Jones, F.W., 1996. Electromagnetic results from the Alberta Basement Transect. Proceedings of the AB transect workshop held in Calgary on 28th February – 1st March. Lithoprobe Report 51, pp. 61–70.
1996, 55	THOT, Saskatoon, 1–2 April	Ferguson, I.J., K.M. Stevens, J.P. Cassells, X. Wu, I. Shiozaki, and A.G. Jones, 1996. THOT MT studies: Eastern Segment. Proceedings of the THOT transect workshop held in Saskatoon on 1st–2nd April. Lithoprobe Report 55, pp. 10–25.
1996, 54	AG, Quebec City, 29–30 November	(1) Senechal, G., Rondenay, S., Mareschal, M., Guilbert, J., and Poupinet, G., 1996. Teleseismic shear wave splitting and electrical anisotropy across the Grenville Front, Canada. Abitibi–Grenville LITHOPROBE Atelier 96 held in Quebec City on 29th–30th November. Lithoprobe Report 54, p. 32.
		(2) Shaocheng, J., Rondenay, S., Mareschal, M., and Seneschal, G., 1996. Obliquity between seismic and electrical anisotropies as potential indicator of movement sense for ductile shear zones. Abitibi–Grenville LITHOPROBE Atelier 96 held in Quebec City on 29th–30th November. Lithoprobe Report 54, p. 20.
1997, 56	SNORCLE, Calgary, 7–9 March	Jones, A.G., and I.J. Ferguson, 1997. Results from 1996 MT studies along SNORCLE profiles 1 and 1A. Proceedings of the SNORCLE transect workshop held in Calgary on 7th–9th March. Lithoprobe Report 56, pp. 42–47.
1997, 59	AB, Calgary, 10–11 March	Boerner, D.E., R.D. Kurtz, J.A. Craven, and F.W. Jones, 1997. Towards a synthesis of electromagnetic results from the Alberta Basement Lithoprobe Transect. Proceedings of the Alberta Basement transect workshop held in Calgary on 10th–11th March. Lithoprobe Report 59, pp. 55–62.
1997, 60		Report for SNORCLE and THOT EM, Nick Grant.
1997, 62	THOT, Saskatoon, 1–2 May	(1) Cassels, J., I.J. Ferguson, and A.G. Jones, 1997. Signal processing and interpretation of magnetotelluric data from the Superior boundary zone. Proceedings of the THOT transect workshop in Saskatoon on 1st–2nd May. Lithoprobe Report 62, pp. 251–268.

Table 2 (*continued*).

Year, Report	Transect Meeting	Reports
		(2) Ferguson, I.J., Y. Sheng, X. Wu, I. Shiozaki, and A.G. Jones, 1997. Electrical conductivity soundings in the central Flin Flon Belt, Trans-Hudson Orogen, Canada. Proceedings of the THOT transect workshop in Saskatoon on 1st–2nd May. Lithoprobe Report 62, pp. 147–167.
		(3) Grant, N., 1997. Processing, interpretation and databasing of magnetotelluric data from the Trans-Hudson orogen: Rapid 2D inversion of the THOT92 regional datasets. Proceedings of the THOT transect workshop in Saskatoon on 1st–2nd May. Lithoprobe Report 62, pp. 16–61.
		(4) Grant, N., 1997. Processing, interpretation and databasing of magnetotelluric data from the Trans-Hudson orogen: Site by site and multi-site, multi-frequency Groom-Bailey decompositions. Proceedings of the THOT transect workshop in Saskatoon on 1st–2nd May. Lithoprobe Report 62, pp. 62–105.
		(5) Jones, A.G., X. Garcia, N.J. Grant, I.J. Ledo, and I.J. Ferguson, 1997. Regional electrical structure of the Trans-Hudson Orogen. Proceedings of the THOT transect workshop held in Saskatoon on 1st–2nd May. Lithoprobe Report 62, pp. 130–146.
		(6) Stevens K., and I.J. Ferguson 1997. 1-D interpretation of high frequency magnetotelluric data across the Glennie Domain of the Trans Hudson Orogen Transect. Proceedings of the THOT transect workshop in Saskatoon on 1st–2nd May. Lithoprobe Report 62, pp. 197–205.
1998, 64	SNORCLE, Vancouver, 6–8 March	(1) Cassels, J., and A.G. Jones, 1998. Source-field contamination of SNORCLE magnetotelluric data. Proceedings of the SNORCLE transect workshop held in Vancouver on 6th–8th March. Lithoprobe Report 64, pp. 130.
		(2) Wu, X., I.J. Ferguson, and A.G. Jones, 1998. Electrical resistivity structure between the Nahanni Terrane and Slave Province. Proceedings of the SNORCLE transect workshop held in Vancouver on 6th–8th March. Lithoprobe Report 64, pp. 93–102.
1998, 65	WS, Toronto, 23–24 March	Craven, J.A., I.J., Ferguson, D.E. Boerner, R.C. Bailey, and R.D. Kurtz, 1998. A recon survey of the electrical structure within the West Superior Province. Proceedings of the WS transect workshop held in Toronto on 23rd–24th March. Lithoprobe Report 65, pp. 3–7.
1999, 70	WS, Ottawa, 1–3 February	Craven, J.A., D.E. Boerner, R.D. Kurtz, I.J. Ferguson, and R.C. Bailey, 1999. Preliminary results from the 1998 EM survey along the Western Superior Transect. Proceedings of the WS transect workshop held in Ottawa on 1st–3rd February. Lithoprobe Report 70, pp. 23–25.
1999, 69	SNORCLE, Calgary, 5–7 March	(1) Jones, A.G., I. Ferguson, G. McNeice, R. Evans, and A. Chave, 1999. Electromagnetic studies of the Slave craton: Preliminary results and ongoing experiments. Proceedings of the SNORCLE transect workshop held in Calgary on 5th–7th March. Lithoprobe Report 69, pp. 56–71.
		(2) Evans, R.L., A.D. Chave, and A.G. Jones, 1999. Deep EM studies of the Slave craton. Proceedings of the SNORCLE transect workshop held in Calgary on 5th–7th March. Lithoprobe Report 69, pp. 72.
2000, 77	WS, Ottawa, 3–4 February	Craven, J.A., R.D. Kurtz, D.E. Boerner, I.J. Ferguson, and R.C. Bailey, 2000. Overview of the 1999 activities. Proceedings of the WS transect workshop held in Ottawa on 3rd–4th February. Lithoprobe Report 77, pp. 137–137.
2000, 72	SNORCLE, Calgary, 25–27 February	(1) Jones, A.G., I. Ferguson, G. McNeice, R. Evans, and A. Chave, 2000. The electric Slave craton. Proceedings of the SNORCLE transect workshop held in Calgary on 25th–27th February. Lithoprobe Report 72, pp. 36–42.
		(2) Wu, X., I.J. Ferguson, and A.G. Jones, 2000. Magnetotelluric response and geoelectric structure of southwestern Northwest Territories, Canada. Proceedings of the SNORCLE transect workshop held in Calgary on 25th–27th February. Lithoprobe Report 72, pp. 43–55.
		(3) Eaton, D.E., I. Asudeh, and A.G. Jones, 2000. Mantle strain beneath the Great Slave Lake shear zone, NWT from measurements of seismic and electrical anisotropy. Proceedings of the SNORCLE transect workshop held in Calgary on 25th–27th February. Lithoprobe Report 72, pp. 56–63.
2000, 74	Pan-Lithoprobe II, Banff, 23–25 May	Jones, A.G., and I.J. Ferguson, 2000. The electric Moho. Proceedings of the Pan-Lithoprobe workshop held in Banff on 23rd–25th May. Lithoprobe Report 74.
2001, 80	WS, Ottawa, February, 5–6 March	(1) Ferguson, I.J., J.A. Craven, X. Wu, M. Norton, and G. Wennberg, 2001. Review and 2-D modelling of magnetotelluric data from Manitoba and Western Ontario on the LITHOPROBE Western Superior Transect. Presentation at the WS transect workshop held in Ottawa on 5th–6th March. Lithoprobe Report 80.
		(2) Craven, J.A., R.D. Kurtz, I.J. Ferguson, X. Wu, D.E. Boerner, and R.C. Bailey, 2001.Towards a 3-D image of electrical lithosphere beneath the Western Superior Transect. Presentation at the WS transect workshop held in Ottawa on 5th–6th March. Lithoprobe Report 80.

Table 2 (*concluded*).

Year, Report	Transect Meeting	Reports
2001, 79	SNORCLE, Sidney, 25–27 February	(1) Ledo, J., A.G. Jones, I.J. Ferguson, and G. Wennberg, 2001*a*. Electromagnetic images of the Tintina fault. Proceedings of the SNORCLE transect workshop held in Sidney on 25th–27th February. Lithoprobe Report 79, pp. 67–73.
		(2) Ledo, J., A.G. Jones, I.J. Ferguson, and G. Wennberg, 2001*b*. Regional electrical conductivity of the northern Cordillera: Corridors 2 and 3. Proceedings of the SNORCLE transect workshop held in Sidney on 25th–27th February. Lithoprobe Report 79, pp. 258.
		(3) Wennberg, G., I.J. Ferguson, J. Ledo, and A.G. Jones, 2001. Preliminary results from SNORCLE magnetotelluric data: Johnson's Crossing to Upper Liard. Proceedings of the SNORCLE transect workshop held in Sidney on 25th–27th February. Lithoprobe Report 79, pp. 284–290.
2001, 81	Pan-Lithoprobe III, "Mantle Lithosphere and Lithoprobe: Views of Continental Evolution from the Bottom Up" Banff, 27–29 October	(1) Craven, J.A., and A.G. Jones, 2001. Comparisons of Slave and Superior electric lithosphere. Proceedings of the Pan-Lithoprobe workshop held in Banff on 27th–29th October. Lithoprobe Report 81, pp. 8–10.
		(2) Craven, J.A., I.J. Ferguson, T. Skulski, R.D. Kurtz, X. Wu, M. Orellana, J. Spratt, and D.E. Boerner, 2001. Electrical images of ancient partial melting. Proceedings of the Pan-Lithoprobe workshop held in Banff on 27th–29th October. Lithoprobe Report 81, p. 11.
		(3) Eaton, D., I.J. Ferguson, A.G. Jones, J. Hope, and X. Wu, 2001. A geophysical shear-sense indicator and the role of mantle lithosphere in transcurrent faulting. Proceedings of the Pan-Lithoprobe workshop held in Banff on 27th–29th October. Lithoprobe Report 81, pp. 12–15.
		(4) Jones, A.G., I.J. Ferguson, A.D. Chave, R. Evans, and J. Spratt, 2001. Slave electromagnetic studies. Proceedings of the Pan-Lithoprobe workshop held in Banff on 27th–29th October. Lithoprobe Report 81, pp. 50–51.
2002, 82	SNORCLE, Sidney, 21–24 February	(1) Jones, A.G., I.J. Ferguson, A.D. Chave, R.L. Evans, P. Lezaeta, and X. Garcia, 2002. Regional-scale electrical structure of the Slave craton. Proceedings of the SNORCLE transect workshop. Lithoprobe Report 82, pp. 12–13.
		(2) Lezaeta, P., A.D. Chave, R.L. Evans, and A.G. Jones, 2002. Three-dimensional electrical conductivity structure beneath the Slave craton. Proceedings of the SNORCLE transect workshop held in Sidney on 21st–24th February. Lithoprobe Report 82, p. 14.
		(3) Ledo, J., A.G. Jones, I.J. Ferguson, and G. Wennberg, 2002. SNORCLE corridor 3 magnetotelluric experiment. Proceedings of the SNORCLE transect workshop held in Sidney on 21st–24th February. Lithoprobe Report 82, pp. 21–23.
		(4) Wennberg, G., I.J. Ferguson, J. Ledo, and A.G. Jones, 2002. Modeling and interpretation of magnetotelluric data: Watson Lake to Stewart (line 2a) and Johnson Crossing to Watson Lake. Proceedings of the SNORCLE transect workshop held in Sidney on 21st–24th February. Lithoprobe Report 82, pp. 145–152.
		(5) Wu, X., I.J. Ferguson, and A.G. Jones, 2002. Geological interpretation of electrical resistivity models along the SNORCLE corridors 1 and 1a. Proceedings of the SNORCLE transect workshop held in Sidney on 21st–24th February. Lithoprobe Report 82, pp. 153–163.

Table 3. List of graduate students, post-doctoral fellows, and visiting scientists trained by Lithoprobe MT scientists.

Post-doctoral fellows

Name	Location	Focus of research	Period	Publications
Dr. Jacek Majorowicz	University of Alberta	British Columbia	1985–1991	Majorowicz and Gough (1991); Gough and Majorowicz (1992); Majorowicz et al. (1993a, 1993b); Majorowicz and Gough (1994)
Dr. Ross Groom	GSC-Ottawa	Distortion decomposition	1989–1992	Groom et al. (1993); Jones and Groom (1993); Jones et al. (1993b)
Dr. Richard Kellett	École Polytechnique	Abitibi–Grenville	1990–1993	Kellett et al. (1992, 1994)
Dr. Dean Livelybrooks	École Polytechnique	Abitibi–Grenville	1993–1996	Livelybrooks et al. (1996)
Dr. Ping Zhang	École Polytechnique	Abitibi–Grenville	1991–1995	Zhang and Chouteau (1992); Zhang et al. (1993, 1995)
Dr. Benoit Tournerie	École Polytechnique	Abitibi–Grenville	1996–2005	Tournerie and Chouteau (1998, 2002)
Dr. Juanjo Ledo	Geological Survey of Canada, Ottawa	THOT, Southern Cordillera, SNORCLE Transects 2 and 3	1997–2002	Ledo and Jones (2001); Ledo et al. (2001, 2002, 2004); Jones et al. (2005b)
Dr. Xavier Garcia	Geological Survey of Canada, Ottawa	SNORCLE Slave: Yellowknife Fault	1998–2001	Garcia and Jones (2002a, 2002b, 2005a); Garcia et al. (2003); Jones and Garcia (2006)
Dr. Pamela Lezaeta	Woods Hole Oceanographic Institution	SNORCLE Slave Lakes data	2001–2003	Jones et al. (2003); Lezaeta et al. (2007)
Dr. Xianghong Wu	University of Manitoba	Western Superior	2001–2003	Wu et al. (2005)
Dr. Wolfgang Soyer	University of Alberta	Alberta–BC	2002–2004	Soyer and Unsworth (2006)

Graduate students

Name	University/institution	Focus of research	Degree and year	Thesis
Carlos Flores	Toronto	Mt. Meager	Ph.D., 1986	Flores-Luna (1986)
Ross Groom	Toronto	Distortion decomposition	Ph.D., 1988	Groom (1988)
Stanley Dosso	UBC	One-dimensional MT inversion	Ph.D., 1990	Dosso (1990)
Rachid Chakridi	École Polytechnique	Distortion decomposition	Ph.D., 1991	Chakridi (1991)
James A. Craven	Toronto	UTEM, Kapuskasing	M.Sc., 1991	Craven (1991)
Francois Aucoin	École Polytechnique	Groundhog River block, Kapuskasing	M.Sc., 1992	Aucoin (1992)
Abd-Errezak Bouzid	École Polytechnique	Saharan Basin	M.Sc., 1992	Bouzid (1992)
Guy Marquis	Victoria	Southern Cordillera	Ph.D., 1992	Marquis (1992)
Stefka Krivochieva	École Polytechnique	Santa Catarina basin	M.Sc., 1993	Krivochieva (1993)
Jorge Arzate-Flores	École Polytechnique	Cocos Plate subduction	Ph.D., 1994	Arzate-Flores (1994)
Estelle Blais	École Polytechnique	Trillabelle Deposit	M.Sc., 1994	Blais (1994)
Jie Chen	Victoria	Analogue modelling	Ph.D., 1994	Chen (1994)
Antonio Correia	Alberta	Faulting in Portugal	Ph.D., 1994	Correia (1994)
Bernard Giroux	École Polytechnique	Senegal Basin	M.Sc., 1994	Giroux (1994)
Helena Poll	Victoria	Numerical forward modelling	Ph.D., 1994	Poll (1994)
Xing-Hua Pu	Victoria	Three-dimensional modelling	Ph.D., 1994	Pu (1994)
Anand Kalvey	Alberta	Alberta	M.Sc., 1994	Kalvey (1994)
Colin Farquharson	UBC	Forward and inverse modelling	Ph.D., 1995	Farquharson (1995)
Shugang Kang	Victoria	Analogue modelling	Ph.D., 1995	Kang (1995)
Stéphane Rondenay	École Polytechnique	Seismic and electric anisotropy	M.Sc.A., 1996	—
Xavier Garcia	Barcelona	THOT Profile X	Ph.D., 1998	—
Gary McNeice	Memorial/GSC-Ottawa	Lithoprobe East	M.Sc., 1998	McNeice (1998)
Kevin Stevens	Manitoba	THOT Eastern Saskatchewan	M.Sc., 1999	Stevens (1999)
Xianghong Wu	Manitoba	SNORCLE Transect 1	Ph.D., 2001	Wu (2001)
Stefka Krivochieva	École Polytechnique	TDEM in aquifers	Ph.D., 2002	Krivochieva (2002)
Shane Evans	Queens/GSC-Ottawa	Baffin Island	M.Sc., 2003	Evans (2003)
Jessica Spratt	Syracuse/GSC-Ottawa	Tibet	M.Sc., 2003	Spratt (2003)
Grant Wennberg	Manitoba	SNORCLE	M.Sc., 2003	Wennberg (2003)
Wen Xiao	Alberta	Rocky Mountain Foothills	M.Sc., 2004	Xiao (2004)
Jean Legault	École Polytechnique	Kidd Creek MT and IP data inversion	M.Sc., 2005	Legault (2005)
Matthew Marchand	École Polytechnique	Noise removal	M.Sc., 2005	Marchand (2005)
Marcelo Orellana	Manitoba	Western Superior	M.Sc., 2006	Orellana (2006)
Volkan Tuncer	Alberta	EXTECH-IV	M.Sc., 2007	Tuncer (2007)
Peter Fernberg	Carleton	GICs on powerlines	Ph.D., 2011	Fernberg (2011)
Matthew Drew	Memorial	Inversion	M.Sc., 2012	Drew (2012)
Ademola Adetunji	Manitoba	Abitibi–Grenville, POLARIS Ontario	Ph.D., 2014	Adetunji (2014)

Table 3 (concluded).

Visiting scientists/students or others

Name	University/institution	Focus of research	Degree and year	Publications/theses
Jim Craven	Carleton/GSC-Ottawa	Prince Edward Island	B.Sc., 1984	—
Isabelle Dumas	École Polytechnique/GSC-Ottawa	Mt. Meager and Mt. Cayley	B.Sc., 1994	Jones and Dumas (1993)
Sheng Yu	Manitoba (1991–1992)	THOT	Ph.D. (Chinese Academy of Sciences)	—
Dr. Ichiro Shiozaki	Manitoba (1996)	THOT/SNORCLE	Assistant Professor (Tottori University, Japan)	—
James Cassels	Manitoba	THOT	B.Sc., 1997	Cassels (1997)
Jessica Spratt	Carleton/GSC-Ottawa	Western Superior	B.Sc., 2000	—
Grant Wennberg	Manitoba	Western Superior	B.Sc., 1999	Wennberg (1999)
Lisa Wolynec	Manitoba	SNORCLE Corridor 1	B.Sc., 2000	Wolynec (2000)
Mark Norton	Manitoba	Western Superior	B.Sc., 2000	Norton (2000)
Xiaobing Ma	Manitoba (2002)	THOT/POLARIS Ontario	Ph.D. (Chinese Academy of Sciences)	—
Evan Gowan	Manitoba	POLARIS Manitoba	B.Sc., 2005	Gowan (2005); Gowan et al. (2009)
Cassandra Tycholiz	Manitoba	Western Superior, Nipigon	B.Sc., 2010	Tycholiz (2010)
Obuneme Akaranta	Manitoba	Trans-Hudson Orogen	B.Sc., 2011	Akaranta (2011)
Joe McLeod	Manitoba	Western Superior, Knee Lake	B.Sc., 2013	McLeod (2013)

Note: UBC, University of British Columbia.

with the trace of the Trans-Hudson Orogen. For the Cordillera, elastic thickness is in the range 20–40 km (Fluck et al. 2003).

Plate motion

For the third type of direction parameters, we compare our anisotropy azimuths and strengths for the deepest determinations with absolute plate motion (red arrows, Fig. 2d) derived using the model HS3-NUVEL1 based on a fixed hot spot reference frame by Gripp and Gordon (2002), obtained using the calculator of Professor Kensaku Tamaki (University of Tokyo) at ofgs.aori.u-tokyo.ac.jp/~okino/platecalc_new.html, for selected geographic points (centres of the red arrows), and estimates of plate motions from global GPS observations (Larson et al. 1997; Prawirodirdjo and Bock 2004) (blue arrows) and from Calais et al. (2006) (green arrows) in a fixed reference frame (ITRF), and from the two Doppler satellite tracking (DORIS) stations in Canada in St. John's, Newfoundland, and Yellowknife, Northwest Territories (Soudarin and Cretaux 2006) (black arrows). These are all shown in Fig. 2d and are all consistent with WSW movement of most of Canada and W–WSW movement for eastern Canada (eastern Ontario, Quebec, and the Maritime provinces). We expect these directions to be indicative of lowermost mantle lithosphere or asthenosphere fabric directions.

Mantle temperature estimates

Estimates of continental mantle temperature at 40, 50, 100, 150, and 200 km are taken from the TC1 model of Artemieva (2006) on the publicly-available 5° × 5° grid downloaded from the web site http://lithosphere.info. Those data are plotted on the appropriate resistivity maps for the corresponding depths. Also included in the TC1 model data are estimates of the depths to temperatures of 550, 900, and 1300 °C, where the latter is taken as the lithosphere–asthenosphere boundary (tLAB, see discussion later in the text) and the depths are plotted in Fig. 2e (circles).

Lithosphere–asthenosphere depth estimates

We wish to compare our resistivity estimates at 200 km with estimates of lithospheric thickness for Canada—unfortunately, apart from thermal models there are few lithosphere–asthenosphere boundary (LAB) estimates that we can appeal to, and most of them are on the Canadian Shield.

Defining the depth to the LAB is fraught with difficulties and contention, not least of which is the plethora of proxies used to derive it (Eaton et al. 2009). Geophysical proxies, be they thermally-based (tLAB), electromagnetically-based (eLAB), or seismically-based (generically sLAB; from receiver functions, sLABrf, from anisotropy studies, sLABa, from surface waves, sLABsw, and from reflection studies, sLABrl), are responding principally to today's thermal field, whereas the petrologically-defined (pLAB) estimates are indicative of the LAB at the time of magmatic eruption (kimberlitic or lamproitic). Even so, estimates of the LAB from geophysical methods can differ significantly, as shown by Jones et al. (2010) for Europe. On Phanerozoic Europe south of the Trans-European Suture Zone (TESZ), the eLAB and sLABrf estimates agree, and the sLABa estimates are consistently deeper, whereas on Precambrian Europe north of the TESZ the sLABa and sLABrf estimates are in agreement, but are significantly shallower than the eLAB ones.

Recent concern has been expressed about sLABrf estimates that yield impossibly shallow LABs, e.g., the global compilation of Rychert and Shearer (2009) with an average of 95 ± 4 km for Precambrian regions of the world, the estimate of 120 km for the southern part of the Slave Craton (Yuan et al. 2006; Kind et al. 2012), and the estimate of <100 km for Indian lithosphere that includes the Dharwar Craton (Kumar et al. 2007). All of these are counter to the overwhelming petrological evidence from recent kimberlitic magmatism as well as other geophysical evidence for thick lithosphere beneath Archean cratons. This concern was addressed by Abt et al. (2010), who suggested that there existed mid-lithosphere discontinuities (MLDs) responsible for the observed shallow receiver functions, and that these MLDs had been routinely misinterpreted as the sLABs in prior studies. A recent paper by Bodin et al. (2014) demonstrates that the supposed "sLABrf" imaged at 110 km beneath the Dharwar Craton is an MLD, and that the real sLABrf is expressed as a mild gradient between 150 and 200 km. This amply highlights the dangers inherent when geophysicists independently label observed physical interfaces.

Estimates of the depth to the LAB for Canada come from both geophysical sources and petrological ones and are shown in Fig. 2e. The contoured LAB depth estimates for Canada come from the spherical harmonic global model of Hamza and Vieira (2012)

Fig. 2. (*a*) Surface heat flow (mW/m²) map of Canada, taken from the North American database of Blackwell and Richards (2004) (circles) plus the recent compilation database of J.-C. Mareschal for the Canadian Shield (Perry et al. 2010, and personal communication, 2013) (squares). The SHF data were contoured using GMT (Wessel and Smith 1991, 1998) *surface* routine, with a 5 min contour interpolation and tension set to 0.95 internally and 0.05 on the boundary. (*b*) Maximum horizontal stress directions (blue vectors) and median-based averages (red vectors) (see text for details). (*c*) Compilation of SKS observations in Canada and northern USA. Red arrows are median-based averages (see text for details). (*d*) Plate motion (PM) velocity vectors from Gripp and Gordon's (2002) model (red arrows), from GPS (blue and green arrows) and DORIS (black arrows) observations (see text for details). (*e*) Estimates to the depth of the lithosphere–asthenosphere boundary (LAB). Contoured are those of the spherical harmonic model of Hamza and Vieira (2012), and the circles are those of Artemieva (2006), both based on thermal arguments (depth to 1300 °C from Artemieva's model TC1). The diamonds are the petrologically derived ones of Snyder and Grütter (2010) based on analyses of xenoliths brought to the surface in kimberlites. The stars are from MT estimates, with the northern Canada one being that of Moorkamp et al. (2010) for the central Slave Craton derived from joint inversion of receiver function data, surface wave dispersion curve data, and magnetotelluric data, and the southern Canada one being that of Jones et al. (2003) for the Carty Lake data (Schultz et al. 1993) on the Superior Craton.
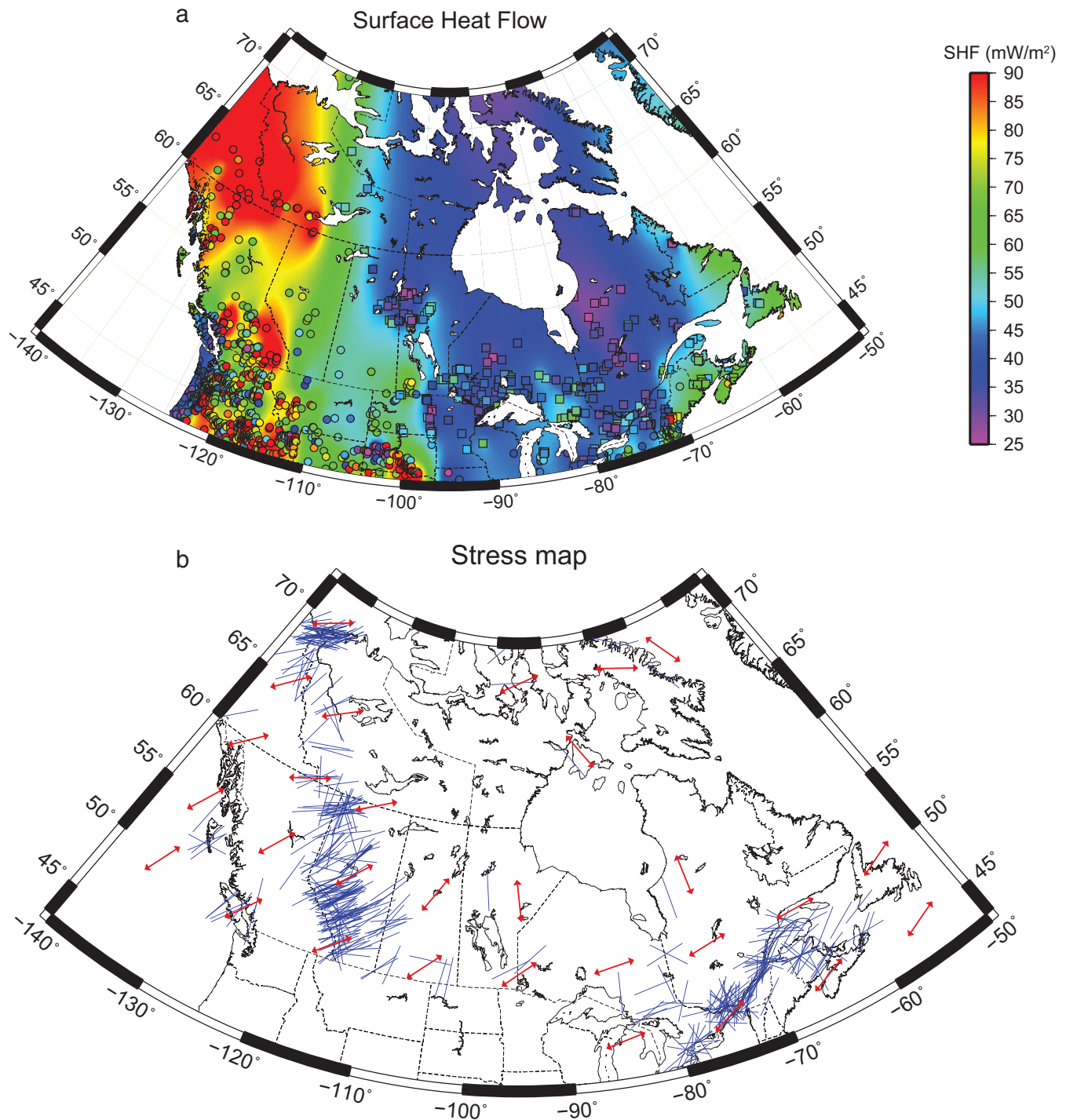
Fig. 2 (*continued*).
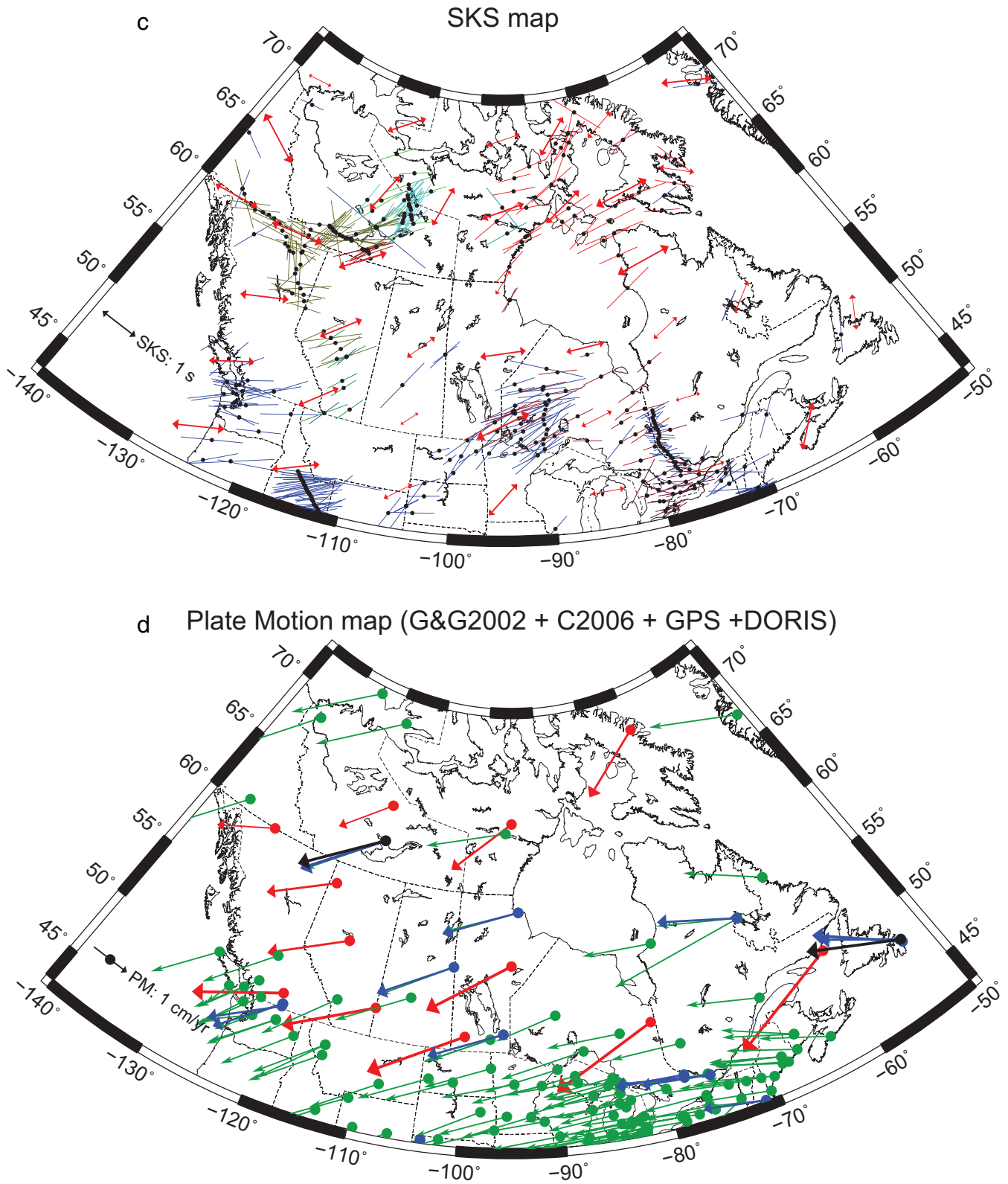
c

SKS map

d

Plate Motion map (G&G2002 + C2006 + GPS +DORIS)

Fig. 2 (*concluded*).

e LAB Depth Estimates
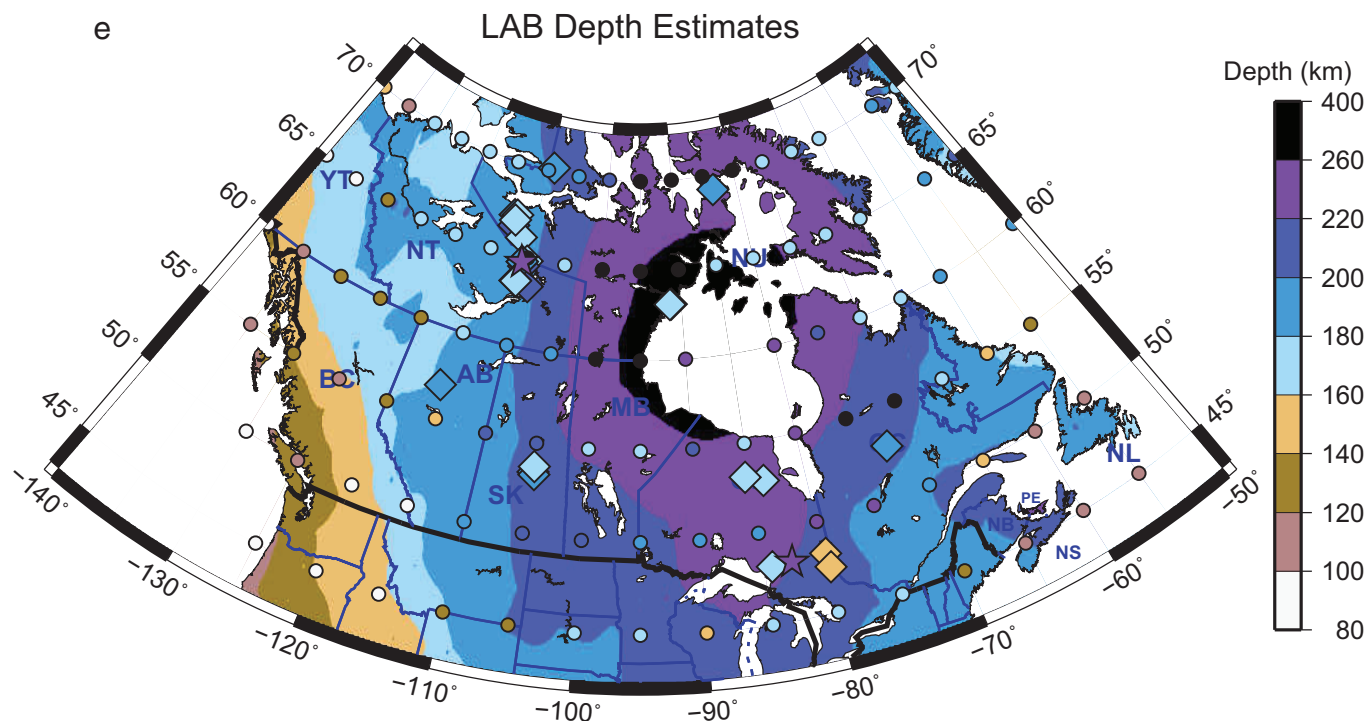
based on thermal arguments using global surface heat flow (SHF) data compilation of Vieira and Hamza (2010) coupled with crustal structure taken from CRUST 5.1 of Mooney et al. (1998). Given the extant SHF information for Canada shown in Fig. 2a, and that the crustal model CRUST 5.1 includes no data for all of northern Canada given the paucity of refraction experiments, much of this thermal LAB (tLAB) map is generated by interpolation between very, very sparse SHF data points. However, the general trend of thick lithosphere beneath the Canadian Shield and thinner lithosphere to the west (Cordillera) and east (Appalachians) is intuitive and undoubtedly correct, so their values will be used here. Similarly, the depth to the 1300 °C isotherm derived by Artemieva (2006) is generally consistent with this trend, with the exception of southern BC and NW USA that exhibits thick lithosphere, presumably as a consequence of Juan de Fuca plate subduction under the SW coastal region of Canada.

The diamonds shown in Fig. 2e are the petrologically-derived LAB (pLAB) depth estimates of Snyder and Grütter (2010), published in the Lithoprobe synthesis volume (Clowes 2010b), based on analyses of xenoliths brought to the surface in kimberlites of eruption ages varying from the Neoproterozoic to Eocene. The pLAB depths are derived from thermobarometry calculations on the deepest xenoliths recovered, using the Cr/Ca-in-garnet barometer of Grütter et al. (2006), and as such should be considered minimum estimates of the "true" LAB. Generally, the pLABs are in excess of 160 km, as required for the kimberlite pipes to be diamondiferous, i.e., sampling from below the graphite–diamond stability field which lies at around 150–160 km beneath the continents (Kennedy and Kennedy 1976). The anomalous ones are those of Jurassic age on the Superior Craton from the Kirkland Lake (pLAB of 144 km) and New Liskeard (Opap) (pLAB of 150 km) clusters, shown as orange diamonds on Fig. 2e. This shallow result is in accord with surface wave investigations of locally thin lithosphere in the southern Superior Craton (Darbyshire et al. 2007; Faure et al. 2011). The xenoliths from the kimberlites do, however, exhibit some evidence of diamonds, so must have had an LAB in excess of 170 km (150 km for graphite–diamond stability field depth plus a minimum 20 km thick "diamond window") at the

time of kimberlitic eruption, estimated at 160–152 Ma (Heaman and Kjarsgaard 2000; Heaman et al. 2003). So either the lithosphere is today thick, and the lower lithosphere was not sampled by xenolith entrainment in the kimberlitic magmas (but nevertheless diamonds were entrained), and the sLABrf estimates are too shallow, or the lowermost lithosphere has been eroded away since eruption, possibly by the movement of the North American plate over the Great Meteor hotspot (Heaman and Kjarsgaard 2000). The Churchill cluster of late-Triassic to mid-Jurassic pipes on the NW part of Hudson's Bay yield pLAB estimates of <190 km, thus not lending conclusive support to the purported very thick lithospheric root (>260 km) beneath Hudson Bay. But again, pLAB estimates should be taken as minimum values. Surface wave studies of Darbyshire and Eaton (2010) indicate sLABsw values around Hudson Bay of 230–240 km.

Two firm LAB estimates come from MT. The star data point in the centre of the Slave Craton in northern Canada (Fig. 2e) is the LAB estimate of Moorkamp et al. (2010), derived from joint inversion of receiver function data, surface wave dispersion curve data, and magnetotelluric data from the EKTN POLARIS station. This eLAB + sLABrf + sLABsw value of 230 km (220–235 km) exceeds by 20–30 km the greatest pLAB values on the Slave Craton of 202 km for the Neoproterozoic Anuri pipe in NW Slave, 208 km from the Jurassic-aged Gahcho Kue pipe (formerly known as Kennedy Lake) in SW Slave, and the 202 km pLAB from the Eocene-aged Diavik pipe in the central Slave (Snyder and Grütter 2010). It is though well within the error limits of the poorly-resolved sLABsw estimate of 220 ± 60 km of Chen et al. (2007) based on only Rayleigh wave inversion from the same station (EKTN); here, the joint inversion of Moorkamp et al. (2010) has served to reduce the uncertainty considerably. Either the pLAB estimates are too low by 20–30 km, which is likely, or the lithosphere has grown by that order over the last 50 million years since the Eocene kimberlite eruptions in the central Slave, which is less likely, or aspects of both are operating.

The second star point in the centre of the Superior Craton (Fig. 2e) is that from the unique Carty Lake MT experiment, located at 82.7°W, 48.2°N, of Schultz et al. (1993), with electrodes set over

a kilometre apart on the lake bottom to ensure thermal and chemical stability and consisting of over 2 years of data recording. To this day, the responses from Carty Lake still represent the best MT data we have for a craton worldwide, and modelling of them by Jones et al. (2003) yielded an eLAB at 253 ± 6 km. This value is consistent with the tLAB thermal modelling of Hamza and Vieira (2012) and reasonably consistent with the tLAB estimates of Artemieva (2006), but significantly deeper than the 166 km pLAB estimate from the nearby late-Mesoproterozoic (1176–1076 Ma) Wawa kimberlites (Snyder and Grütter 2010) to the west. The sLABsw estimates of Darbyshire et al. (2007) for two-station paths, with one end-station taken as the one closest to the Carty Lake site, namely Canadian National Seismic Network station KAPO at 82.5°W, 49.5°N, are of 160–180 km for a path to the west (to station PKLO), and 220–240 km for a path to the southeast (to station BANO). Picking the sLABsw is subject to uncertainty (Eaton et al. 2009), and particularly, the PKLO–KAPO models exhibit a very shallow gradient with depth, suggesting the sLABsw could be chosen to be deeper (see fig. 6 in Darbyshire et al. 2007).

One area that deserves more attention is the Canadian Cordillera, where there is an apparent contradiction in that the inferred shallow LAB (40–60 km), based on the sLABrl estimate of 48 km from a mantle reflector interpreted as the LAB by Clowes et al. (1995), pLAB estimates from xenolith analyses (Saruwatari et al. 2001; Harder and Russell 2006; Greenfield et al. 2013), and tLAB estimates from consideration of the thermal field (Hyndman 2010), are all seemingly falsified by the electrical resistivity model of Soyer and Unsworth (2006). The model, from long-period MT data acquired along a 350 km long NE–SW profile from the Intermontane Belt to the SW coast of Vancouver Island, exhibits moderate upper mantle resistivity >100 Ω·m beneath the Intermontane Belt to depths of 80 km below the Cordillera. In contrast, asthenospheric resistivity is typically in the range of 5–25 Ω·m below oceanic, active, and young regions (see Jones 1999b and references therein). More recent MT modelling, however, using data from this profile extended to the NE to Edmonton plus a second parallel NE–SW profile some 200 km to the northwest (Rippe et al. 2013) yields a rather more complex result; the lithosphere below the westernmost part of the Omineca Belt has low resistivity, of the order of 50–60 Ω·m, for the whole lithospheric extent on the northwestern profile; otherwise, the lithosphere beneath the Omineca Belt is resistive (>200 Ω·m) on both profiles. In contrast, the lithosphere beneath the western part of the Intermontane Belt is resistive to a depth of 100 km on the northwestern profile of the two, and otherwise more conductive (~50–60 Ω·m) on both profiles; the lithosphere beneath the Intermontane Belt on the southeastern profile was previously interpreted as resistive (>100 Ω·m) by Soyer and Unsworth (2006) (discussed earlier in the text). Rippe et al. (2013) suggest that the low resistivities modelled at shallow lithospheric mantle depths beneath the Intermontane Belt cannot be accounted for by proton conduction in wet peridotite alone, using either the Wang et al. (2006) or the Yoshino et al. (2009) models (see discussion later in the text), and proposed that 1.5% partial melt is required. This would suggest a shallower eLAB beneath most of the Intermontane Belt and a deeper eLAB beneath the western part of the Intermontane Belt on the northern profile of the two and beneath the Omineca Belt. This conclusion is though counter to indications from topography; the higher relief of the Omineca Belt compared to the lower relief of the Intermontane Belt, given the flat Moho at the same depth beneath both of them, infers thinner lithosphere beneath the Omineca than beneath the Intermontane Belt. Cleary more work is required to reconcile all of these observations, and this is best done in a self-consistent, petrological–geophysical reference frame, such as was recently performed for Ireland (Fullea et al. 2014; Jones et al. 2014) using the LitMod approach (Afonso et al. 2008; Fullea et al. 2009).

Electrical parameters: bulk resistivity, dimensionality, geoelectric strike, anisotropy, and integrated conductivity

The most dominant electrical parameter that can be deduced from the Earth's surface by MT is the depth-integrated conductivity — or conductance — given by thickness times conductivity (i.e., thickness divided by resistivity) between two depths (Weidelt 1985). This is particularly true in one-dimensional (1-D) for a conductive layer sandwiched between two resistive ones, where the conductance of the layer is well resolved, and the resistance (resistivity–thickness product) is poorly resolved (Edwards et al. 1981; Jones 1982). Generally though, we attempt to determine bulk isotropic electrical resistivity (more precisely, log(resistivity) or equivalently log(conductivity)). One-, two-, and three-dimensional models of the electrical resistivity are mostly derived formally from magnetotelluric data in terms of isotropic layers (one-dimension) or blocks (two- or three-dimension) of resistivity, and some anisotropic modelling/inversion methods are available.

Depth of penetration

Some MT practitioners display maps of various MT response parameters at a given period, with the notion that period is a proxy for depth given the skin depth relationship. However, electrical resistivity varies over many orders of magnitude, and hence depth of investigation at a given period varies significantly over large regions due to crustal and mantle conductivity variations. This is shown in Hamilton et al. (2006) for South Africa, Miensopust et al. (2011) for Botswana, and Adetunji et al. (2014) for Ontario. An example of the dangers in using period as a proxy for depth is the interpreted imaging of the asthenospheric flow direction beneath Scandinavia from MT phases at a period of 2049 s by Bahr and Simpson (2002), whereas these long-period MT phase anisotropy effects were shown to be due to crustal artefacts by Lahti et al. (2005). In addition, if there is significant difference in the resistivity in orthogonal lateral directions, due to either extrinsic (structure) or intrinsic (grain) anisotropy, the two different modes of MT will sample different depths at the same period (Jones 2006).

For Canada, the scale of the problem can be appreciated by plotting an estimate of the depth of penetration for various periods. This depth is derived from the skin depth of the rotationally-invariant Berdichevsky arithmetic average of the off-diagonal elements at each site. The maps, generated using the same GMT algorithms and parameters as all other maps, are shown in Figs. 3a–3d for 10, 100, 1000, and 10 000 s period, respectively. The colour scale is logarithmic depth (in km), from 10 km (red) to 1000 km (purple), with 100 km in green–blue. Note that penetration is far more limited in Western Canada compared to on the Canadian Shield. This is a consequence of the more conducting crust, particularly within deep sedimentary basins, and of the shallower asthenosphere. At 10 s period (Fig. 3a), average penetration in the Prairies is <10 km, whereas in NW Ontario it is >150 km. Similarly, at 1000 s period (Fig. 3c), penetration for most of the Canadian Shield is in excess of 300 km, whereas for North Dakota, due to the presence of the North American Central Plains conductor that has conducting elements both in the crust and in the mantle (Jones et al. 2005a), penetration is only of order 70–80 km. Surprisingly, penetration in northern BC and much of the Yukon is also limited, but conducting crust is noted in the formal two-dimensional (2-D) modelling of the MT data in Jones et al. (2005b). At 10 000 s period (Fig. 3d), average penetration is more uniform at 300–400 km, except for the shallower penetration in North Dakota and the far greater penetration in the northern Arctic.

To counter these effects to first order, we construct the images based on an approximate transformation from MT response parameters (apparent resistivity and phase) versus period to approximate resistivity and approximate depth using the Niblett–Bostick transformation (Niblett and Sayn Wittgenstein 1960; Bostick 1977;

Fig. 3. (*a*) Penetration depth of the averaged impedance at 10 s period. (*b*) Penetration depth of the averaged impedance at 100 s period. (*c*) Penetration depth of the averaged impedance at 1000 s period. (*d*) Penetration depth of the averaged impedance at 10 000 s period.

a   DepAV 10 s depth penetration map

b   DepAV 100 s depth penetration map
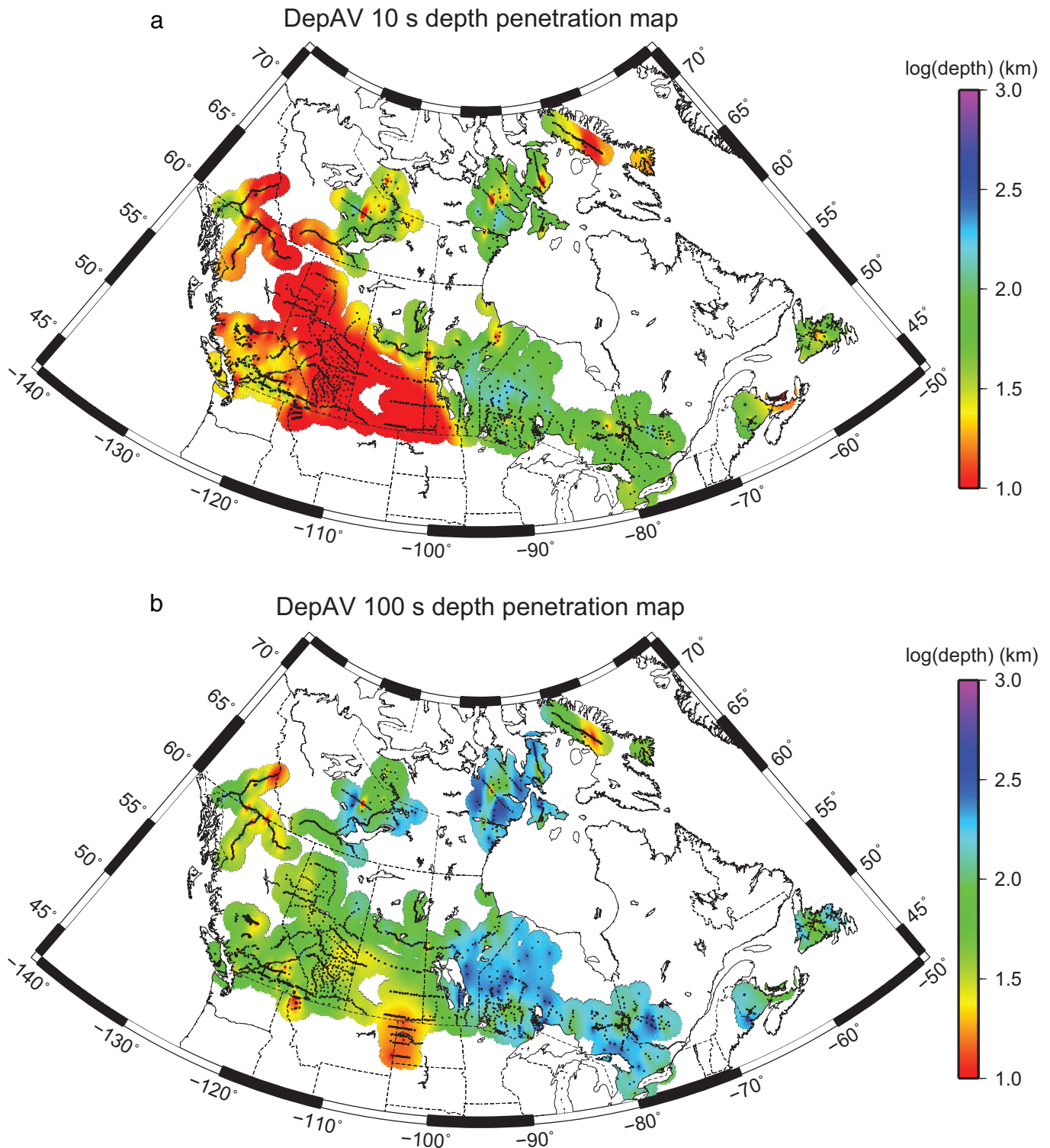
Jones 1983). This transform takes the apparent resistivity and phase data as a function of period, and converts it to approximate depth by

$$\rho_{NB}(h_{NB}) = \rho_a(T)\left(\frac{\pi}{2\phi(T)} - 1\right) \quad \text{and} \quad h_{NB} = \sqrt{\frac{\rho_a(T)\,T}{2\pi\mu_0}}$$

where T, $\rho_a(T)$ and $\phi(T)$ are the data, namely the apparent resistivity and phase at period T, μ_0 is the free space permeability, and ρ_{NB} and h_{NB} are the transformed data, namely the Niblett–Bostick (NB) resistivity ρ_{NB} at Niblett–Bostick depth h_{NB}. It must be appreciated that this is an approximate transformation from period to depth; it is not a formal inversion but one that performs remarkably well.

Fig. 3 (*concluded*).

c   DepAV 1000 s depth penetration map

d   DepAV 10000 s depth penetration map
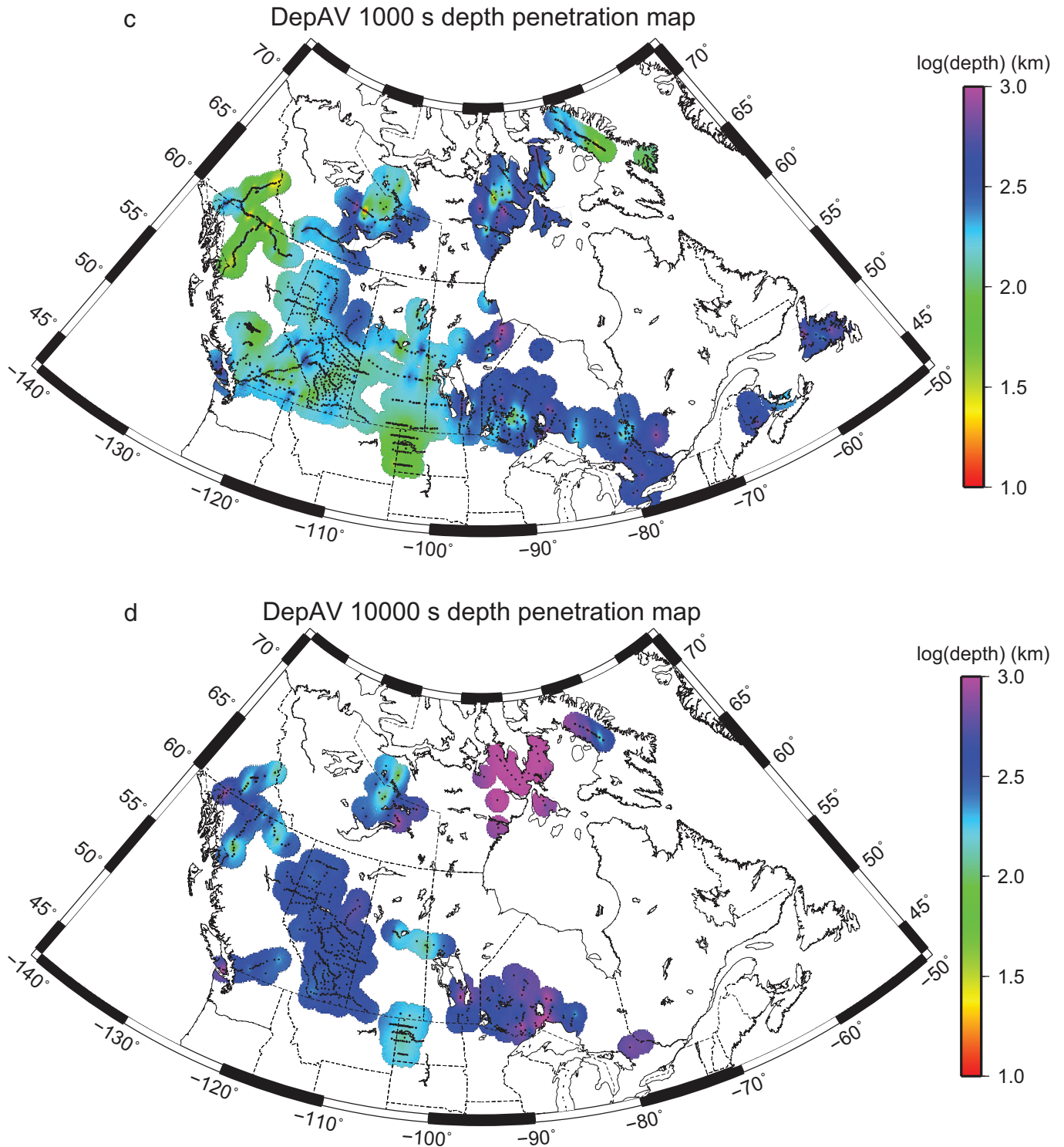
An example of the depth transformation is shown in Fig. 4. The black line is the true layered-Earth model, whereas the red stepped line is the NB transform of synthetic data generated from the true model. Less resistive (i.e., conductive) regions are easily identified on the NB transform, but the resistivity of resistive regions is typically underestimated. This is, however, a general problem of the "masking" effect in MT data whereby the parameters of a resistive region below a conductive one are difficult to determine (Jones 1999a).

An example of the transformation on real data is shown in Fig. 5, which displays MT data from one site in North Dakota both in standard form (Fig. 5A) and against NB depth (Fig. 5B). It must also be appreciated that this is a 1-D approximation applied to a three-dimensional (3-D) world, but comparisons show that this approximate imaging usually yields resistivity estimates that are generally within half an order of magnitude or less of the resistivity derived through more exacting modelling and inversion. An

Fig. 4. One-dimensional resistivity–depth model of the Earth (black line) and the Niblett–Bostick transformation of synthetic data generated from it (red stepped line).

Niblett−Bostick Transform Model
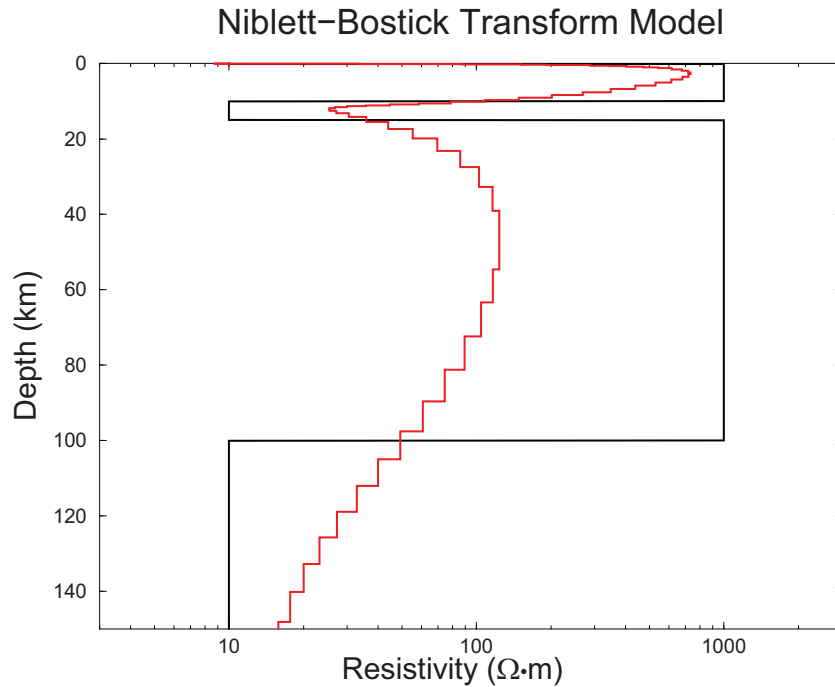
Fig. 5. (A) MT data, plotted in conventional log(period) format, from above the North American Central Plains conductivity anomaly showing the large difference in response between the along-strike currents (TE-mode, full circles; TM-mode, open circles) and the across-strike currents. Data at 300, 1000, and 3000 s are highlighted using oppositely-filled circles. (B) The same data after Niblett–Bostick transformation into approximate depth. Data for the two modes have dramatically different depth sensitivity, with the TE-mode responses stalled in the crust due to the presence of the crustal conductors.
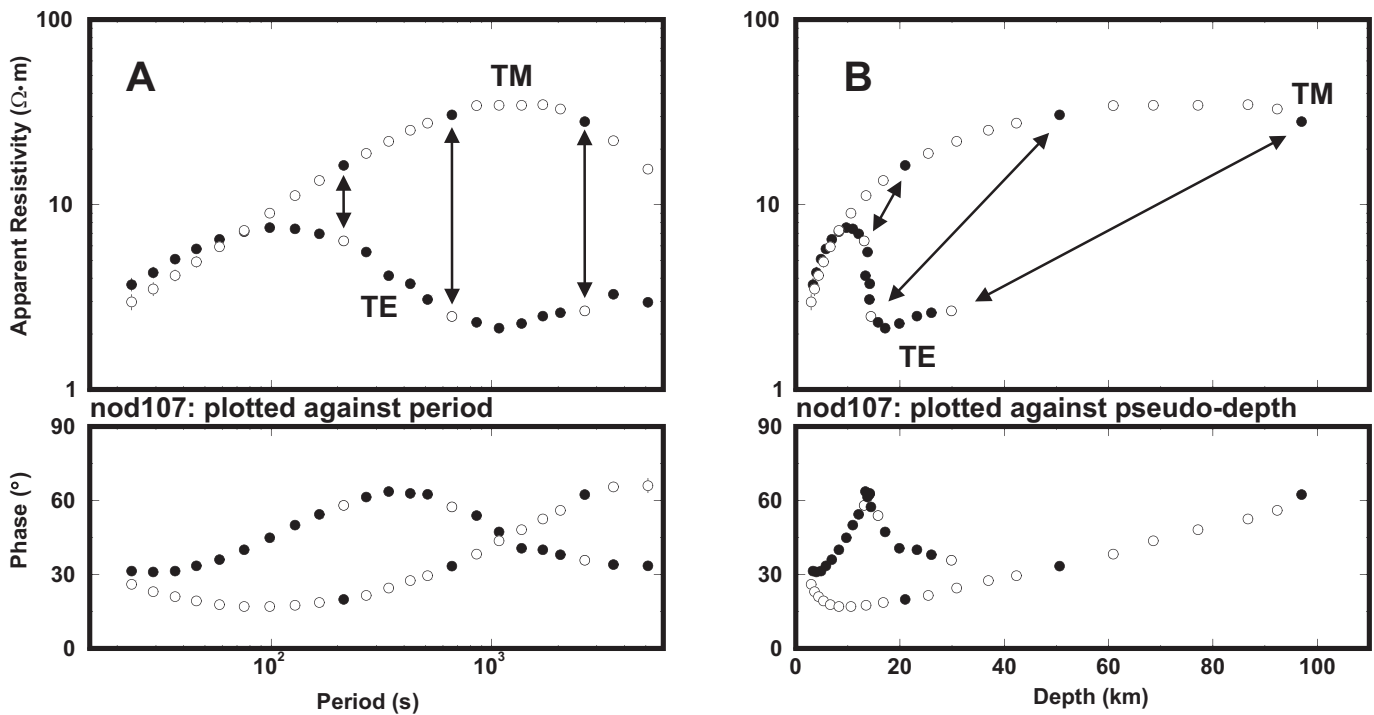
example is given in Jones et al. (2013) for locations in southern Africa where the approximate mapping approach yielded resistivity estimates within errors of those derived from 1-D and 2-D inversion. Of course there is no substitute for precise 3-D model-ling for confidence in the modelled resistivities, but approximate

imaging is highly useful at the regional scale for identifying large-scale features. Note that the NB estimated resistivity is biased to be an *overestimate* for conducting regions, and an *underestimate* for resistive regions, but this is similarly true of any Tikhonov-regularized smooth inversions in 1-D, 2-D and 3-D.

Fig. 6. Schematic diagram portraying the MT response at one frequency to the two quarter-space fault model. The variations of the TE (red symbols) and TM (blue symbols) modes across the fault for a given frequency are shown. On the more conductive side of the fault, the TM mode apparent resistivity is the more conductive, whereas on the resistive side of the fault, the TE mode apparent resistivity is the more conductive. This results in the more conductive directions being parallel to the geological strike on one side of the fault (the resistive side), and perpendicular on the other (the conductive side). ρ, resistivity.
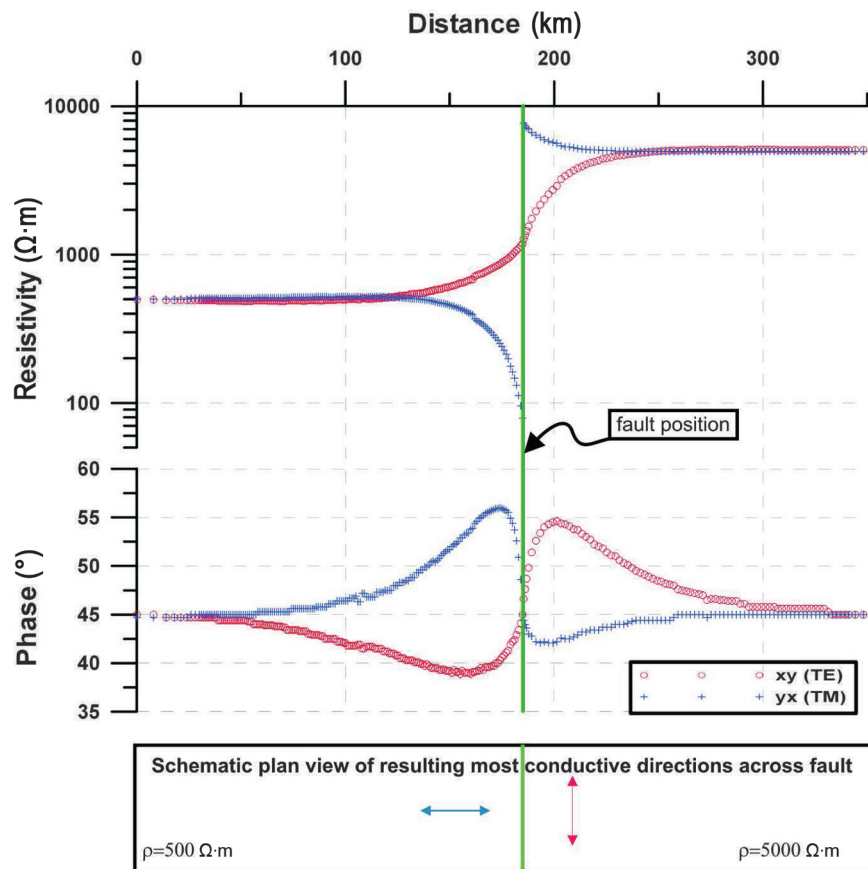
We show image maps of estimated bulk resistivity, dimensionality, geoelectric strike, and a measure of anisotropy for certain depths, and maps of the integrated conductivity between two depth ranges. The depths we have chosen are 20, 40, 100, and 200 km. The first is approximately the middle of the crust and the second is the approximate base of the crust, i.e., depth to the Moho, for much of Canada. The third is in the middle of the lithospheric mantle, and the fourth within the lower lithosphere for much of Canada, and in the asthenosphere for some parts. For integrated conductivity we show two depth ranges, 0–40 km, i.e., the crust, and 40–200 km, i.e., the mantle lithosphere.

Bulk resistivity and anisotropy direction

For bulk resistivity, the parameter we choose to present is the maximum resistivity (RhoMAX) at each site at the particular depth. This is obtained by rotating the apparent resistivity and phase data through 180° in 1° increments, deriving the NB transformed resistivity–depth data at each angle, storing the resistivity value at the desired depth, and, from the ensemble, determining the largest value of resistivity at the specified depth and the direction of that maximum value. This maximum resistivity is robust in that it is only affected by significant conductivity bodies, and will lead to conservative maps. In contrast, the minimum resistivity (RhoMIN) is highly sensitive to noise, distortion, and dimensionality as the electric fields are far smaller than in the RhoMAX direction.

The RhoMAX direction for most localities is parallel to one of the axes of the phase tensor (Caldwell et al. 2004); thus, the maps

of RhoMAX directions are not too dissimilar to maps of phase tensor directions. This is due to the galvanic distortion effects generally operating in a statistical manner, and the averaging procedures used reduce their effects. Herein we plot the phase tensor direction maps, to avoid any potential criticism related to residual effects of galvanic distortion. We plot the direction of the major axis of the phase tensor ellipse. However, this direction changes by 90° when crossing a strong contrast in resistivity. This is because on the *conductive* side of a discontinuity, the most conductive, or least resistive, direction is given by the mode in which currents are flowing *perpendicular* to structural strike, the so-called Transverse Magnetic (TM) mode in magnetotellurics, whereas on the *resistive* side of a discontinuity, the most conductive direction is given by the mode in which currents are flowing *parallel* to strike, the Transverse Electric (TE) mode. This is illustrated in Fig. 6. To account for this behaviour in our anisotropy azimuth maps, we rotate through 90° rather than 180°.

Anisotropy magnitude

Over the last decade, there have been significant efforts made by EM practitioners to try to determine electrical anisotropy of subsurface structures, and to differentiate between anisotropy and structure (Wannamaker 2005). Whether the anisotropy is intrinsic, as in due to differences in resistivity along various grain axis, or extrinsic, as in due to, for example, repeated interlaying of resistive and conductive sequences, is often impossible to differentiate given the spatial resolving kernels of EM data. An example of the former is olivine anisotropy, with a factor of three between

Fig. 7. Crustal conductance map of Canada showing total averaged conductance in the top 40 km.
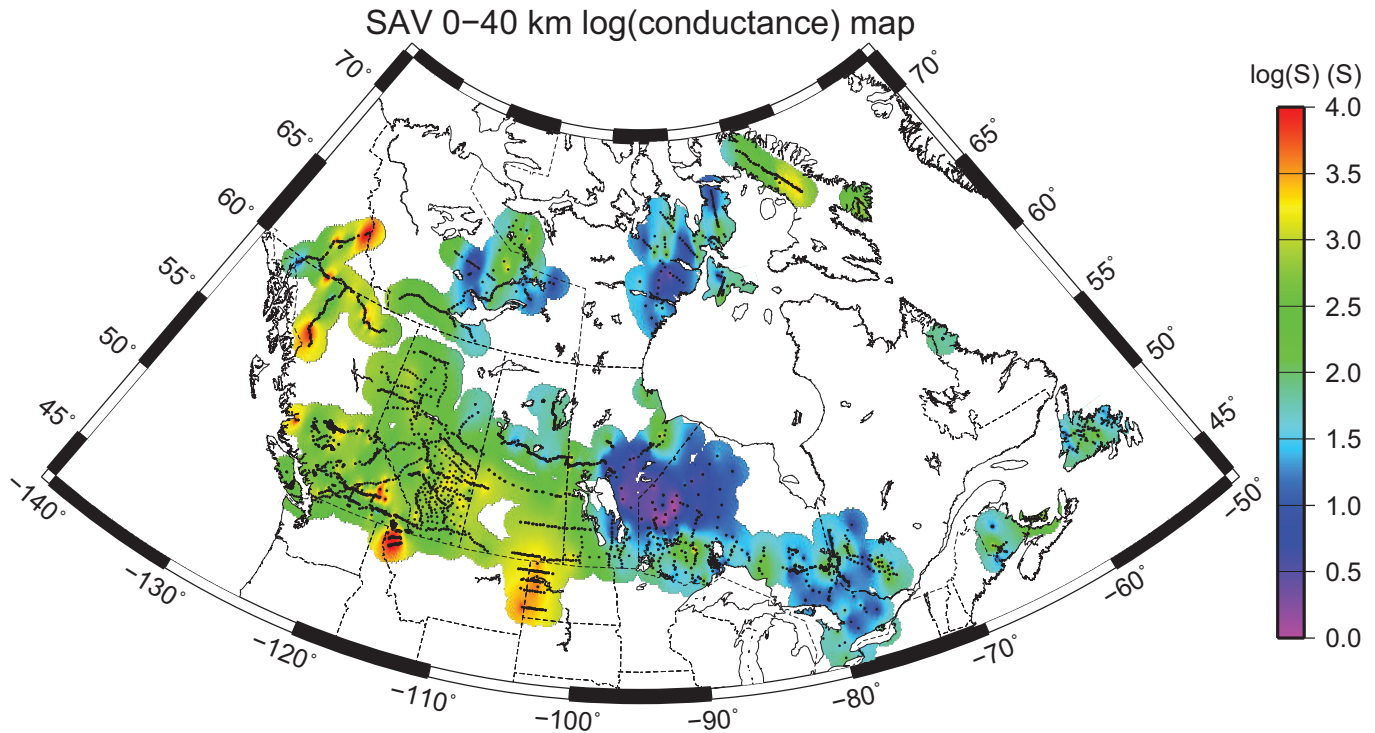
the most conductive (*c*-axis) compared to the least conductive (*a*- and *b*-axes) directions in "dry" olivine (Xu et al. 2000; Du Frane et al. 2005), but this anisotropy can rise to two orders of magnitude due to hydrogen diffusion if the olivine is "wet" (Kohlstedt and Mackwell 1998; Wang et al. 2006; Poe et al. 2010), although there is significant debate between the laboratories that make these difficult proton conduction measurements (Jones et al. 2012). Regardless of which water model is correct, the dominance of the effect has led to the suggestion that deep-probing EM is the optimum method to deduce the amount of water in the mantle (Karato 2006), and an example of applying this to a subcontinent is shown in Jones et al. (2013) for southern Africa.

An estimate of the sensitivity of the maximum resistivity to direction is obtained from mapping anisotropy magnitude. The anisotropy at a given depth was derived from determining the maximum NB resistivity at that depth, and determining the NB resistivity in the direction 90° from it, and computing the anisotropy as

$$\text{Anisotropy} = \log[\rho_{NB}(h, \Theta_{max})] - \log[\rho_{NB}(h, \Theta_{max} + 90)]$$

where h is the desired depth, and Θ_{max} is the direction of the RhoMAX direction. A value of one in anisotropy means that log(RhoMAX) is one order of magnitude larger than log(RhoMIN). Note that this value is derived from NB resistivities at *different* periods for each site and for each of the two directions at any one site, to address the issue illustrated in Fig. 5B and discussed by Jones (2006). For this value to be computed, then there has to be penetration to the required depth in both the RhoMAX direction and the direction perpendicular to it (not necessarily the RhoMIN direction, although for most sites this is the case). This anisotropy is a measure of the true electrical anisotropy, and cannot be separated into either macro, i.e., structural, or micro, i.e., grain boundary, anisotropy; other information must be used to distinguish between these two. Also, as RhoMAX is generally an underestimate of the true maximum resistivity of a resistive region, and RhoMIN is generally an underestimate of the true conductivity

(overestimate of the true resistivity) of a conducting region, then this anisotropy measure is generally a minimum estimate of the true electrical anisotropy.

Conductances

Finally, the conductance value for each site and each depth range is derived by converting the NB resistivity–depth profile into a layered Earth profile and summing the conductances of each layer between the depths of interest.

Map construction

Maps of Canada displaying electrical parameters were generated from the Canadian MT database using GMT (Wessel and Smith 1991, 1998). Maps of the same or similar responses for specific regions of Canada have been presented in the past for southern BC (Jones and Gough 1995), the Trans-Hudson Orogen (Jones et al. 2005*a*), and the SNORCLE transect region (Jones et al. 2005*b*), and the same procedure is followed here, with the addition of calculation of 5° averages. The parameters estimated are $\log_{10}$(NB resistivity), anisotropy, and conductance.

1. Spatial smoothing using median filter routine *blockmedian* with an increment of 30 min.
2. Creating an interpolated grid from the median smoothed data using a continuous curvature gridding algorithm *surface* with a 10 min grid spacing and a tension of 0.5.
3. The grid is plotting using *gridimage*.
4. For regional estimates, the data are spatially smoothed using *blockmedian* with an increment of 7.5° in longitude and 5° in latitude, and are plotted using *psxy*.

Continental electrical parameter maps of Canada

Canada's crust

Crustal conductance

The crustal conductance map for 0–40 km is shown in Fig. 7, where the conductances have been derived from the arithmetical (Berdichevsky) average at each site. The crust of NW Ontario (NW

Fig. 8. Bulk log(resistivity) at (*a*) 20 km and (*b*) 40 km (approximately the middle and the base of the crust for much of Canada). Also shown on the 40 km map are the temperature (Temp) estimates from model TC1 of Artemieva (2006).
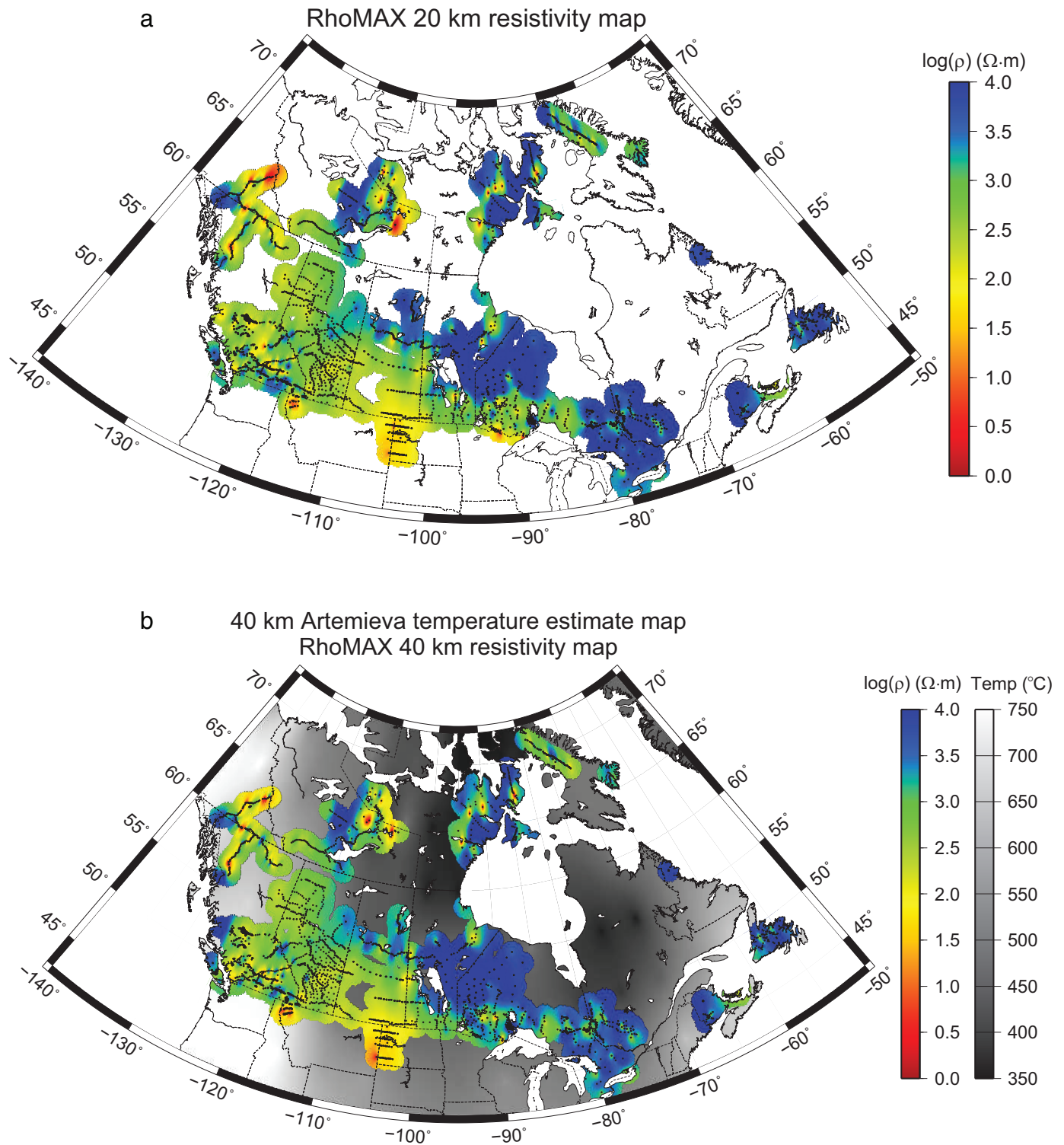
Superior Shield) and northern Hudson Bay (Rae Craton) exhibit the lowest conductances in Canada, with average total crustal conductance of <3 S, which is the expected value for dry crustal rocks at low-temperature conditions without any conducting components in the crust. The highest conductances are observed in North Dakota (NACP crustal anomaly) and in NW Montana (Flathead Basin). Generally, conductance is low on the Canadian

Shield, and higher off it, both to the west (Cordillera) and east (Appalachians).

Crustal resistivity

Bulk crustal resistivity at 20 and 40 km is shown in the maps of Fig. 8; the 40 km map (Fig. 8*b*) additionally shows the temperature estimates from the TC1 model of Artemieva (2006) at that depth.

Fig. 9. Crustal anisotropy at (*a*, *b*) 20 km and (*c*, *d*) 40 km. Anisotropy directions are shown in (*a*) and (*c*), and anisotropy strength in (*b*) and (*d*). Also shown on the anisotropy direction maps are median directions (black arrows, scaled by the arrow in the bottom left corner that signifies one decade of anisotropy strength) and median crustal stress directions (green arrows). Max. hor., maximum horizontal; TN, True North.
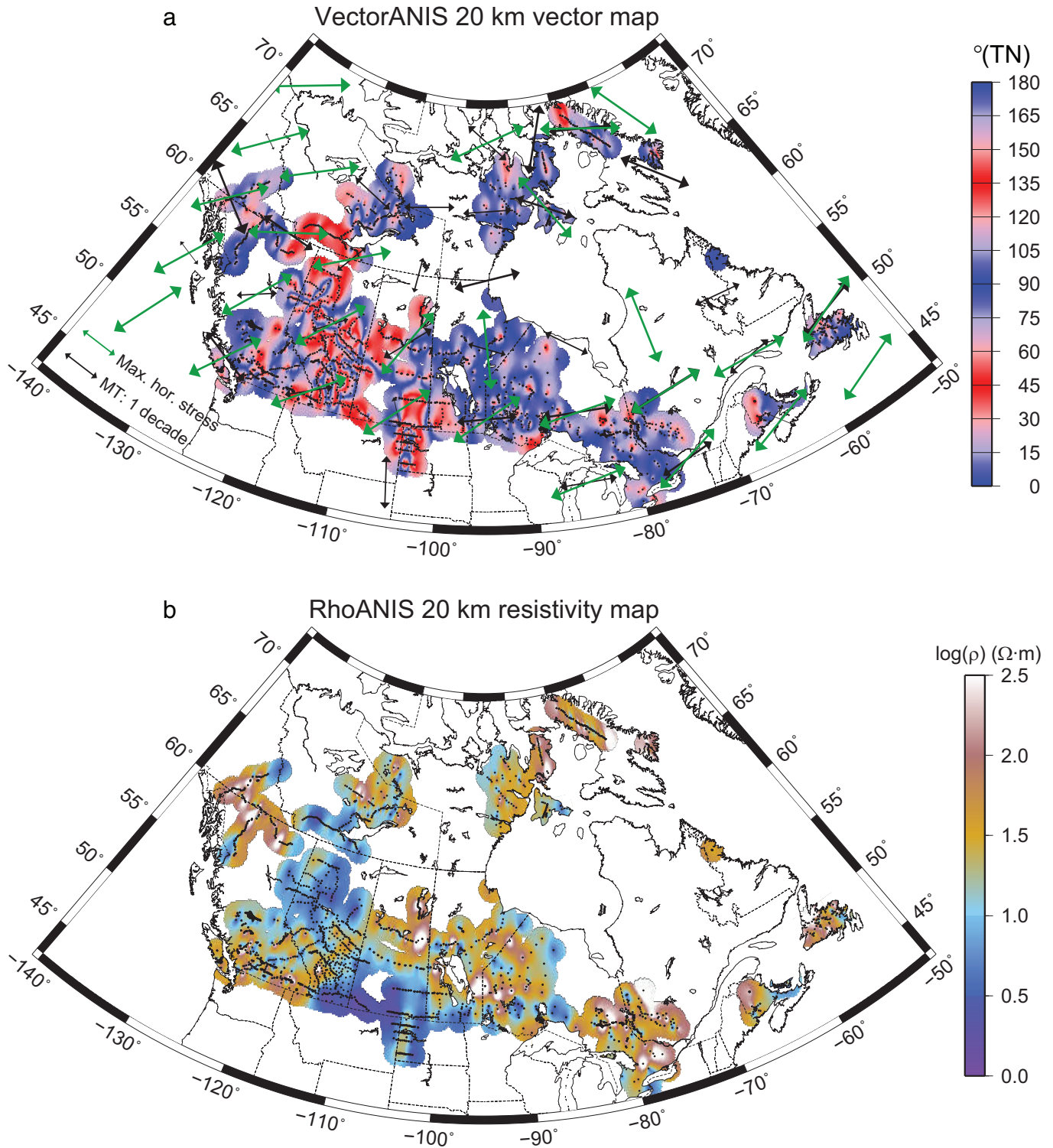
Generally, as is to be expected, the crust of the Canadian Shield is far more resistive than the crust beneath the Cordillera, with the exception of the westernmost parts of BC, including Vancouver Island. Crustal resistivity also spatially correlates, to first order, with the temperature model. Local crustal anomalies are identified within the Canadian Shield, as is the highly-conducting NACP within the Trans-Hudson Orogen.

Crustal anisotropy

Crustal anisotropy is shown in the four maps of Fig. 9 that depict anisotropy direction and strength at 20 km (Figs. 9*a*, 9*b*) and 40 km (Figs. 9*c*, 9*d*) depths. Also plotted on the maps are the median-averaged stress vectors from Fig. 2*b* (plotted as red vectors in Fig. 2*b* but as green vectors on Figs. 9*a* and 9*c*). As noted earlier in the text, due to the "flip" of 90° in direction at a

Fig. 9 (*concluded*).

c VectorANIS 40 km vector map

d RhoANIS 40 km resistivity map
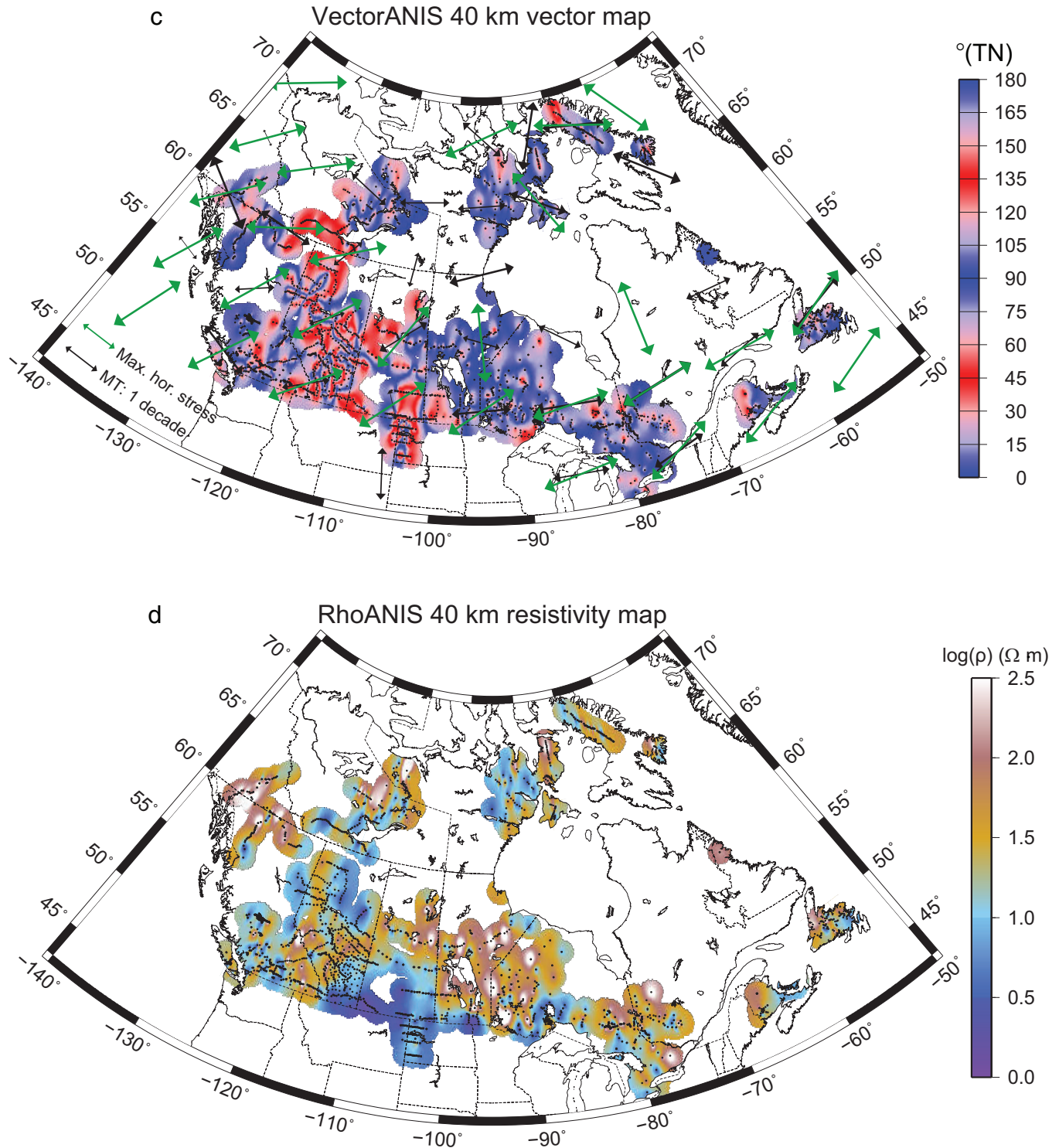
vertical interface, the anisotropy directions are plotted with a 90° repetition rate, so that blue indicates NS and EW, and red indicates NE–SW and NW–SE. The overall pattern is of EW on much of the exposed Canadian Shield and NE–SW beneath western Manitoba and North Dakota, northern Saskatchewan, Alberta, and BC, except for the western part of BC which is EW. These directions generally parallel the measured crustal stress directions. This may be an artefact of sampling bias, or it may indeed signify that crustal electrical anisotropy is caused by

alignment of conducting features structurally controlled by the prevailing stress direction rather than being controlled by prevailing stress directions during formation and prior deformation.

Canada's mantle lithosphere

Canada's mantle lithosphere varies in thickness from its greatest extent below Hudson Bay to its thinnest beneath the Cordillera (Fig. 2*e*). Its tectonic age also presumably varies from

Fig. 10. Lithospheric mantle conductance, i.e., the depth-integrated conductivity from 40 to 200 km, in log units. Olivine-dominated dry cratonic lithosphere would have a value of the order of 12 S (1.1 log units).
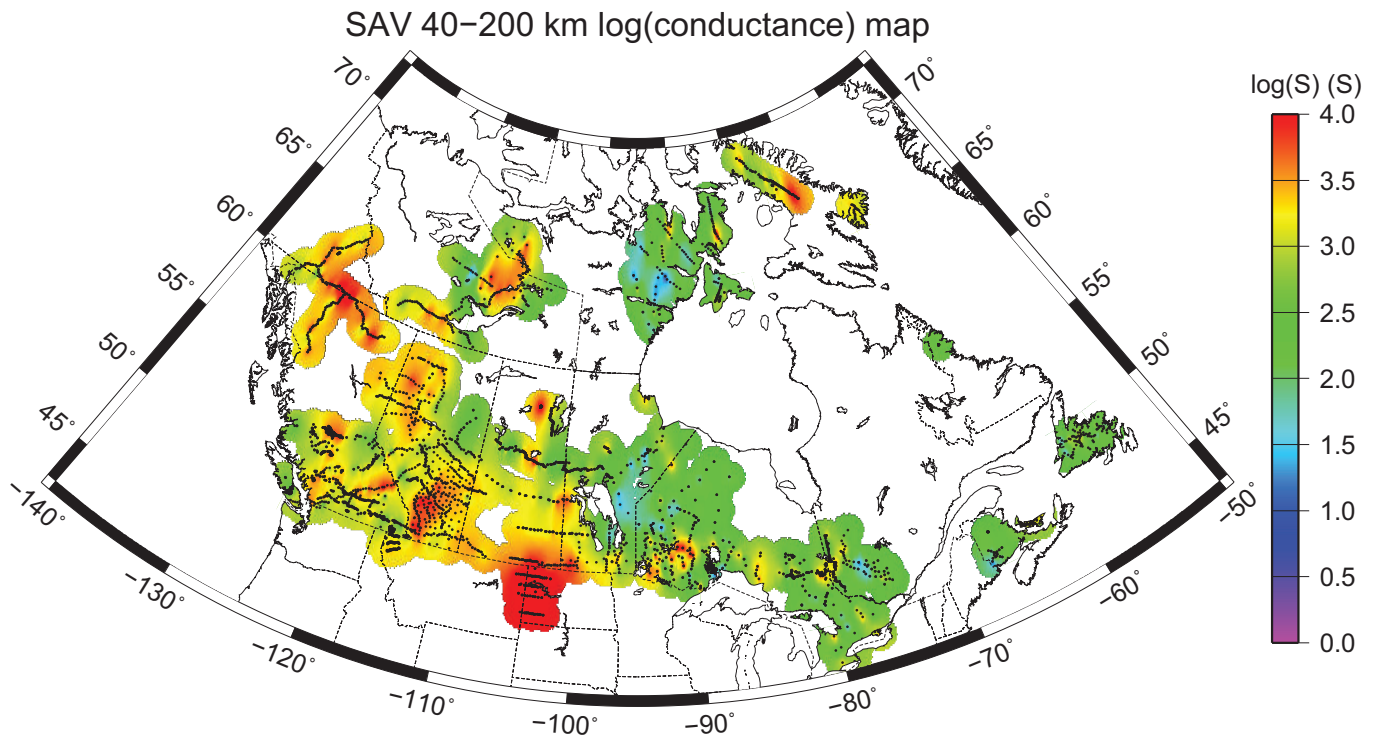
Archean to Phanerozoic, consistent with surface geology shown in Fig. 1*c*.

Mantle lithosphere conductance

The rotationally-invariant integrated lithospheric conductance from 40 to 200 km is plotted in Fig. 10. The depth-integrated conductance for dry, olivine-dominated cratonic lithosphere is of the order of 12 S (blue), i.e., If a dry olivine-dominant mineralogy and a cratonic geotherm are assumed, then laboratory studies suggest that the sum of the conductance in the lithospheric mantle would be of the order of 12 S (e.g., Jones et al. 2013). The only significantly sized coherent regions that have conductances close to this value are parts of the Rae Craton. Otherwise, there is additional conducting material present, which may be either electrically isotropic or anisotropic.

Mantle lithosphere resistivity

The bulk lithospheric mantle resistivity is represented in the two maps of maximum resistivity at 100 km depth (Fig. 11*a*) and 200 km (Fig. 11*b*). Also plotted on the maps are the contoured temperature estimates of Artemieva (2006) (note the different temperature scales). The Canadian Shield is generally cold and resistive, the one main exception being the centre of the Slave Craton, with its Central Slave Mantle Conductor at mid-lithospheric depths (Jones et al. 2003). The dominant mantle anomaly in the rest of Canada is that of the North American Central Plains conductivity anomaly lying within the Trans-Hudson Orogen and associated with the putative Sask Craton (Jones et al. 2005*a*). There is also some variation within Alberta — there seems to be a zone of low resistivity beneath the Archean Loverna Block — compared to the younger Proterozoic regions northwest of the Snowbird Tectonic Zone. This was noted originally by Boerner et al. (1995) based on 2-D TM-mode only inversions. A much more complete study by Nieuwenhuis et al. (2013), using an array of long-period MT stations and 3-D inversion, confirmed this result with the boundaries

of the low-resistivity Loverna Block coinciding with the Snowbird Tectonic Zone on the NW and Vulcan structure on the south side.

Mantle lithosphere anisotropy

Mantle anisotropy directions, shown in Fig. 12*a* (100 km) and Fig. 12*c* (200 km), are generally more complex than in the crust, and for the most part are parallel or sub-parallel to the averaged SKS directions and absolute plate motion (APM) directions. This supports the notion that the lower mantle and asthenospheric fabric directions should parallel the APM. That this also appears to be true at 100 km depth for the Canadian Shield is a quandary, as one would expect fossil directions to dominate. Again, this may be sampling bias, but it is an observation that is worthy of further investigation.

Temperature and water content estimates in the middle and base of mantle lithosphere

We can determine ambient temperature from electrical resistivity, given the exponential effect of temperature on resistivity, if we know the mineral composition of the mantle (a second-order effect) and water content of these minerals (Fullea et al. 2011; Jones et al. 2013), and there is no contribution to conduction from exotic minor phases, such as carbon in graphite form (Duba and Shankland 1982; Jones et al. 2003) or sulphides (Ducea and Park 2000). These are reasonable assumptions for cratonic mantle lithosphere (Jones et al. 2009), and have been used by Ledo and Jones (2005) to put bounds on the temperature of the upper mantle beneath part of the Yukon, NW Canada (discussed later in the text).

Given olivine's dominance of mineral composition in the lithosphere, especially cratonic lithosphere, and that it lies virtually in the middle of the range of laboratory conductivity estimates for olivine, orthopyroxene, clinopyroxene, and garnet (e.g., Ledo and Jones 2005), we can use the olivine resistivity–temperature relationship to convert from resistivity to temperature. The dry

Fig. 11. Bulk log(resistivity) at (*a*) 100 km and (*b*) 200 km (approximately the middle and the base of the mantle lithosphere for much of Canada). Also shown on the maps are the temperature estimates from model TC1 of Artemieva (2006).
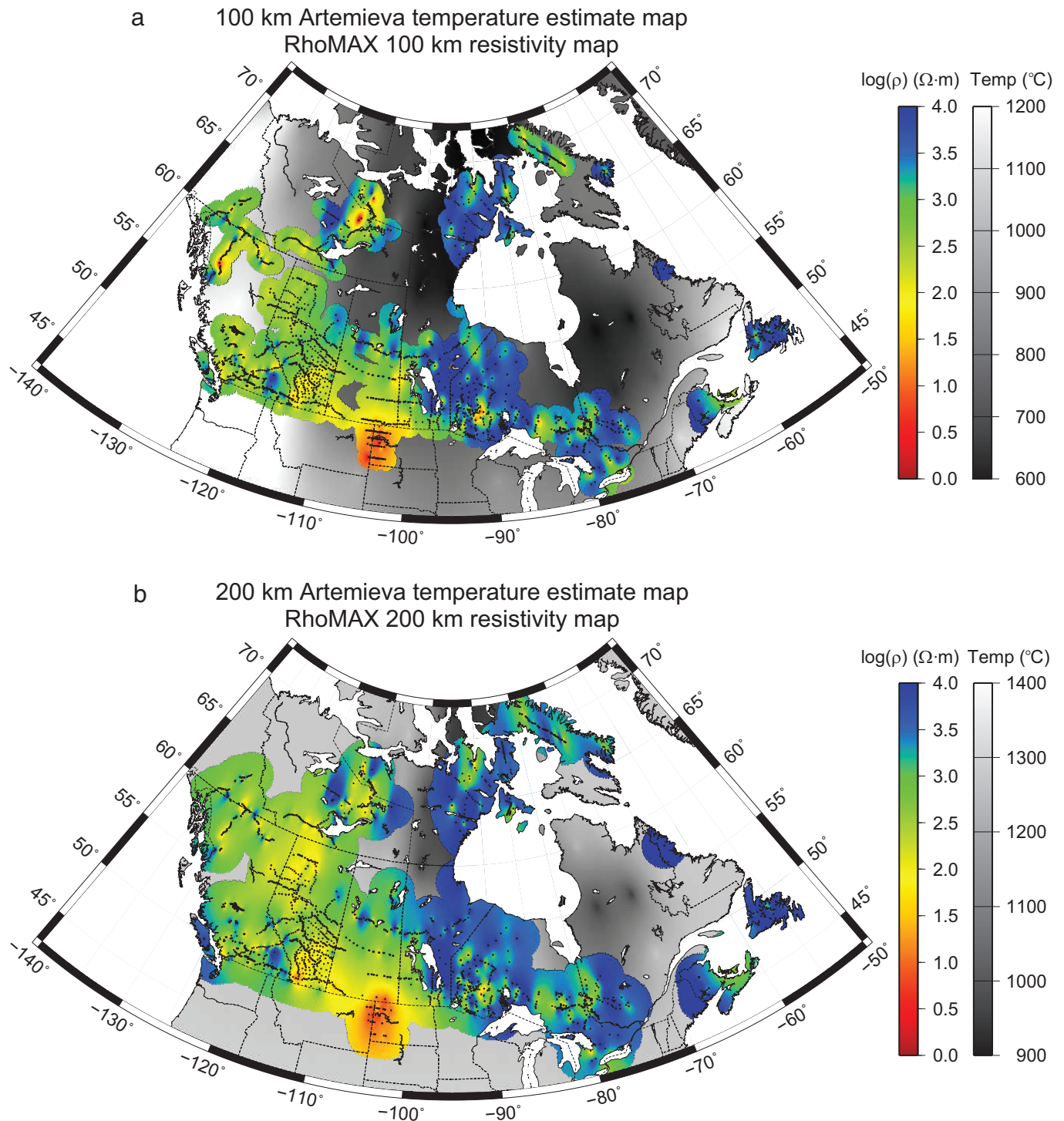
olivine resistivity–temperature relation for small polaron and magnesium vacancy conduction, derived using the formulae in Fullea et al. (2011), is shown in Fig. 13 (solid black line). Also shown on Fig. 13 are the expected resistivities for wet olivine, with water in the matrix of the order of 15, 30, 50, 100, and 200 ppm, using the water model of Jones et al. (2012) that was derived based on fitting field observations. (Note that there is a vigorous debate in the literature between the laboratories making these measurements, and the three main laboratories of Karato, Yoshino, and Poe are not in agreement, and their results are very different from each other by orders of magnitude and do not agree with field observations; see Jones et al. (2012) for details.) The reasonable range of water contents in olivine is from almost dry up to 150 ppm or even 200 ppm, as observed in kimberlitic mantle xenoliths for the Kaapvaal Craton (Peslier et al. 2010; Baptiste et al. 2012), although recent results from Udachnaya on the Siberian Craton suggest anomalously high values of up to 325 ppm are observed at the base of the lithosphere (Doucet et al. 2013). Such high values in

Fig. 12. Lithospheric anisotropy at (*a*, *b*) 100 km and (*c*, *d*) 200 km. Anisotropy directions are shown in (*a*) and (*c*), and anisotropy strength in (*b*) and (*d*). Also shown on the anisotropy direction maps are median directions (black arrows) and median SKS directions (green arrows).
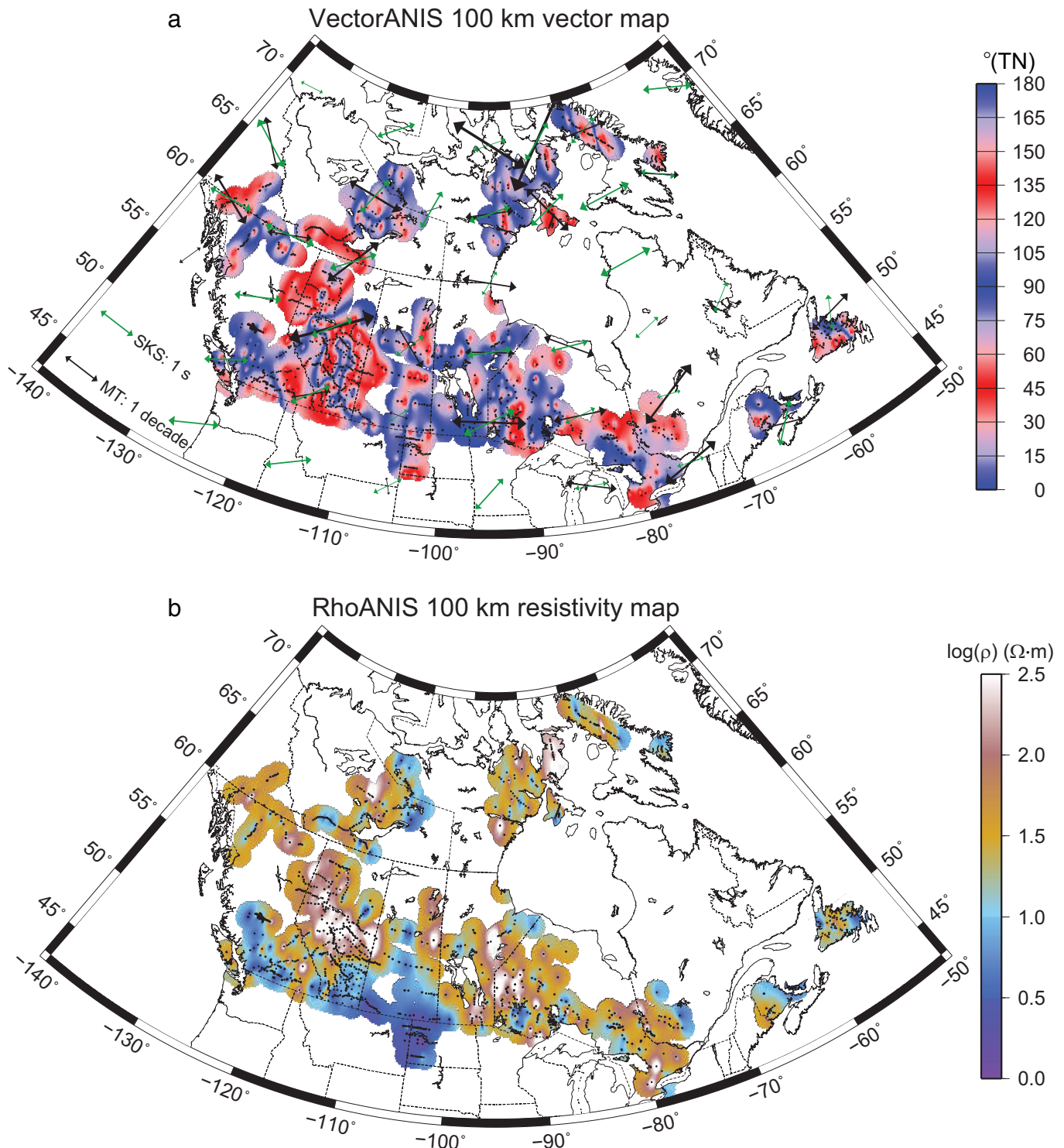
the lower lithosphere are though counter to the suggestion of the requirement of low water contents to ensure craton longevity (Peslier et al. 2010), and are unlikely to be representative of the bulk of the lithosphere. These water content values observed in cratonic lithosphere are certainly well below water saturation levels; the storage capacity of olivine is a function of pressure and at lithospheric pressures varies from 300 ppm at 40 km to 800 ppm at 100 km to 2000 ppm at 200 km (Hirschmann et al. 2005).

The point here is that our estimates of temperature based on a dry olivine composition provide a *maximum* bound on mantle temperature. For a given resistivity, temperature can be lower than that we estimate, i.e., above the solid black line in Fig. 13, but not higher (below it). Any additional conducting mechanism, due to water or melt or other phases, will result in lower estimates of resistivity, which implies higher estimates of temperature. Also, any bias in our estimate of resistivity of the lithosphere will be

Fig. 12 (*concluded*).

c VectorANIS 200 km vector map

d RhoANIS 200 km resistivity map
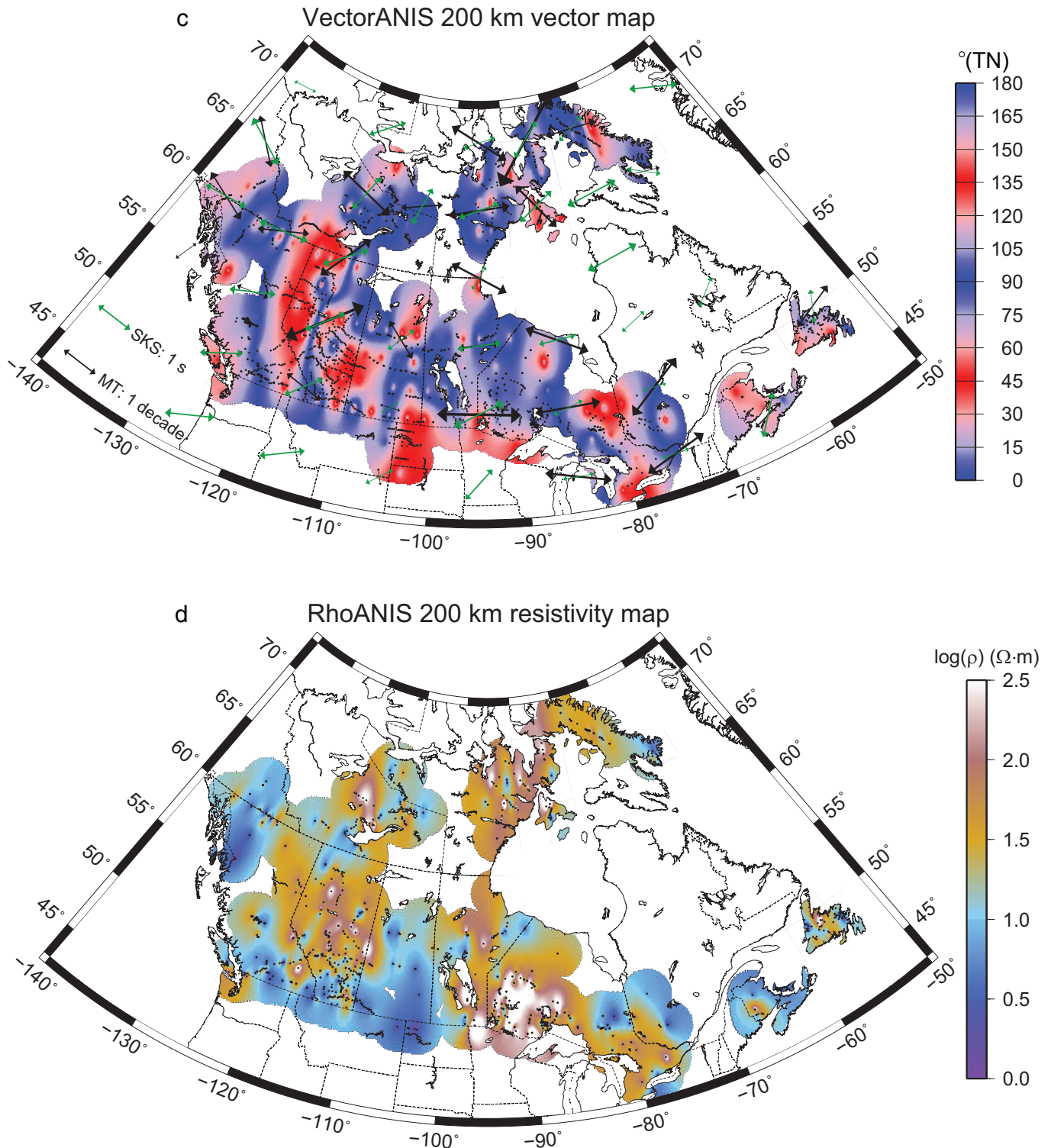
towards lower rather than higher resistivity (see Fig. 4 and earlier discussion), so again yielding an upper bound on temperature — it can be lower but unlikely to be any higher. Take for example a resistivity of 1000 Ω·m, this can be explained by dry olivine at a temperature of 1075 °C, or by wet olivine as cold as 700 °C for 200 wt. ppm water. The ambient temperature *cannot* be any higher than 1075 °C. Note the assumption we make here that our Rho-MAX estimates are the ones that are most likely to correctly

represent the thermal state, whereas the RhoMIN values are likely perturbed by additional conducting components to the host rocks.

That we derive maximum bounds on temperature from resistive zones was exploited by Ledo and Jones (2005) who demonstrated that the explanation of a seismic low-velocity compressional wave (Vp) anomaly detected with teleseismic studies in the upper mantle beneath the northern Canadian Cordillera in terms of elevated tempera-

Fig. 13. Log(resistivity)–temperature (*T*) relationships defined by pure olivine that is dry or contains 15, 30, 100, or 200 ppm water, including small polaron, magnesium vacancy, and proton conduction, using the equations given in Fullea et al. (2011) with the water model of Jones et al. (2012). The dots are the resistivity–temperature pairs for 100 km depth (red) and 200 km depth (black).

Olivine Resistivity-Temperature relationships
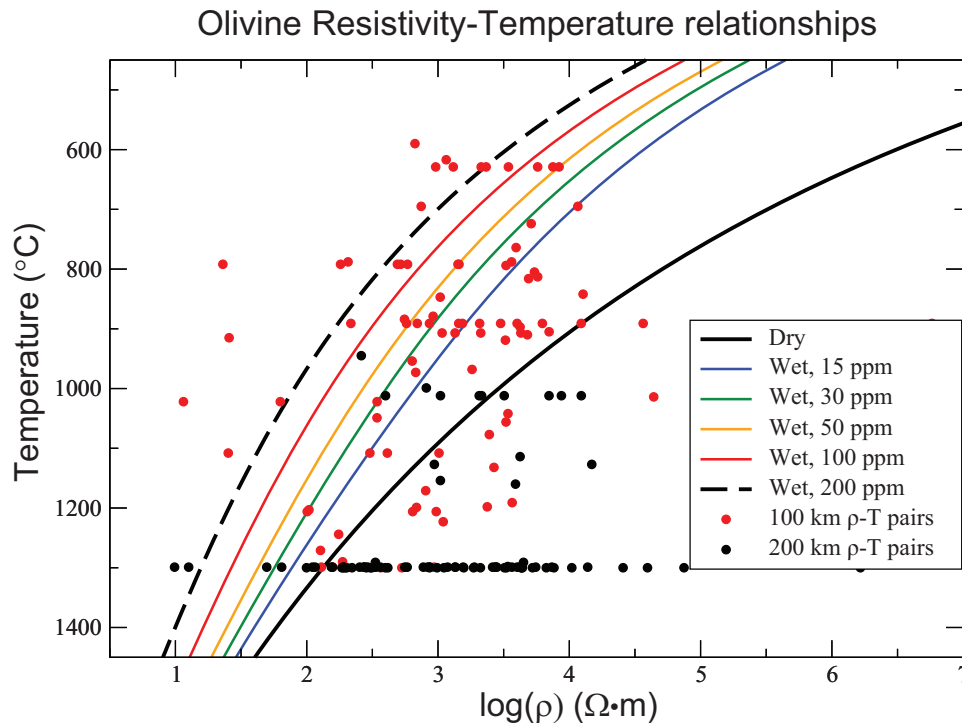
ture by Frederiksen et al. (1998) must be incorrect. The MT data does not allow the zone to be any hotter than 200 °C less than that interpreted from the seismic data.

In a similar manner, resistivity can place bounds on water content if the ambient temperature is known. For a temperature of 1000 °C, then dry olivine resistivity will be 3000 Ω·m, and the presence of water will reduce resistivity to a reasonable low of 150 Ω·m for 100 ppm water, and a maximum permissible low of 75 Ω·m for 200 ppm water (50 Ω·m for 325 ppm water, as recently reported for the base of the Siberian Craton (Doucet et al. 2013)). Any lower than that requires the presence of other conducting phases. If we know the ambient temperature and the resistivity, and the resistivity lies within the range of 80–3000 Ω·m, then we can estimate the amount of water in the olivine. A water content map of southern Africa was derived by Jones et al. (2013), who used seismological information on velocities to control the temperature. Here, we will use Artemieva's (2006) temperature estimates as our thermal calibration.

Resistivity-derived temperature estimates at depths of 100 and 200 km, using the conversion from resistivity to temperature for dry olivine shown in Fig. 13, are shown in Fig. 14*a* (100 km) and Fig. 14*b* (200 km). Figure 14*a* and 14*b* also includes the publicly-available mantle temperature estimates by Artemieva (2006) on a 5° × 5° grid (coloured circles). Plotted in Fig. 15 are cross sections from Vancouver Island to north of Ottawa along the swath shown in Fig. 1*b* of (*a*) the estimated resistivity, (*b*) temperature derived from resistivity using the dry olivine curve in Fig. 13, and (*c*) temperature estimated by Artemieva (2006).

From petrological and thermal considerations, the base of cratonic lithosphere is thought to be at the adiabat with temperature in the range of 1250–1350 °C (see, e.g., Artemieva 2009; Eaton et al. 2009). Dry mantle minerals in the temperature range 1250–1350 °C have a resistivity of the order of 100–250 Ω·m (Jones et al. 2009), whereas the asthenosphere is often observed with a resistivity of an order of magnitude less, around 5–25 Ω·m (e.g., Jones 1999*a*), so an additional conducting component is required and

this is generally thought to be either partial melting or increased water content (Hirth et al. 2000), or both. In either situation the transformation from resistivity to temperature based on the conductive, solid-state arguments used earlier in the text is invalid, and temperature estimates from resistivity >1400 °C are indicative of either the presence of water (within the limits shown on Fig. 13) or of exotic phases such as graphite (at depths above the graphite–diamond stability field) and sulphides.

At 200 km depth (Fig. 11*b*), electrical resistivities suggest that, generally, the exposed Canadian Shield is at a temperature of the order of 1000–1100 °C (Fig. 14*b*), which is consistent with a conductive cratonic geotherm for a lithosphere of approx. 250–260 km thickness and a moderate surface heat flow. Such a lithospheric thickness was found for the central part of the Slave Craton and the Superior Craton by Moorkamp et al. (2010) and Jones et al. (2003), respectively (stars in Fig. 2*e*). Coldest temperatures (850–950 °C), implying thickest lithosphere, is suggested for the region on the west side of Hudson Bay, consistent with the thermal modelling of Hamza and Vieira (2012), with the elastic thickness modelling of Audet and Mareschal (2004, 2007), and with the surface wave studies of Darbyshire and Eaton (2010). Western Canada is much warmer, with the exception of the Cascadia forearc region in southwest BC that is cold because of the currently active subduction of the Juan de Fuca plate, a component of the former, far larger Farallon Plate. The bright red anomaly beneath southern Saskatchewan, NW Dakota, and NE Montana is the mantle expression of the North American Central Plains anomaly discussed in Jones et al. (2005*a*), and is not a thermally-activated conduction process.

At 200 km depth, the estimates of Artemieva infer higher temperatures, by some 200 °C, for most of the Canadian Shield than do the MT data. It can be concluded that these estimates must be inaccurate, as they significantly exceed the MT estimates, which are, by their nature, maximum bounds. This is due to Artemieva's estimate of the LAB thickness being too shallow for much of the Canadian Shield. Similarly, Artemieva's estimates for SW BC are

Fig. 14. Temperature estimates based on the (*a*) 100 km and (*b*) 200 km resistivity maps of Fig. 11 and a dry olivine mineralogy mantle (Fig. 13). The coloured circles are temperature estimates from the global model of Artemieva (2006). The swath A–B shows the track of the section plotted in Fig. 15.

a RhoMAX 100 km temperature map

b RhoMAX 200 km temperature map
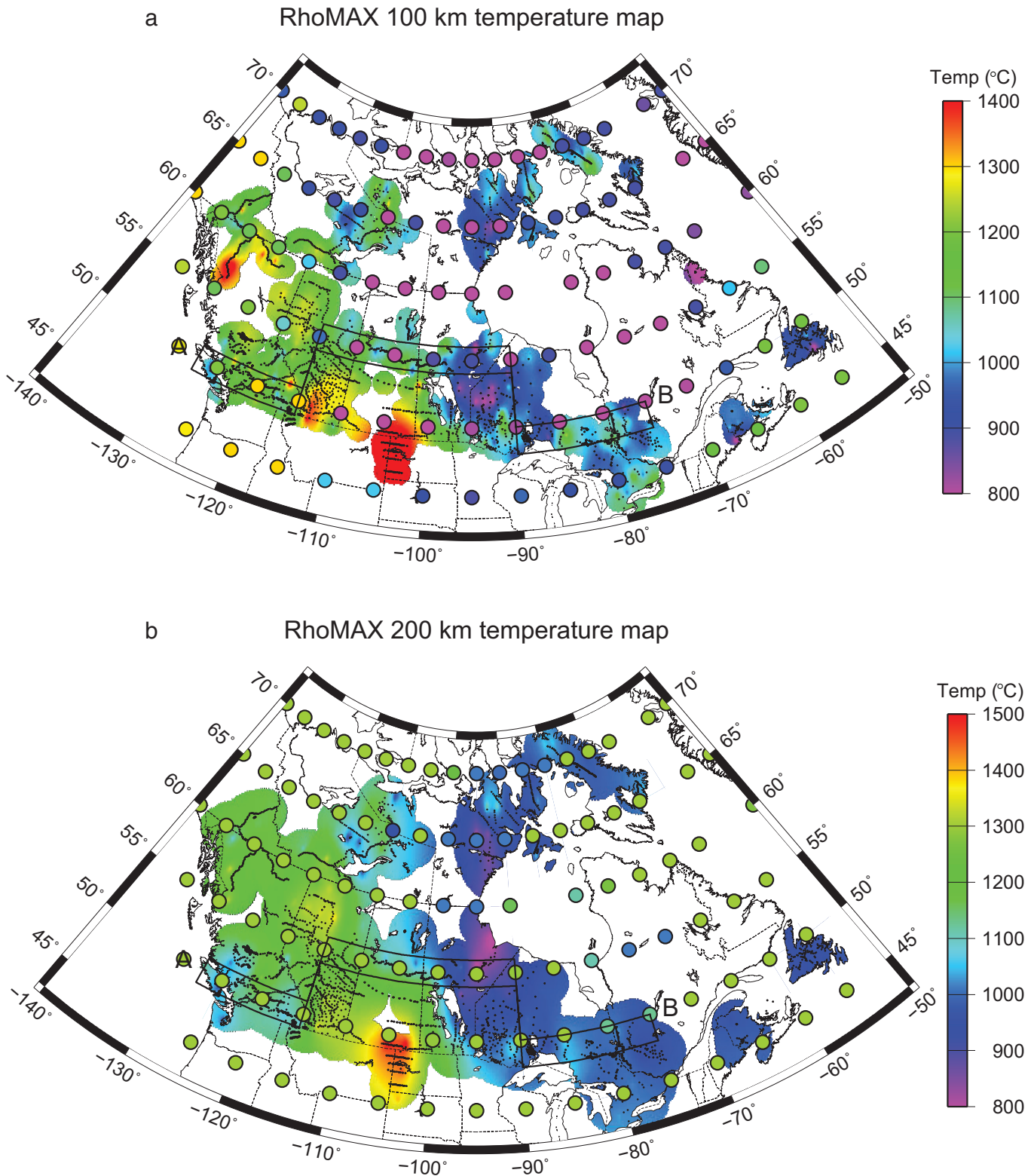
too high, and are inconsistent with the cold subducting slab. The MT data for the Churchill and Rae provinces and in northern Nunavut are consistent with Artemieva's low temperatures, which is complete coincidence, as there are no heat flow esti-

mates on the Canadian Shield north of 60° with the exception of three on the Slave Craton and one on northernmost Quebec (Fig. 16*a*), so Artemieva's estimates come from interpolation and extrapolation effects.

Fig. 15. Section of (*a*) resistivity, (*b*) temperatures implied from resistivity using dry olivine, and (*c*) Artemieva's temperature estimates, along the swath transect shown in Fig. 1*b*. Note the highly compressed resistivity scale in (*a*) from 300 to 30 000 Ω·m, and that the two temperature sections are plotted on different temperature scales to highlight lateral variations. Depth is given in terms of Earth radius, and is from the surface to 200 km below the surface.
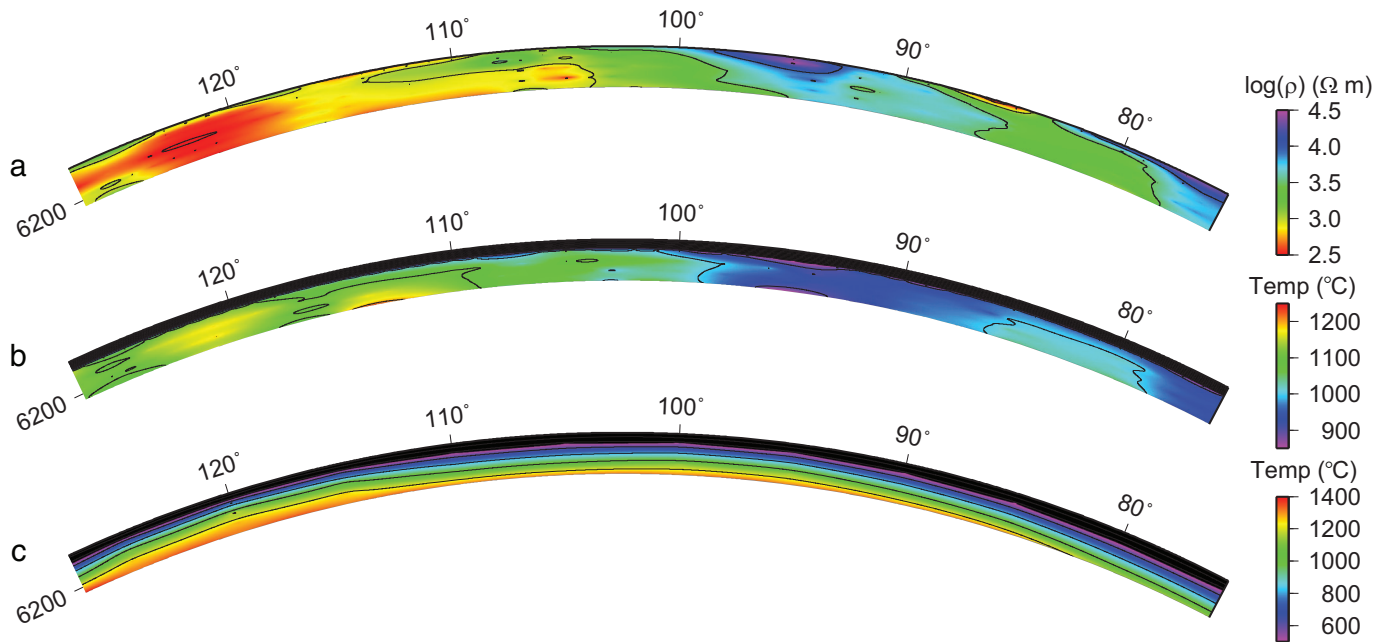
For western Canada, with the exception of Vancouver Island and the neighbouring mainland, Artemieva's temperature estimates are within error of the MT ones, implying that temperature is the only control on electrical resistivity for this region. Taking the point at (–120°W, 60°N) as representative of the region, i.e., the Northwest Territories – Alberta–BC triple point, Artemieva's estimate is of 1300 °C (the adiabat), whereas the resistivity-based estimate is of 1250 °C, assuming dry olivine mantle with small polaron and magnesium vacancy conduction. Remarkably, exotic phases and (or) water do not need to be invoked to explain the observed MT responses; dry olivine at the temperatures predicted by Artemieva's model is sufficient.

This latter result is surprising. A dry lower lithosphere for the Canadian Shield is expected, given the results for the Kaapvaal Craton of Peslier et al. (2010) and Baptiste et al. (2012) that show quite large water content (50–100 ppm) in olivine at mid-lithospheric depths (100 km), but reducing water content with increasing depth to 10 ppm at 200 km. So resistivity should be almost exclusively a function of ambient temperature. For the Cordillera, however, where the LAB is thought to be shallower than 200 km (Fig. 2*e*), then, at 200 km, we are in the sub-lithospheric mantle, or asthenosphere, and there should be evidence of lower resistivity than temperature alone would incur due to the presence of either partial melt, water, or both.

The resistivity-based temperature map at 100 km (Fig. 14*a*) also exhibits colder temperatures beneath the Canadian Shield than the rest of Canada. However, comparison with the estimates of Artemieva (coloured circles on Fig. 14*a*) shows that the resistivity-based estimates are "hotter", i.e., lower resistivity, than Artemieva's estimates, indicative of additional conducting contributions in addition to thermally-induced small polaron activity.

Smoothing and interpolating the resistivities at 100 and 200 km onto a 5° × 5° grid for direct comparison with Artemieva's grid yields the resistivity–temperature pairs shown in Fig. 13 at 100 km depth (red points) and 200 km depth (black points). Points below the solid black line for dry olivine must have temperature estimates that are in error, as the resistivity is far too high. The actual

maximum resistivity values can be higher than RhoMAX estimates, but will not be lower. To a first-order approximation, we can assume that the lithosphere is dry (water content Cw = 0.0) so we correct the value by taking the resistivity-based temperature of the point from going vertically upwards from the point until we intersect the dry olivine line.

For points above the solid black line, we assume to first order that the temperature estimate of Artemieva is correct, and that the resistivity is lower than that of dry olivine due to the presence of water, and we estimate the water content by deriving the intersection of the point with the appropriate water content line. Note that at 100 km depth about half the points are above the dry olivine line, meaning that there is water in the lithosphere. In contrast, at 200 km depth, almost all of the points are below the dry olivine line, meaning that the temperatures of Artemieva are systematically too high.

Maps of the thus derived corrected temperature and estimated water content are shown in Fig. 16. Consistent with the information on Fig. 13, the water content map at 200 km (Fig. 16*d*) shows the mantle at that depth to be virtually dry everywhere, with the exception of NW North Dakota. This anomaly is known to be associated with the North American Central Plains mantle conductor, so is unlikely to be related to proton conduction.

At 100 km depth, the water content map (Fig. 16*b*) shows much of the Canadian Shield and the Cordillera to be dry, with significant conductivity enhancement over and above the thermal effect in southern Saskatchewan – SE Alberta, the Slave Craton, in the northern Arctic in NE Nunavut, and parts of the Superior Craton. Enhanced conductivity in the mantle beneath SW Alberta was discussed by Boerner et al. (1995) and Boerner et al. (1999) in terms of mineralization effects from mantle metasomatism. An alternative suggestion comes from our analysis, which is that the area contains water of the order of 150 ppm in olivine; whether the water is primary or was emplaced as a consequence of mantle metasomatism is open to debate, as of course we have no idea of the age of the water in the olivine.

Note again that these water content estimates come from our RhoMAX values. These we consider robust in that they represent

Fig. 16. Estimates of ambient temperature and water content (Cw) combining the temperature estimates of Artemiva with the resistivity estimates derived: (*a*) corrected temperature at 100 km; (*b*) water content at 100 km; (*c*) corrected temperature at 200 km; (*d*) water content at 200 km.
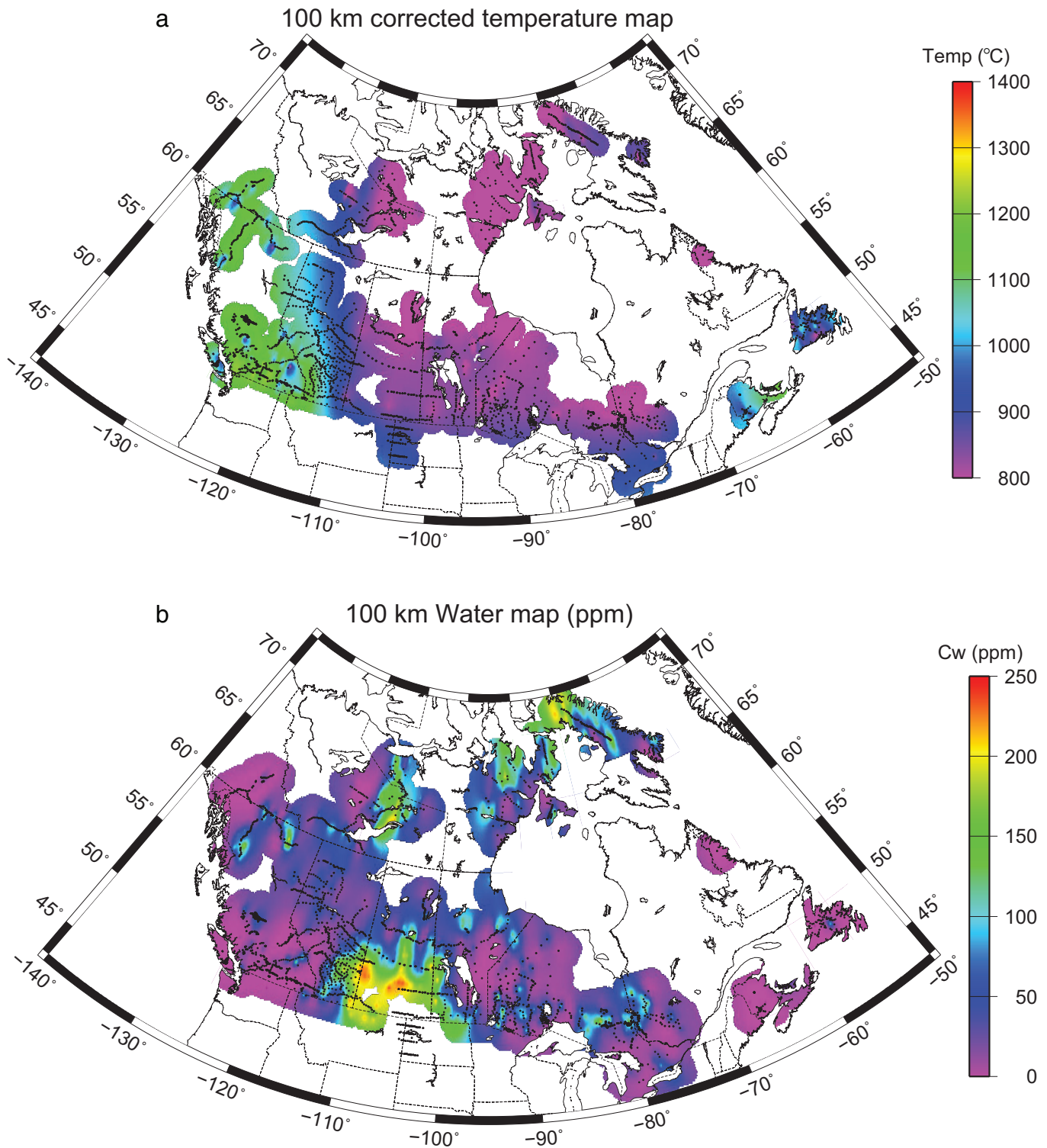
the minimum possible value of the maximum resistivity and are likely little affected by distortion or 3-D effects. There may indeed be value in considering the RhoMIN estimates, but these imply high anisotropy in many locations in Canada (see resistivity anisotropy, RhoANIS, plotted in Fig. 12*b* for 100 km depth and Fig. 12*d* for 200 km depth). Although electrical anisotropy in wet

olivine single crystals was suggested to be up to one and a half orders of magnitude, based on measurements of diffusion rates and the Nernst–Einstein equation relating diffusion to conductivity (Kohlstedt and Mackwell 1998), far lower values (factor of up to 1.5) are reported at lithospheric temperatures and water contents (<1350 °C and <200 wt. ppm) from a laboratory study of conductivity

Fig. 16 (*concluded*).

c 200 km corrected temperature map

d 200 km Water map (ppm)
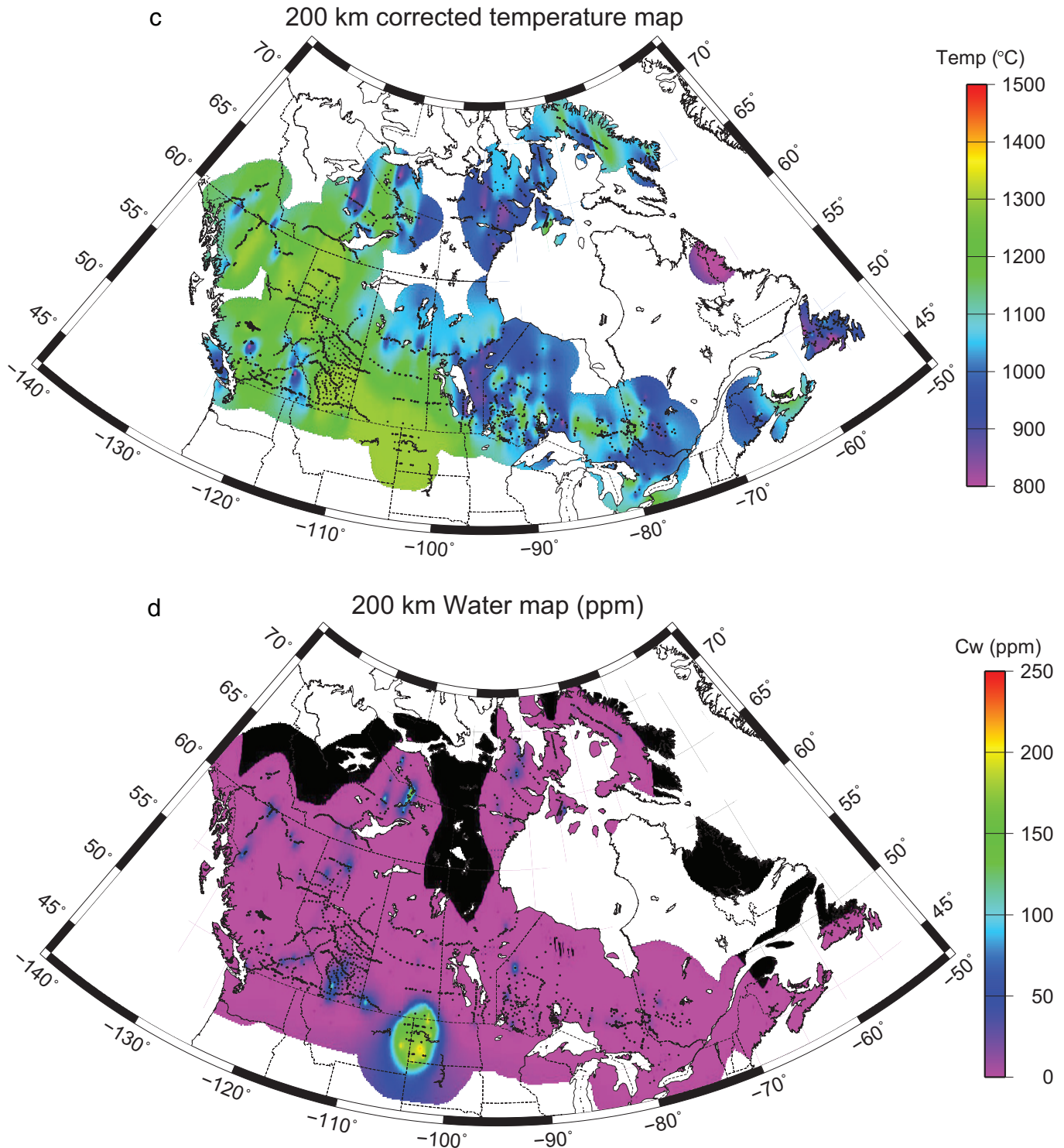
anisotropy (Poe et al. 2010). In addition, numerical simulations, although not completely applicable as they were conducted only in two dimensions and considered direct-current (DC) conduction and not alternating-current (AC) induction, suggest factors of up to three for the bulk maximum anisotropy (Simpson and Tommasi 2006).

The region that is most puzzling is the Cordillera, where water in peridotite would be expected. Indeed, Rippe et al. (2013) suggest that the upper mantle at 100 km beneath parts of the Intermon-

tane Belt must contain water to explain the low resistivities modelled there. But the anisotropy at 200 km depth for about half of the Cordillera is low to absent (Fig. 12d), thus in those regions certainly there is little water present. Where there is high anisotropy in NE BC, of about 1.5 orders of magnitude, the anisotropy direction is NE–SW, consistent with absolute plate motion. This region is below the lithosphere in the asthenosphere, and some process results in conductivity higher in the APM direction compared to perpendicular to it. Whether that process is aligned wet

olivine (Evans et al. 2005*a*) or partial melt (e.g., Caricchi et al. 2011), particularly carbonatitic melts (Gaillard et al. 2008; Yoshino et al. 2012), is vigorously debated in the literature (Hirth 2006; Wang et al. 2006; Yoshino et al. 2006).

Major contributions from Lithoprobe MT studies

Magnetotelluric studies on Lithoprobe transects have contributed significantly to instrumentation, acquisition, and method development and to geoscientific knowledge. However, the two overarching legacies of Lithoprobe MT studies are the postgraduate and post-doctoral training received by many (see Table 3) and a dataset of over 2000 MT sites crossing the continent from sea to sea to sea — east–west from the Atlantic to the Pacific Oceans and north to the Arctic Ocean (Figs. 1*b*, 1*c*). During the Lithoprobe years, Canada was a hotbed of MT activity that was the envy of the world. Numerous post-doctoral fellows and graduate and undergraduate students participated as field assistants and received training in geophysical field techniques, and many of these have proceeded on to careers in geophysics, including in MT. Sadly, there is no lasting legacy of the intellectual capital from those years in terms of related permanent positions in Canadian government and academic institutions, and ironically the number of MT specialists active now in these institutions in Canada is far less than at the initiation of Lithoprobe; a situation also reflected in other areas of geophysics that were very active in Lithoprobe, such as seismic reflection, seismic refraction, and potential field studies. In contrast, MT expertise in the commercial sector has increased dramatically since the start of Lithoprobe, in some part as a consequence of the Lithoprobe project and the exposure it gave to MT results.

In the following text, we list the major contributions made by MT scientists during Lithoprobe

Instrumentation development

- A new-generation long-period magnetotelluric system, called LiMS for Long-period Intelligent Magnetotelluric System (Andersen et al. 1988), was developed by Lithoprobe scientists at the Earth Physics Branch and then the GSC in the mid- and late 1980s to allow information to be gathered during Lithoprobe surveys on the lithospheric and sub-lithospheric mantle resistivity structure. LiMS took advantage of the developments in ring-core magnetometers during the 1980s (Narod and Bennest 1990) to design a modern, state-of-the-art system. A set of 15 LiMSs were built by the GSC and were used extensively across Canada on the SNORCLE, Alberta Basement, Trans-Hudson Orogen, and Western Superior transects, as well as other investigations. Phoenix Geophysics, under licence from the Government of Canada, made clones of the LiMS that they called LRMTs (long-range magnetotellurics). As a consequence of having this instrument through the 1990s and 2000s, the electrical properties and structures of the mantle lithosphere of Canada is known better than for any other country.
- In the late 1980s Lithoprobe scientists at the Geological Survey of Canada collaborated with Phoenix Geophysics in their development of their new 24-bit MT system V5. In particular, Lithoprobe scientists worked on developing and testing high-frequency MT (audio-MT) acquisition.

Acquisition development

- The very long period experiment of Schultz et al. (1993), with 1 km long electrode lines deployed in Carty Lake, northern Ontario, is still the finest experiment of its kind performed. Data were obtained that permitted resolution of electrical resistivity structure to depths >1000 km. In particular, a definitive change in electrical conductivity was found at the 410 km discontinuity, and such a change was later substantiated by laboratory experiments (Xu et al. 1998) who demonstrated a two orders of magnitude increase in conductivity at the olivine–wadsleyite phase transformation.

- Measuring MT fields in the dead of winter was perfected on the Slave Craton part of the SNORCLE transect (McNeice and Jones 1998), resulting in coverage along the whole of the world's longest heavy haul ice road going from Tibbit Lake east of Yellowknife north to the former Lupin gold mine at Contwoyto Lake, plus other profiles (Jones et al. 2001*b*; Jones and Garcia 2003*a*; Jones et al. 2003). Recordings were accomplished in temperatures as low as –40 °C using frozen lakes traversed by the ice road. Electrode lines crossed the lake surface with electrodes lowered to the lake floor through holes drilled in the ice. Magnetometers were deployed adjacent to the lakes because movement of the frozen lake ice introduced noise into the recordings at 10–100 s periods.
- The novel concept of using ocean-bottom magnetotelluric equipment in freshwater lakes was proposed, tested, and found to provide excellent deep-probing information on the Slave Craton as part of SNORCLE (Jones et al. 2003).
- Deep-probing into the crust using large-scale UTEM (University of Toronto EM system) transmitter loops was tested and perfected by Lithoprobe scientists (Bailey et al. 1989; Kurtz et al. 1989; Jones et al. 1994).

MT technique development

- The problem of electric field distortion by local, near-surface inhomogeneities is the Achilles heel of magnetotelluric studies, and major progress in quantifying and removing this distortion has been made by Lithoprobe scientists on a variety of fronts. This distortion arises from structures that are small scale (smaller than the smallest experimental scale, which may be the electrode line length or the smallest induction length at the shortest period) and that produce a frequency independent shift in the measured apparent resistivity. The Groom–Bailey technique (Bailey and Groom 1987; Groom and Bailey 1989, 1991) treats galvanic electric-field distortions through a decomposition of the MT impedance tensor into determinable and indeterminable parts, and has additional superior properties to other techniques and tensor decompositions (Jones 2012). The approach was refined and developed in the early 1990s (Groom et al. 1993; Jones and Groom 1993), with subsequent extension to multiple frequencies and multiple sites (McNeice and Jones 1996; McNeice and Jones 2001); the McNeice–Jones "strike" code is freely distributed and is in use by over 150 scientists and students worldwide. Significant advances in understanding and removing the effect of the distortion of the vertical magnetic field response have also made use of Lithoprobe MT data (Zhang et al. 1993), as have consideration of the magnetic effects of the galvanic charges (Chave and Jones 1997). Finally, 3-D distortion of responses from 3-D structures was explored by Garcia and Jones (2002*c*).
- Conventional MT data analysis assumes that the source fields are plane waves. Non-uniform source fields can be problematic in MT studies, particularly close to auroral regions. Given the location of the auroral oval over Northern Canada, this is an important issue for Canadian researchers. Garcia et al. (1997) examined the effect of non-uniform fields associated with high auroral activity on local night-time recordings from MT data recorded on the northernmost Lithoprobe THOT, and showed that a robust controlled-leverage processing algorithm could extract stable uniform field estimates of the MT impedance tensor. Source field effects were most acute on the Slave part of the SNORCLE transect, and methods for dealing with non-uniform sources fields were advanced by Jones and Spratt (2002) and Lezaeta et al. (2007). The former used the property that the vertical magnetic field tipper response is far more sensitive to non-uniform fields than is the MT response, whereas

the latter approach was more mathematical in nature using a frequency domain principal component method.

- The application of high-frequency AMT for mineral exploration was advanced by Lithoprobe scientists on a number of fronts (Garcia and Jones 2000), from instrumentation (Phoenix Geophysics' V5A and MTU-5A developments), understanding of AMT source fields (Garcia and Jones 2002a), acquisition methodologies (Jones and McNeice 2002), including a proposed novel telluric–telluric–magnetotelluric (TT–MT) method (Garcia and Jones 2005b), down-mine measurements (Queralt et al. 2007), specialized wavelet processing (Garcia and Jones 2008), distortion of controlled-source AMT data (Boerner et al. 1993), 3-D distortion analysis (Garcia and Jones 2002c), and implementation and interpretation (Zhang and Chouteau 1992; Livelybrooks et al. 1996; Chouteau et al. 1997; Jones and Garcia 2006), including a cautionary tale resulting from regional current systems (Jones and Garcia 2003b). AMT is now being used extensively for mineral exploration, with over 30 000 sites measured over the last decade in Canada alone, and particularly 3-D modelling and inversion are being employed. The method is gaining particular importance in settings for which deposits are located near or beyond the limits of controlled-source electromagnetic studies, for example, deep nickel deposits in the Sudbury basin as part of Abitibi–Grenville transect studies (Livelybrooks et al. 1996; Stevens and McNeice 1998; Boerner et al. 2000a), within the Chibougamau camp in Quebec (Chouteau et al. 1997), the world-class Voisey's Bay massive sulphide deposit in Labrador (Balch et al. 1998; Watts and Balch 2000), modelling and resolution appraisal of the Bathurst No. 9 body (Queralt et al. 2007) and of an enigmatic body in northern Labrador on Okak Bay (Jones and Garcia 2003b), the lithospheric-scale geometry of the gold-bearing Yellowknife Fault as part of SNORCLE (Jones and Garcia 2006), and unconformity uranium deposits in the Athabasca basin as part of EXTECH-IV (Tuncer et al. 2006; Tuncer 2007; Farquharson and Craven 2009).

- Lithoprobe scientists were the first basic research scientists to purchase access to the Geotools integrated MT workstation package, the first of its kind, in 1989 and were heavily involved in improving and augmenting it.

- Lithoprobe MT data from the Trans-Hudson Orogen and Southern Cordillera were used as part of a global comparison of 2-D MT inversion algorithms, the so-called COPROD2 (Jones 1993b) and BC87 (Jones 1993a) datasets. Papers appear in the special issues of *Journal of Geomagnetism and Geoelectricity* devoted to the MT–DIWs (MT Data Interpretation Workshops, Jones 1993d; Jones and Schultz 1997).

- MT and AMT methods have been applied increasingly in engineering infrastructure studies and Lithoprobe MT data, along with newly-collected MT soundings, have been used in the planning of high-voltage, direct-current (HVDC) power systems in multiple Canadian provinces and for predicting levels of geomagnetically induced currents on powerlines and pipe-to-soil potentials on pipelines (Ferguson and Odwar 1998; Fernberg et al. 2007). Magnetotelluric methods were also used in site investigations for the development of nuclear waste disposal technologies (Kurtz et al. 1986b).

Results with global consequences

- One of the most significant global questions addressed by Lithoprobe scientists is the cause of the enhanced conductivity in the continental lower crust. This is an almost (but not completely) ubiquitous observation, particularly in Phanerozoic re-

gions, with resistivities some two or more orders of magnitude lower than laboratory studies on candidate dry rocks would suggest. Gough (1986, 1992), Jones (1987, 1992), and Hyndman and students (Hyndman and Shearer 1989; Marquis and Hyndman 1992; Hyndman et al. 1993; Marquis et al. 1995) all brought attention to the apparent correlation between the top of a conducting layer and the top of reflective lower crust, and sought to explain the coincidence though the presence of existence of fluids in the lower crust. M. Mareschal, together with Katsube's laboratory studies on rocks, suggested that for Precambrian regions, grain-boundary graphite was the explanation (Mareschal et al. 1992; Katsube and Mareschal 1993; Mareschal et al. 1994), although recent laboratories studies suggest that such thin films would be unstable (Yoshino and Noritake 2011).

Although this phenomenon of lower crustal enhanced conductivity has not been fully explained to everybody's satisfaction (Yardley and Valley 1997), there is broad consensus that in active or recently-active regions a fluid explanation for low resistivity is plausible (Wannamaker 2000). In contrast, for ancient (Precambrian) regions a fluid explanation is implausible and other mechanisms must be responsible for the almost ubiquitous observation of low resistivity. Perhaps what is anomalous, akin to Holmes's Dog[2], are the rare lower crustal regions that are *not* conductive, but can be explained in terms of dry rocks. These have been found to exist in the southwesternmost part of the Slave Craton (Jones and Ferguson 2001), the North Caribou terrane of the Superior Province (Ferguson et al. 2005a), the Rae Province (Jones et al. 2002a), and in the Bear Province (Spratt et al. 2009). They are shown by the dark blue to purple regions in the crustal conductance map (Fig. 7). All of these regions have exposed crustal rocks that are Archean in age, predominantly Mesoarchean, which suggests that tectonic processes active at that time did not result in emplacement of conducting material deep into the crust. Either subduction, sensu stricto, was not yet operating in the manner in which it is today, or the sediments did not contain any conducting material, sulphides, graphite, or iron oxides, that could be taken to depth in the crust.

- Electrical anisotropy in the continental lithospheric mantle over regional-scale distances was definitively established in the pioneering paper by Mareschal et al. (1995) following observations of anisotropy in the lower crust of the central part of the Superior Province (Kellett et al. 1992) and in the upper mantle below the Kapuskasing Uplift (Kurtz et al. 1993). The crustal and lithospheric mantle electrical anisotropy were confirmed in the novel experiment conducted by Tournerie and Chouteau (1998) who used telephone lines to construct 100 km long electric field dipoles. Very high quality MT responses out to 20 000 s that were free of distortion and static shift effects (Langlois et al. 2000) provided firm unequivocal evidence of anisotropy of the order of 30:1, with the more conducting direction approximately EW in both the lower crust and the lithospheric mantle.

Others have now made similar interpretations elsewhere in Canada and worldwide (Boerner et al. 1999; Simpson 2001; Bahr and Simpson 2002; Hamilton et al. 2006; Padilha et al. 2006), although some of these interpretations are coming under closer scrutiny (Lahti et al. 2005; Nieuwenhuis et al. 2013). Also pioneered in Canada, and fully consistent with the multidisciplinary ethos of Lithoprobe, are qualitative comparisons between electrical and seismic anisotropy, with the first being the key publication by Ji et al. (1996) in which the obliquity between the seismic and electrical anisotropy directions was interpreted

---

[2]Gregory (Scotland Yard detective): "Is there any other point to which you wish to draw my attention?" Holmes: "To the curious incident of the dog in the night time." Gregory: "The dog did nothing in the night time." Holmes: "That was the curious incident," remarked Sherlock Holmes. (Arthur Conan Doyle, "Silver Blaze").

as an indicator of mantle ductile shearing. Others have followed this lead and have demonstrated the advantages of a joint analysis of seismic and electrical data in anisotropic regions (Senechal et al. 1996b; Simpson 2002; Eaton et al. 2004b; Eaton and Jones 2006; Frederiksen et al. 2006; Hamilton et al. 2006; Padilha et al. 2006), including formal joint inversion (Roux et al. 2011), although a caution that differential EM penetration in orthogonal directions must be taken into account when undertaking qualitative comparisons (Jones 2006).

- The North American Central Plains (NACP) conductivity anomaly, discovered fortuitously by Gough and colleagues in the late 1960s (Reitzel et al. 1970; Camfield et al. 1971; Alabi et al. 1975), was identified with a Proterozoic plate boundary in a highly insightful paper by Camfield and Gough (1977). Camfield and Gough (1977) were the first to suggest that a Paleoproterozoic suture lay beneath the Williston Basin, a proposal shown to be correct through later geoscientific studies. As part of GSC and Lithoprobe studies, the NACP anomaly was shown to lie wholly within the Paleoproterozoic Trans-Hudson Orogen (Jones et al. 2005a and references therein), and in northern Saskatchewan to be associated with sulphides, deposited as the arc advanced on the Rae–Hearne hinterland, that were compressed and concentrated along fold hinges leading to very high electrical anisotropy at hand sample scale (Jones et al. 1997). This was the first time that a causative mechanism had been identified for a major conductivity anomaly; an anomaly that is possibly the longest in the world (Jones 1993c). Elsewhere along the NACP, where it lies at depth within the crust, graphite has been postulated to be a contributor to the enhanced conductivity. Graphite within the Black Hills of South Dakota was first noted by Gough and Camfield (1972) and followed up by Rankin and Reddy (1973), Alabi et al. (1975), and Camfield and Gough (1977), with the latter two noting the spatial coincidence of the southern end of the NACP with the Black Hills. Jones et al. (1997) suggested that the Black Hills conductivity anomaly is in fact not related to the NACP anomaly but is likely caused by a different mechanism related to the Hartville Arch, which connects the Black Hills to the Laramie uplift, within which are mapped exposures of graphite (Osterwald et al. 1959).

    The exact geometry of the conductor has been refined over the course of the Lithoprobe project and in subsequent MT surveys, and its crustal extent is now interpreted to lie along the western margin of the Sask Craton (Jones et al. 2005a), with additional crustal conductors, the TOBE (Jones and Craven 1990) and ALCA (Gowan et al. 2009) conductors, lying along the eastern margin of this craton. In addition, analyses of long-period MT responses revealed, for the first time, that the NACP anomaly was not only in the crust, but also had a mantle expression, and that the mantle conductor lies directly beneath the areally largest kimberlite deposit in the world, namely the 104–95 Ma Fort à la Corne kimberlite field (Jones et al. 2005a) that lies within the Sask Craton. A crustal conductor alone is insufficient to explain the anomalies in the vertical magnetic field component seen at daily variation periods of 8 h and 12 h by Camfield and Gough (1975).

    In the early to mid-1990s, the MT data from the southern profile in Saskatchewan were used by the global MT community for testing 2-D inversion codes (Jones 1993b). The dataset, called COPROD2, was acquired by PanCanadian in the mid-1980s and donated to Lithoprobe, and some 20 publications have used the comparison data to date.

- One significant synthesis that has global consequences is that of Boerner et al. (1996) on an explanation for the conductivity of Paleoproterozoic foredeeps. Euxinic carbonaceous shales deposited on pre-foredeep continental margin facies appear to be the conductive lithology.

- Magnetotelluric data were used for the first time to give bounds on upper mantle temperature (Ledo and Jones 2005). Given

knowledge of mantle mineralogy from xenoliths and the highly resistive nature of the crust and upper mantle beneath the Intermontane Belt on SNORCLE's Corridor 3 in the Yukon, it was possible to use extremal bound theory (Hashin–Shtrikman bounds) to determine the minimum (820 °C) and maximum (1020 °C) possible temperatures for an upper mantle region given appropriate mixtures of the dominant mantle minerals (olivine, orthopyroxene, and clinopyroxene). These bounds do not permit the interpretation of a seismic low-velocity body in the same location as being due to high temperatures (Frederiksen et al. 1998; Shi et al. 1998).

- The magnetotelluric method was established as an effective area selection tool for diamond exploration (Jones and Craven 2004) during Lithoprobe surveys on the Slave Craton. The high sensitivity of conductivity to the onset of partial melt and (or) high water content in the electrically conducting asthenosphere means that high-quality MT studies can define the depth to the (electrical) lithosphere–asthenosphere boundary (eLAB) with a precision of 10% or better in 1-D situations (Jones 1999a). In addition, anomalies in the upper lithospheric mantle beneath Archean cratons are most plausibly interpreted as due to graphite or interconnected carbon on grain boundaries (Jones et al. 2003; Jones and Craven 2004), with the implication being that below the graphite–diamond stability field the carbon will be in the form of diamond. Other upper mantle conductors have also been discovered beneath Canada's cratonic regions, such as the western part of the Superior Craton (Ferguson et al. 2005a) and beneath the Sask Craton in north-central Saskatchewan (Jones et al. 2005a). The Kirkland Lake and Cobalt (Rapide des Quinze) kimberlite fields in the southern Superior Craton occur along strike from a mantle conductor (Adetunji et al. 2014). In contrast, work by Turkoglu et al. (2009) on the Buffalo Head Hills terrane in northern Alberta that hosts diamondiferous kimberlites shows no evidence for a conductor in the lithospheric mantle, nor is there a conductor associated with kimberlitic magmatism in the Kaapvaal Craton (Evans et al. 2011). A consequence of establishing MT as a viable tool for regional reconnaissance is that one major diamond exploration company has invested in MT technology, with one of their staff (Shane Evans) being trained in Canada (at Queen's and GSC-Ottawa under Jones) and with the purchase of MT equipment, for studies in primarily Southern Africa but also elsewhere globally.

- A novel very long period (VLOP) MT experiment in Carty Lake, Kapuskasing, northern Ontario, involved deploying an electrode array in the lake bottom and recording MT data for over 2 years. The responses from those data were used to infer electrical conductivity structure to depths in excess of 1000 km (Schultz et al. 1993), and in particular, high gradients in conductivity with depth at around 410 and 660 km were required to fit the data. Subsequent laboratory studies on olivine demonstrated that such rapid changes in electrical resistivity are to be expected at these phase-change boundaries (Xu et al. 1998).

- Lithoprobe magnetotelluric studies from the active western margin of the North American continent, from Proterozoic suture zones, and from the Archean core of the continent, allow the examination of structures produced by ocean–continent collision zones over 2.7 billion years of geological time and provide insight into the processes controlling the electrical conductivity of these zones. Studies from the southern Cordillera provided one of the first electrical images of dipping structures associated with a subducting oceanic plate, and comparison with seismic reflection images permitted an interpretation in terms of thermally-driven fluid processes associated with the subduction (Kurtz et al. 1986a). Larger-scale and deeper studies of this region have revealed deeper zones of enhanced conductivity east of the volcanic arc that have been interpreted to indicate the presence of a shallow asthenosphere (Soyer and

Unsworth 2006; Rippe et al. 2013). In the northern Canadian Cordillera, active subduction was replaced by transform motion around 50 million years ago. However, Lithoprobe SNORCLE Corridors 2 and 3 both image a residual dipping conductor interpreted to be associated with the former subduction of the Kula plate (Jones et al. 2005*b*). This conductor has two distinct parts: a part occurring at crustal depth is interpreted to be caused by subducted metasedimentary rocks, whereas a part at mantle depths is interpreted to be caused by irreversible interactions between fluids from the subducting plate and the overlying mantle wedge (Ledo et al. 2004), for example, hydration of nominally anhydrous mantle minerals (Karato 2006). These observations allow localized mantle conductors observed in Proterozoic suture zones, for example, in the Wopmay Orogen (Wu et al. 2005), to be interpreted in terms of subduction. They also provide insight into conductors observed within Archean cratons (Jones et al. 2003) and infer plate tectonic processes somewhat similar to those observed today.

- One of the seminal results of the Lithoprobe magnetotelluric studies was the first definitive observation of the electrical conductivity structure of the Moho (Jones and Ferguson 2001; Jones 2013). This observation was enabled by the absence in the Mesoarchean crust of the southeast Slave Craton of any enhancement of conductivity in the middle to lower crust. The Lithoprobe results thus place an important constraint on the source of this globally-observed enhancement (see earlier in the text) by indicating that whatever is the cause of the enhanced conductivity, usually hypothesized to be either fluids or graphite, is absent in the oldest crust. The availability of Lithoprobe magnetotelluric results from lithosphere of varying age and tectonic setting placed additional constraints on the source of the enhanced conductivity. In particular, high-resolution studies in the Kapuskasing Structural Zone reveal an absence of enhanced conductivity in rocks interpreted to be derived from the lower crust but now present at the surface (Jones et al. 1994; Mareschal et al. 1994). More detailed Lithoprobe studies suggested that grain-boundary graphite may be an important contribution to the enhanced conductivity, as discussed earlier.

Conclusions

Lithoprobe and other MT studies have contributed greatly to advancing the method, to improved knowledge of the geoscience of Canada, to improved insight into Earth processes, and, most importantly, to the high-quality training of young research personnel. Electromagnetic studies within Lithoprobe, principally using the magnetotelluric technique, have been part of this contribution and this lasting legacy.

Using the Lithoprobe MT dataset together with MT data from many other sources acquired over the last 30 years, we are able to construct continental-scale maps of electrical properties over a region in excess of 7 million km² covering much of Canada. These maps, generated from approximate mapping methods rather than formal 3-D inversions (which will be a long time coming at this scale!), locate the presence of crustal and lithospheric mantle conductors that can be related to tectonic processes, both ancient and modern. Such detail is beyond the scope of this overview paper, but the results of the detailed Lithoprobe MT studies along the various transects have contributed significantly to our understanding of modern and ancient tectonic processes (see subsection "Results with global consequences"). The Canadian Shield is in most parts as cold and resistive as expected for a craton, and SW BC is also cold and resistive, with a thick lithosphere as a consequence of the subduction of the Juan de Fuca plate. The Cordillera has resistivities at a depth of 200 km that are consistent with the temperature estimates from Artemieva's (2006) TC1 model, surprisingly indicative of dry conditions. Anisotropy directions in the crust generally parallel stress directions, and in the mantle generally parallel SKS directions and plate motion directions.

Ironically, MT research in Canada was far more diverse and more robust at the beginning of Lithoprobe than now after its end. In the mid-1980s, there were some 20 permanent university faculty and GSC staff scientists undertaking high-quality MT and EM studies, from theory to instrumentation development to processing and analysis developments to numerical and analogue modelling to interpretation, on both the land and at sea. Today, that number is sadly only six pursuing a smaller range of activities.

The majority of the figures were produced using Wessel and Smith's GMT package (Wessel and Smith 1991, 1998), a wonderful resource for the whole scientific community.

References

Abt, D.L., Fischer, K.M., French, S.W., Ford, H.A., Yuan, H.Y., and Romanowicz, B. 2010. North American lithospheric discontinuity structure imaged by Ps and Sp receiver functions. Journal of Geophysical Research-Solid Earth, **115**(B9). doi:10.1029/2009JB006914.

Adetunji, A.Q. 2014. Resistivity structure and the electrical anisotropy of the Precambrian Grenville Province. University of Manitoba, Winnipeg, Canada, Department of Geological Sciences. pp. 357.

Adetunji, A.Q., Ferguson, I.J., and Jones, A.G. 2014. Crustal and lithospheric scale structures of the Precambrian Superior-Grenville margin. Tectonophysics, **614**: 146–169. doi:10.1016/j.tecto.2013.12.008.

Afonso, J.C., Fernandez, M., Ranalli, G., Griffin, W.L., and Connolly, J.A.D. 2008. Integrated geophysical-petrological modeling of the lithosphere and sublithospheric upper mantle: Methodology and applications. Geochemistry, Geophysics, Geosystems, **9**, Q05008. doi:10.1029/2007GC001834.

Agarwal, A.K., and Weaver, J.T. 1993. Inversion of the COPROD2 data by a method of modeling. Journal of Geomagnetism and Geoelectricity, **45**: 969–983. doi:10.5636/jgg.45.969.

Akaranta, O. 2011. Evaluation of the resistivity structure of the Flin Flon Belt and the Chisel Lake Area using the magnetotelluric method. University of Manitoba, Winnipeg, Canada.

Alabi, A.O., Camfield, P.A., and Gough, D.I. 1975. North-American Central Plains conductivity anomaly. Geophysical Journal of the Royal Astronomical Society, **43**: 815–833. doi:10.1111/j.1365-246X.1975.tb06197.x.

Andersen, F., Boerner, B.B., Harding, K., Jones, A.G., Kurtz, R.D., Parmelee, J., and Trigg, D. 1988. LIMS: Long period intelligent magnetotelluric system. 9th Workshop on EM Induction in the Earth, Sochi, USSR.

Artemieva, I.M. 2006. Global 1 degrees x 1 degrees thermal model TC1 for the continental lithosphere: Implications for lithosphere secular evolution. Tectonophysics, **416**: 245–277. doi:10.1016/j.tecto.2005.11.022.

Artemieva, I.M. 2009. The continental lithosphere: Reconciling thermal, seismic, and petrologic data. Lithos, **109**: 23–46. doi:10.1016/j.lithos.2008.09.015.

Arzate-Flores, J.A. 1994. Magnetotelluric interpretation of the subduction Cocos Plate in Oaxaca's continental margin. Ecole Polytechnique, Montreal, Quebec, Canada.

Atkinson, G., Adams, J., Asudeh, I., Bostock, M., Cassidy, J., Eaton, D., Ferguson, I., Jones, A.G., Snyder, D., and White, D. 2003. POLARIS Update: Fall 2002. Seismological Research Letters, **74**: 41–43. doi:10.1785/gssrl.74.1.41.

Aucoin, F. 1992. Signature électromagnétique du bloc de la rivière Groundhog, zone structurale du Kapuskasing, Ontario. Ecole Polyechnique, Montreal, Quebec, Canada.

Audet, P., and Mareschal, J.C. 2004. Variations in elastic thickness in the Canadian Shield. Earth and Planetary Science Letters, **226**: 17–31. doi:10.1016/j.epsl.2004.07.035.

Audet, P., and Mareschal, J.C. 2007. Wavelet analysis of the coherence between Bouguer gravity and topography: application to the elastic thickness anisotropy in the Canadian Shield. Geophysical Journal International, **168**: 287–298. doi:10.1111/j.1365-246X.2006.03231.x.

Bahr, K., and Simpson, F. 2002. Electrical anisotropy below slow- and fast-moving plates: Paleoflow in the upper mantle? Science, **295**: 1270–1272. doi:10.1126/science.1066161. PMID:11847335.

Bailey, R.C., and Groom, R.W. 1987. Decomposition of the magnetotelluric impedance tensor which is useful in the presence of channeling. 57th annual international Society of Exploration Geophysicists meeting and exposition, Tulsa, OK. Abstract 57, pp. 154–156.

Bailey, R.C., Craven, J.A., Macnae, J.C., and Polzer, B.D. 1989. Imaging of deep fluids in Archean crust. Nature, **340**: 136–138. doi:10.1038/340136a0.

Balch, S.J., Crebs, T.J., King, A., and Verbiski, M. 1998. Geophysics of the Voisey's Bay Ni-Cu-Co deposits. SEG Technical Program Expanded Abstracts 17, pp. 784–787.

Bank, C.G., Bostock, M.G., Ellis, R.M., and Cassidy, J.F. 2000. A reconnaissance teleseismic study of the upper mantle and transition zone beneath the Archean Slave craton in NW Canada. Tectonophysics, **319**: 151–166. doi:10.1016/S0040-1951(00)00034-2.

Baptiste, V., Tommasi, A., and Demouchy, S. 2012. Deformation and hydration of the lithospheric mantle beneath the Kaapvaal craton, South Africa. Lithos, **149**: 31–50. doi:10.1016/j.lithos.2012.05.001.

Bastow, I.D., Kendall, J.M., Brisbourne, A.M., Snyder, D.B., Thompson, D., Hawthorn, D., Helffrich, G.R., Wookey, J., Horleston, A., and Eaton, D. 2011. The Hudson Bay Lithospheric Experiment. Astronomy and Geophysics, **52**(6): 6.21–6.24. doi:10.1111/j.1468-4004.2011.52621.x.

Blackwell, D.D., and Richards, M. 2004. Geothermal map of North America. American Association of Petroleum Geologist (AAPG).

Blais, E. 1994. Application de la magnétotellurique à l'exploration minière profonde: anomalie de Trillabelle structure de Sudbury. Ecole Polytechnique, Montreal, Quebec, Canada.

Bodin, T., Yuan, H.L., and Romanowicz, B. 2014. Inversion of receiver functions without deconvolution. Geophysical Journal International, **196**: 1025–1033.

Boerner, D.E., Wright, J.A., Thurlow, J.G., and Reed, L.E. 1993. Tensor CSAMT studies at the Buchans mine in central Newfoundland. Geophysics, **58**: 12–19. doi:10.1190/1.1443342.

Boerner, D.E., Kellett, R., and Mareschal, M. 1994. Inductive source EM sounding of the Sudbury structure. Geophysical Research Letters, **21**: 943–946. doi:10.1029/93GL02316.

Boerner, D.E., Kurtz, R.D., Craven, J.A., Rondenay, S., and Qian, W. 1995. Buried Proterozoic foredeep under the Western Canada Sedimentary Basin. Geology, **23**: 297–300. doi:10.1130/0091-7613(1995)023<0297:BPFUTW>2.3.CO;2.

Boerner, D.E., Kurtz, R.D., and Craven, J.A. 1996. Electrical conductivity and Paleo-Proterozoic foredeeps. Journal of Geophysical Research-Solid Earth, **101**: 13775–13791. doi:10.1029/96JB00171.

Boerner, D.E., Craven, J.A., Kurtz, R.D., Ross, G.M., and Jones, F.W. 1998. The Great Falls Tectonic Zone: suture or intracontinental shear zone? Canadian Journal of Earth Sciences, **35**(2): 175–183. doi:10.1139/e97-104.

Boerner, D.E., Kurtz, R.D., Craven, J.A., Ross, G.M., Jones, F.W., and Davis, W.J. 1999. Electrical conductivity in the Precambrian lithosphere of western Canada. Science, **283**: 668–670. doi:10.1126/science.283.5402.668. PMID:9924022.

Boerner, D.E., Kurtz, R.D., and Craven, J.A. 2000a. A summary of electromagnetic studies on the Abitibi–Grenville transect. Canadian Journal of Earth Sciences, **37**(2–3): 427–437. doi:10.1139/e99-063.

Boerner, D.E., Kurtz, R.D., Craven, J.A., Ross, G.M., and Jones, F.W. 2000b. A synthesis of electromagnetic studies in the Lithoprobe Alberta Basement Transect: constraints on Paleoproterozoic indentation tectonics. Canadian Journal of Earth Sciences, **37**(11): 1509–1534. doi:10.1139/e00-063.

Bostick, F.X. 1977: A simple almost exact method of MT analysis. Workshop on Electrical Methods in Geothermal Exploration.

Bouzid, A.-E. 1992. Étude multidisciplinaire d'un bassin saharien près d'In Salah, Algérie: apport de la magnétotellurique. Ecole Polytechnique, Montreal, Quebec, Canada.

Calais, E., Han, J.Y., DeMets, C., and Nocquet, J.M. 2006. Deformation of the North American plate interior from a decade of continuous GPS measurements. Journal of Geophysical Research-Solid Earth, **111**: B06402. doi:10.1029/2005JB004253.

Caldwell, T.G., Bibby, H.M., and Brown, C. 2004. The magnetotelluric phase tensor. Geophysical Journal International, **158**: 457–469. doi:10.1111/j.1365-246X.2004.02281.x.

Camfield, P.A., and Gough, D.I. 1975. Anomalies in daily variation magnetic-fields and structure under northwestern United States and southwestern Canada. Geophysical Journal of the Royal Astronomical Society, **41**: 193–218. doi:10.1111/j.1365-246X.1975.tb04148.x.

Camfield, P.A., and Gough, D.I. 1977. A possible Proterozoic plate boundary in North America. Canadian Journal of Earth Sciences, **14**(6): 1229–1238. doi:10.1139/e77-112.

Camfield, P.A., Gough, D.I., and Porath, H. 1971. Magnetometer array studies in North-Western United-States and South-Western Canada. Geophysical Journal of the Royal Astronomical Society, **22**: 201–222. doi:10.1111/j.1365-246X.1971.tb03592.x.

Caricchi, L., Gaillard, F., Mecklenburgh, J., and Trong, E.L. 2011. Experimental determination of electrical conductivity during deformation of melt-bearing olivine aggregates: Implications for electrical anisotropy in the oceanic low velocity zone. Earth and Planetary Science Letters, **302**: 81–94. doi:10.1016/j.epsl.2010.11.041.

Cassels, J.P. 1997. A magnetotelluric study of the Superior Boundary Zone. University of Manitoba, Winnipeg, Canada.

Chakridi, R. 1991. Interprétation magnétotellurique dans des régions complexes. Ecole Polytechnique, Montreal, Quebec, Canada.

Chakridi, R., Chouteau, M., and Mareschal, M. 1992. A simple technique for analyzing and partly removing galvanic distortion from the magnetotelluric impedance tensor - application to Abitibi and Kapuskasing data (Canada). Geophysical Journal International, **108**: 917–929. doi:10.1111/j.1365-246X.1992.tb03480.x.

Chave, A.D., and Jones, A.G. 1997. Electric and magnetic field galvanic distortion decomposition of BC87 data. Journal of Geomagnetism and Geoelectricity, **49**: 767–789. doi:10.5636/jgg.49.767.

Chen, C.W., Rondenay, S., Weeraratne, D.S., and Snyder, D.B. 2007. New constraints on the upper mantle structure of the Slave craton from Rayleigh wave inversion. Geophysical Research Letters, **34**: L10301. doi:10.1029/2007GL029535.

Chen, J. 1994. Electromagnetic induction in the New Zealand region. Department of Physics. University of Victoria, Victoria, B.C., Canada.

Chouteau, M., Zhang, P., Dion, D.J., Giroux, B., Morin, R., and Krivochieva, S. 1997. Delineating mineralization and imaging the regional structure with magnetotellurics in the region of Chibougamau (Canada). Geophysics, **62**: 730–748. doi:10.1190/1.1444183.

Clowes, R.M. 2010a. Initiation, development, and benefits of Lithoprobe - shaping the direction of Earth science research in Canada and beyond. Canadian Journal of Earth Sciences, **47**(4): 291–314. doi:10.1139/E09-074.

Clowes, R.M. 2010b. Preface to CJES Lithoprobe Special Issues 1 and 2. Canadian Journal of Earth Sciences, **47**: v–vi.

Clowes, R.M., Zelt, C.A., Amor, J.R., and Ellis, R.M. 1995. Lithospheric structure in the southern Canadian Cordillera from a network of seismic refraction lines. Canadian Journal of Earth Sciences, **32**(10): 1485–1513. doi:10.1139/e95-122.

Cook, F.A., and Jones, A.G. 1995. Seismic reflections and electrical conductivity: A case of Holmes' curious dog? Geology, **23**: 141–144. doi:10.1130/0091-7613(1995)023<0141:SRAECA>2.3.CO;2.

Correia, A. 1994. A magnetotelluric study in the region of the intersection of the Messejana Fault and the Ferreira-Ficalho overthrust in Portugal. Department of Physics. University of Alberta, Edmonton, Alberta, Canada.

Courtier, A.M. 2008. Mantle Dynamics, Composition, and State in Regions Associated with Active and Ancient Subduction. N. H. Winchell School of Earth Sciences. University of Minnesota, Minneapolis MN.

Courtier, A.M., Gaherty, J.B., Revenaugh, J., Bostock, M.G., and Garnero, E.J. 2010. Seismic anisotropy associated with continental lithosphere accretion beneath the CANOE array, northwestern Canada. Geology, **38**: 887–890. doi:10.1130/G31120.1.

Craven, J.A. 1991. Electromagnetic imaging of deep fluids in Archean crust. Department of Physics. University of Toronto, Toronto, Ont., Canada.

Craven, J.A., Ferguson, I.J., Skulski, T., Kurtz, R.D., Wu, X., Orellana, M., Spratt, J., and Boerner, D.E. 2001. Electrical images of ancient partial melting. Pan-Lithoprobe Workshop III, Banff, Canada, Lithoprobe Report 81: 11.

Craven, J.A., Sanborn-Barrie, M., Roberts, B.J., Stefanescu, M., and Young, M. 2013. Preliminary insights into the architecture of southern Cumberland Peninsula from magnetotelluric data. Pp. 15. Current Research. Geological Survey of Canada.

Darbyshire, F.A., and Eaton, D.W. 2010. The lithospheric root beneath Hudson Bay, Canada from Rayleigh wave dispersion No clear seismological distinction between Archean and Proterozoic mantle. Lithos, **120**: 144–159. doi:10.1016/j.lithos.2010.04.010.

Darbyshire, F.A., Eaton, D.W., Frederiksen, A.W., and Ertolahti, L. 2007. New insights into the lithosphere beneath the Superior Province from Rayleigh wave dispersion and receiver function analysis. Geophysical Journal International, **169**: 1043–1068. doi:10.1111/j.1365-246X.2006.03259.x.

deGroot-Hedlin, C. 1995. Inversion of regional 2-D resistivity structure in the presence of galvanic scatterers. Geophysical Journal International, **122**: 877–888. doi:10.1111/j.1365-246X.1995.tb06843.x.

Dosso, S.E. 1990. Inversion and appraisal for the one-dimensional magnetotellurics problem. Department of Astronomy and Geophysics. University of British Columbia, Vancouver, B.C., Canada.

Doucet, L.S., Peslier, A.H., Ionov, D.A., Brandon, A.D., Golovin, A.V., and Ashchepkov, I.V. 2013. High water contents in the Siberian cratonic mantle: an FTIR study of Udachnaya peridotite xenoliths. Fall AGU, San Francisco, CA, USA.

Drew, M. 2012. 3D inversion modelling of the Nechako Basin, British Columbia, magnetotelluric data set. Memorial University of Newfoundland, St. John's, Canada.

Du Frane, W.L., Roberts, J.J., Toffelmier, D.A., and Tyburczy, J.A. 2005. Anisotropy of electrical conductivity in dry olivine. Geophysical Research Letters. American Geophysical Union. pp. 1–4.

Duba, A.G., and Shankland, T.J. 1982. Free carbon and electrical conductivity in the Earth's mantle. Geophysical Research Letters, **9**: 1271–1274. doi:10.1029/GL009i011p01271.

Ducea, M.N., and Park, S.K. 2000. Enhanced mantle conductivity from sulfide minerals, southern Sierra Nevada, California. Geophysical Research Letters, **27**: 2405–2408. doi:10.1029/2000GL011565.

Eaton, D.W., and Jones, A.G. 2006. Tectonic fabric of the subcontinental lithosphere: Evidence from seismic, magnetotelluric and mechanical anisotropy - Preface. Physics of the Earth and Planetary Interiors, **158**: 85–91. doi:10.1016/j.pepi.2006.05.005.

Eaton, D., Ferguson, I.J., Jones, A.G., Hope, J., and Wu, X. 2001. A geophysical shear-sense indicator and the role of mantle lithosphere in transcurrent faulting. In Pan-Lithoprobe Workshop III. Lithoprobe, Banff, Canada. Edited by R.M. Clowes. pp. 12–15.

Eaton, D., Frederiksen, A., and Miong, S.K. 2004a. Shear-wave splitting observations in the lower Great Lakes region: Evidence for regional anisotropic domains and keel-modified asthenospheric flow. Geophysical Research Letters, **31**: L07610. doi:10.1029/2004GL019438.

Eaton, D.W., Jones, A.G., and Ferguson, I.J. 2004b. Lithospheric anisotropy structure inferred from collocated teleseismic and magnetotelluric observations: Great Slave Lake shear zone, northern Canada. Geophysical Research Letters, **31**: L19614. doi:10.1029/2004GL020939.

Eaton, D.W., Adams, J., Asudeh, I., Atkinson, G.M., Bostock, M.G., Cassidy, J.F., Ferguson, I.J., Samson, C., Snyder, D.B., Tiampo, K.F., and Unsworth, M.J. 2005. Investigating Canada's Lithosphere and Earthquake Hazards with Portable Arrays. EOS Transactions, **86**: 169–173. doi:10.1029/2005EO170001.

Eaton, D.W., Darbyshire, F., Evans, R.L., Gruetter, H., Jones, A.G., and Yuan, X. 2009. The elusive lithosphere-asthenosphere boundary (LAB) beneath cratons. Lithos, **109**: 1–22. doi:10.1016/j.lithos.2008.05.009.

Edwards, R.N., Bailey, R.C., and Garland, G.D. 1981. Conductivity anomalies - Lower crust or asthenosphere. Physics of the Earth and Planetary Interiors, **25**: 263–272. doi:10.1016/0031-9201(81)90070-4.

Eisel, M., and Bahr, K. 1993. Electrical anisotropy in the lower crust of British-Columbia - an interpretation of a magnetotelluric profile after tensor decomposition. Journal of Geomagnetism and Geoelectricity, **45**: 1115–1126. doi:10.5636/jgg.45.1115.

Ellis, R.G., Farquharson, C.G., and Oldenburg, D.W. 1993. Approximate inverse mapping inversion of the COPROD2 data. Journal of Geomagnetism and Geoelectricity, **45**: 1001–1012. doi:10.5636/jgg.45.1001.

Evans, R.L., Hirth, G., Baba, K., Forsyth, D., Chave, A., and Mackie, R. 2005a. Geophysical evidence from the MELT area for compositional controls on oceanic plates. Nature, **437**: 249–252. doi:10.1038/nature04014. PMID:16148932.

Evans, R.L., Jones, A.G., Garcia, X., Muller, M., Hamilton, M., Evans, S., Fourie, S., Spratt, J., Webb, S., Jelsma, H., and Hutchins, D. 2011. The electrical lithosphere beneath the Kaapvaal Craton, Southern Africa. Journal of Geophysical Research - Solid Earth. pp. 16.

Evans, S. 2003. A magnetotelluric investigation of the northern margin of the Trans-Hudson Orogen on Baffin Island, Nunavut, Canada. Department of Geological Sciences. Queen's University, Kingston, Ontario, Canada.

Evans, S., Jones, A.G., Spratt, J., and Katsube, J. 2003. Central Baffin electromagnetic experiment (CBEX), Phase 2. Geological Survey of Canada. pp. 10 pages.

Evans, S., Jones, A.G., Spratt, J., and Katsube, J. 2005b. Central Baffin electromagnetic experiment (CBEX) maps the NACP in the Canadian arctic. Physics of the Earth and Planetary Interiors, **150**: 107–122. doi:10.1016/j.pepi.2004.08.032.

Farquharson, C.G. 1995. Approximate sensitivities for the multi-dimensional electromagnetic inverse problem. Department of Astronomy and Geophysics. University of British Columbia, Vancouver, B.C., Canada.

Farquharson, C.G., and Craven, J.A. 2009. Three-dimensional inversion of magnetotelluric data for mineral exploration: An example from the McArthur River uranium deposit, Saskatchewan, Canada. Journal of Applied Geophysics, **68**: 450–458. doi:10.1016/j.jappgeo.2008.02.002.

Faure, S., Godey, S., Fallara, F., and Trepanier, S. 2011. Seismic architecture of the Archean North American Mantle and its relationship to diamondiferous kimberlite fields. Economic Geology, **106**: 223–240. doi:10.2113/econgeo.106.2.223.

Ferguson, I.J., and Odwar, H.D. 1998. Review of conductivity soundings in Canada (Appendix 3).

Ferguson, I.J., Jones, A.G., Sheng, Y., Wu, X., and Shiozaki, I. 1999. Geoelectric response and crustal electrical-conductivity structure of the Flin Flon Belt, Trans-Hudson Orogen, Canada. Canadian Journal of Earth Sciences, **36**(11): 1917–1938. doi:10.1139/e99-119.

Ferguson, I.J., Craven, J.A., Kurtz, R.D., Boerner, D.E., Bailey, R.C., Wu, X., Orellana, M.R., Spratt, J., Wennberg, G., and Norton, A. 2005a. Geoelectric response of Archean lithosphere in the western Superior Province, central Canada. Physics of the Earth and Planetary Interiors, **150**: 123–143. doi:10.1016/j.pepi.2004.08.025.

Ferguson, I.J., Stevens, K.M., and Jones, A.G. 2005b. Electrical-resistivity imaging of the central Trans-Hudson orogen. Canadian Journal of Earth Sciences, **42**(4): 495–515. doi:10.1139/e05-017.

Fernberg, P.A. 2011. Earth resistivity structures and their effects on geomagnetic induction in pipelines. Carleton University, Ottawa, Canada. pp. 272.

Fernberg, P.A., Samson, C., Boteler, D.H., Trichtchenko, L., and Larocca, P. 2007. Earth conductivity structures and their effects on geomagnetic induction in pipelines. Annales Geophysicae, **25**: 207–218. doi:10.5194/angeo-25-207-2007.

Flores, C., Kurtz, R.D., and DeLaurier, J. 1985. Magnetotelluric exploration in the Meager Mountain Geothermal Area, Canada. Acta Geodaetica, Geophysica et Montanistica. Academy Sciences Hungary, **20**: 165–171.

Flores-Luna, C.F. 1986. Electromagnetic induction studies over the Meager Creek geothermal area, British Columbia. Department of Physics. University of Toronto, Toronto, Ontario, Canada.

Fluck, P., Hyndman, R.D., and Lowe, C. 2003. Effective elastic thickness T-e of the lithosphere in western Canada. Journal of Geophysical Research-Solid Earth, **108**: 2430. doi:10.1029/2002JB002201.

Frederiksen, A.W., Bostock, M.G., VanDecar, J.C., and Cassidy, J.F. 1998. Seismic structure of the upper mantle beneath the northern Canadian Cordillera from teleseismic travel-time inversion. Tectonophysics, **294**: 43–55. doi:10.1016/S0040-1951(98)00095-X.

Frederiksen, A.W., Ferguson, I.J., Eaton, D., Miong, S.K., and Gowan, E. 2006. Mantle fabric at multiple scales across an Archean-Proterozoic boundary, Grenville Front, Canada. Physics of the Earth and Planetary Interiors, **158**: 240–263. doi:10.1016/j.pepi.2006.03.025.

Frederiksen, A.W., Miong, S.K., Darbyshire, F.A., Eaton, D.W., Rondenay, S., and Sol, S. 2007. Lithospheric variations across the Superior Province, Ontario, Canada: Evidence from tomography and shear wave splitting. Journal of Geophysical Research-Solid Earth, **112**: B07318. doi:10.1029/2006JB004861.

Fullea, J., Afonso, J.C., Connolly, J.A.D., Fernandez, M., Garcia-Castellanos, D., and Zeyen, H. 2009. LitMod3D: An interactive 3-D software to model the thermal, compositional, density, seismological, and rheological structure of the lithosphere and sublithospheric upper mantle. Geochemistry, Geophysics, Geosystems, **10**: Q08019. doi:10.1029/2009GC002391.

Fullea, J., Muller, M.R., and Jones, A.G. 2011. Electrical conductivity of continental lithospheric mantle from integrated geophysical and petrological modeling: Application to the Kaapvaal Craton and Rehoboth Terrane, southern Africa. Journal of Geophysical Research-Solid Earth, **116**: B10202. doi:10.1029/2011JB008544.

Fullea, J., Muller, M.R., Jones, A.G., and Afonso, J.C. 2014. The lithosphere-asthenosphere system beneath Ireland from integrated geophysical-petrological modelling II: 3D thermal and compositional structure. Lithos, **189**: 49–64. doi:10.1016/j.lithos.2013.09.014.

Gaillard, F., Malki, M., Iacono-Marziano, G., Pichavant, M., and Scaillet, B. 2008. Carbonatite melts and electrical conductivity in the asthenosphere. Science, **322**: 1363–1365. doi:10.1126/science.1164446. PMID:19039132.

Garcia, X., and Jones, A.G. 2000. Advances in aspects of the application of magnetotellurics for mineral exploration. 70th SEG, Calgary, Alberta. pp. 1115–1118.

Garcia, X., and Jones, A.G. 2002*a*. Atmospheric sources for audio-magnetotelluric (AMT) sounding. Geophysics, **67**: 448–458. doi:10.1190/1.1468604.

Garcia, X., and Jones, A.G. 2002*b*. Decomposition of three-dimensional magnetotelluric data. *In* Three-Dimensional Electromagnetics, Proceedings. *Edited by* M.S. Zhdanov and P.E. Wannamaker. pp. 235–250.

Garcia, X., and Jones, A.G. 2002*c*. Extended decomposition of MT data. *In* Three-Dimensional Electromagnetics. *Edited by* M.S. Zhdanov and P.E. Wannamaker. Elsevier. pp. 235–250.

Garcia, X., and Jones, A.G. 2005*a*. Electromagnetic image of the Trans-Hudson orogen - THO94 transect. Canadian Journal of Earth Sciences, **42**(4): 479–493. doi:10.1139/e05-016.

Garcia, X., and Jones, A.G. 2005*b*. A new methodology for the acquisition and processing of audio-magnetotelluric (AMT) data in the AMT dead band. Geophysics, **70**: G119–G126. doi:10.1190/1.2073889.

Garcia, X., and Jones, A.G. 2008. Robust processing of magnetotelluric data in the AMT dead-band using the Continuous Wavelet Transform. Geophysics, 01/2008; **73**: F223–F234. doi:10.1190/1.2987375.

Garcia, X., Chave, A.D., and Jones, A.G. 1997. Robust processing of magnetotelluric data from the auroral zone. Journal of Geomagnetism and Geoelectricity, **49**: 1451–1468. doi:10.5636/jgg.49.1451.

Garcia, X., Boerner, D., and Pedersen, L.B. 2003. Electric and magnetic galvanic distortion decomposition of tensor CSAMT data. Application to data from the Buchans Mine (Newfoundland, Canada). Geophysical Journal International, **154**: 957–969. doi:10.1046/j.1365-246X.2003.02019.x.

Giroux, B. 1994. Application de la magnétotellurique à l'étude des aquifères profonds du bassin sénégalais. Ecole Polytechnique, Montreal, Quebec, Canada.

Gough, D.I. 1986. Seismic reflectors, conductivity, water and stress in the continental crust. Nature, **323**: 143–144. doi:10.1038/323143a0.

Gough, D.I. 1992. Electromagnetic exploration for fluids in the Earth's crust. Earth-Science Reviews, **32**: 3–18. doi:10.1016/0012-8252(92)90009-I.

Gough, D.I., and Camfield, P.A. 1972. Convergent geophysical evidence of a metamorphic belt through Black Hills of South Dakota. Journal of Geophysical Research, **77**: 3168. doi:10.1029/JB077i017p03168.

Gough, D.I., and Majorowicz, J.A. 1992. Magnetotelluric soundings, structure, and fluids in the Southern Canadian Cordillera. Canadian Journal of Earth Sciences, **29**(4): 609–620. doi:10.1139/e92-053.

Gowan, E. 2005. Investigation of the electrical resistivity of the crust in southern Manitoba using the magnetotelluric method. University of Manitoba, Winnipeg, Canada.

Gowan, E.J., Ferguson, I.J., Jones, A.G., and Craven, J.A. 2009. Geoelectric structure of the northeastern Williston basin and underlying Precambrian lithosphere. Canadian Journal of Earth Sciences, **46**(6): 441–464. doi:10.1139/E09-028.

Greenfield, A.M.R., Ghent, E.D., and Russell, J.K. 2013. Geothermobarometry of spinel peridotites from southern British Columbia: implications for the thermal conditions in the upper mantle. Canadian Journal of Earth Sciences, **50**(10): 1019–1032. doi:10.1139/cjes-2013-0037.

Gripp, A.E., and Gordon, R.G. 2002. Young tracks of hotspots and current plate velocities. Geophysical Journal International, **150**: 321–361. doi:10.1046/j.1365-246X.2002.01627.x.

Groom, R.W. 1988. The effects of inhomogeneities on magnetotellurics. Department of Physics. University of Toronto, Toronto, Ontario, Canada.

Groom, R.W., and Bailey, R.C. 1989. Decomposition of magnetotelluric impedance tensors in the presence of local three dimensional galvanic distortion. Journal of Geophysical Research, **94**: 1913–1925. doi:10.1029/JB094iB02p01913.

Groom, R.W., and Bailey, R.C. 1991. Analytical investigations of the effects of near surface three dimensional galvanic scatterers on MT tensor decomposition. Geophysics, **56**: 496–518. doi:10.1190/1.1443066.

Groom, R.W., Kurtz, R.D., Jones, A.G., and Boerner, D.E. 1993. A quantitative methodology for determining the dimensionality of conductive structure from magnetotelluric data. Geophysical Journal International, **115**: 1095–1118. doi:10.1111/j.1365-246X.1993.tb01512.x.

Grütter, H., Latti, D., and Menzies, A. 2006. Cr-saturation arrays in concentrate garnet compositions from kimberlite and their use in mantle barometry. Journal of Petrology, **47**: 801–820. doi:10.1093/petrology/egi096.

Gupta, J.C., and Jones, A.G. 1990. Electrical resistivity structure of the Flahhead basin in south-eastern British Columbia, Canada. Canadian Journal of Earth Sciences, **27**(8): 1061–1073. doi:10.1139/e90-101.

Gupta, J.C., and Jones, A.G. 1995. Electrical conductivity structure of the Purcell Anticlinorium in southeast British Columbia and northwest Montana. Canadian Journal of Earth Sciences, **32**(10): 1564–1583. doi:10.1139/e95-127.

Hamilton, M.P., Jones, A.G., Evans, R.L., Evans, S., Fourie, C.J.S., Garcia, X., Mountford, A., Spratt, J.E., and Team, S.M. 2006. Electrical anisotropy of South African lithosphere compared with seismic anisotropy from shear-wave splitting analyses. Physics of the Earth and Planetary Interiors, **158**: 226–239. doi:10.1016/j.pepi.2006.03.027.

Hamza, V.M., and Vieira, F.P. 2012. Global distribution of the lithosphere-asthenosphere boundary: a new look. Solid Earth, **3**: 199–212. doi:10.5194/se-3-199-2012.

Harder, M., and Russell, J.K. 2006. Thermal state of the upper mantle beneath the Northern Cordilleran Volcanic Province (NCVP), British Columbia, Canada. Lithos, **87**: 1–22. doi:10.1016/j.lithos.2005.05.002.

Heaman, L.M., and Kjarsgaard, B.A. 2000. Timing of eastern North American kimberlite magmatism: continental extension of the Great Meteor hotspot track? Earth and Planetary Science Letters, **178**: 253–268. doi:10.1016/S0012-821X(00)00079-0.

Heaman, L.M., Kjarsgaard, B.A., and Creaser, R.A. 2003. The timing of kimberlite magmatism in North America: implications for global kimberlite genesis and diamond exploration. Lithos, **71**: 153–184. doi:10.1016/j.lithos.2003.07.005.

Hirschmann, M.M., Aubaud, C., and Withers, A.C. 2005. Storage capacity of H2O in nominally anhydrous minerals in the upper mantle. Earth and Planetary Science Letters, **236**: 167–181. doi:10.1016/j.epsl.2005.04.022.

Hirth, G. 2006. Geophysics - Protons lead the charge. Nature, **443**: 927–928. doi:10.1038/443927a. PMID:17066024.

Hirth, G., Evans, R.L., and Chave, A.D. 2000. Comparison of continental and oceanic mantle electrical conductivity: Is the Archean lithosphere dry? Geochemistry, Geophysics, Geosystems, **1**: 1030. doi:10.1029/2000GC000048.

Hyndman, R.D. 2010. The consequences of Canadian Cordillera thermal regime in recent tectonics and elevation: a review. Canadian Journal of Earth Sciences, **47**(5): 621–632. doi:10.1139/E10-016.

Hyndman, R.D., and Shearer, P.M. 1989. Water in the lower continental crust - modeling magnetotelluric and seismic reflection results. Geophysical Journal International, **98**: 343–365. doi:10.1111/j.1365-246X.1989.tb03357.x.

Hyndman, R.D., Vanyan, L.L., Marquis, G., and Law, L.K. 1993. The origin of electrically conductive lower continental crust - saline water or graphite. Physics of the Earth and Planetary Interiors, **81**: 325–344. doi:10.1016/0031-9201(93)90139-Z.

Ingham, M.R., Gough, D.I., and Parkinson, W.D. 1987. Models of conductive structure under the Canadian Cordillera. Geophysical Journal of the Royal Astronomical Society, **88**: 477–485. doi:10.1111/j.1365-246X.1987.tb06654.x.

Ji, S.C., Rondenay, S., Mareschal, M., and Senechal, G. 1996. Obliquity between seismic and electrical anisotropies as a potential indicator of movement sense for ductile shear zones in the upper mantle. Geology, **24**: 1033–1036. doi:10.1130/0091-7613(1996)024<1033:OBSAEA>2.3.CO;2.

Jones, A.G. 1982. On the electrical crust-mantle structure in Fennoscandia: no Moho and the asthenosphere revealed? Geophysical Journal of the Royal Astronomical Society, **68**: 371–388. doi:10.1111/j.1365-246X.1982.tb04906.x.

Jones, A.G. 1983. On the equivalence of the Niblett and Bostick transformations in the magnetotelluric method. Journal of Geophysics-Zeitschrift Fur Geophysik, **53**: 72–73.

Jones, A.G. 1987. MT and reflection: an essential combination. Geophysical Journal of the Royal Astronomical Society, **89**: 7–18. doi:10.1111/j.1365-246X.1987.tb04380.x.

Jones, A.G. 1988*a*. Discussion of "A magnetotelluric investigation under the Williston Basin" by J.M. Maidens and K.V. Paulson. Canadian Journal of Earth Sciences, **25**(7): 1132–1139. doi:10.1139/e88-111.

Jones, A.G. 1988*b*. Static shift of magnetotelluric data and its removal in a sedimentary basin environment. Geophysics, **53**: 967–978. doi:10.1190/1.1442533.

Jones, A.G. 1992. Electrical Conductivity of the Continental Lower Crust. *In* Continental Lower Crust. *Edited by* D.M. Fountain, R.J. Arculus, and R.W. Kay. Elsevier. pp. 81–143.

Jones, A.G. 1993*a*. The BC87 dataset - tectonic setting, previous EM results, and recorded MT data. Journal of Geomagnetism and Geoelectricity, **45**: 1089–1105. doi:10.5636/jgg.45.1089.

Jones, A.G. 1993*b*. The COPROD2 dataset - tectonic setting, recorded MT data, and comparison of models. Journal of Geomagnetism and Geoelectricity, **45**: 933–955. doi:10.5636/jgg.45.933.

Jones, A.G. 1993*c*. Electromagnetic images of modern and ancient subduction zones. Tectonophysics, **219**: 29–45. doi:10.1016/0040-1951(93)90285-R.

Jones, A.G. 1993*d*. Introduction to MT-DIW1 special section. Journal of Geomagnetism and Geoelectricity, **45**: 931–932. doi:10.5636/jgg.45.931.

Jones, A.G. 1999*a*. Imaging the continental upper mantle using electromagnetic methods. Lithos, **48**: 57–80. doi:10.1016/S0024-4937(99)00022-5.

Jones, A.G. 1999*b*. Information about the continental mantle from deep electromagnetic studies. Short Course on Geophysical and Geochemical Imaging of Canada's Upper Mantle Yellowknife, NWT, Canada.

Jones, A.G. 2006. Electromagnetic interrogation of the anisotropic Earth: Looking into the Earth with polarized spectacles. Physics of the Earth and Planetary Interiors, **158**: 281–291. doi:10.1016/j.pepi.2006.03.026.

Jones, A.G. 2012. Distortion of magnetotelluric data: its identification and removal *in* A.D. Chave and A.G. Jones, eds. The Magnetotelluric Method: Theory and Practice. Cambridge University Press, Cambridge (UK).

Jones, A.G. 2013. Imaging and observing the electrical Moho. Tectonophysics, **609**: 423–436. doi:10.1016/j.tecto.2013.02.025.

Jones, A.G., and Craven, J.A. 1990. The North American Central Plains conductivity anomaly and its correlation with gravity, magnetics, seismic, and heat flow data in the Province of Saskatchewan. Physics of the Earth and Planetary Interiors, **60**: 169–194. doi:10.1016/0031-9201(90)90260-5.

Jones, A.G., and Craven, J.A. 2004. Area selection for diamond exploration using deep-probing electromagnetic surveying. Lithos, **77**: 765–782. doi:10.1016/j.lithos.2004.03.057.

Jones, A.G., and Dumas, I. 1993. Electromagnetic images of a volcanic zone. Physics of the Earth and Planetary Interiors, **81**: 289–314. doi:10.1016/0031-9201(93)90137-X.

Jones, A.G., and Ferguson, I.J. 2000. The electric Moho. Pan-Lithoprobe Workshop II, Banff, Canada.

Jones, A.G., and Ferguson, I.J. 2001. The electric moho. Nature, **409**: 331–333. doi:10.1038/35053053. PMID:11201739.

Jones, A.G., and Garcia, X. 2003a. Electrical resistivity structure of the Yellowknife Fault Zone and surrounding region. *In* Gold in the Yellowknife Greenstone Belt, Northwest Territories: Results of the EXTECH III Multidisciplinary Research Project, Chapter 10, pp. 126–141.

Jones, A.G., and Garcia, X. 2003b. Okak Bay AMT data-set case study: Lessons in dimensionality and scale. Geophysics, **68**: 70–91. doi:10.1190/1.1543195.

Jones, A.G., and Garcia, X. 2006. Electrical resistivity structure of the Yellowknife River Fault Zone and surrounding region. Gold in the Yellowknife Greenstone Belt, Northwest Territories: Results of the EXTECH III Multidisciplinary Research Project, published by Geological Association of Canada, Mineral Deposits Division, Special Publication No. 3, pp. 126–141.

Jones, A.G., and Garland, G.D. 1986. Preliminary interpretation of the upper crustal structure beneath Prince Edward Island. Annales Geophysica, **4B**: 157–164.

Jones, A.G., and Gough, D.I. 1995. Electromagnetic images of crustal structures in southern and central Canadian Cordillera. Canadian Journal of Earth Sciences, **32**(10): 1541–1563. doi:10.1139/e95-126.

Jones, A.G., and Groom, R.W. 1993. Strike angle determination from the magnetotelluric impedance tensor in the presence of noise and local distortion - rotate at your peril. Geophysical Journal International, **113**: 524–534. doi:10.1111/j.1365-246X.1993.tb00905.x.

Jones, A.G., and McNeice, G. 2002. Audio-magnetotellurics (AMT) for steeply-dipping mineral targets: importance of multi-component measurements at each site. 72nd SEG, Salt Lake City, Utah. pp. 496–499.

Jones, A.G., and Savage, P.J. 1986. North-American Central Plains conductivity anomaly goes East. Geophysical Research Letters, **13**: 685–688. doi:10.1029/GL013i007p00685.

Jones, A.G., and Schultz, A. 1997. Introduction to MT-DIW2 special issue. Journal of Geomagnetism and Geoelectricity, **49**: 727–737. doi:10.5636/jgg.49.727.

Jones, A.G., and Spratt, J. 2002. A simple method for deriving the uniform field MT responses in auroral zones. Earth Planets and Space, **54**: 443–450.

Jones, A.G., Kurtz, R.D., Oldenburg, D.W., Boerner, D.E., and Ellis, R. 1988. Magnetotelluric observations along the Lithoprobe Southeastern Canadian Cordilleran transect. Geophysical Research Letters, **15**: 677–680. doi:10.1029/GL015i007p00677.

Jones, A.G., Gough, D.I., Kurtz, R.D., Delaurier, J.M., Boerner, D.E., Craven, J.A., Ellis, R.G., and McNeice, G.W. 1992a. Electromagnetic images of regional structure in the Southern Canadian Cordillera. Geophysical Research Letters, **19**: 2373–2376. doi:10.1029/92GL01457.

Jones, A.G., Kurtz, R.D., Boerner, D.E., Craven, J.A., McNeice, G.W., Gough, D.I., Delaurier, J.M., and Ellis, R.G. 1992b. Electromagnetic constraints on strike-slip-fault geometry - the Fraser River fault system. Geology, **20**: 561–564. doi:10.1130/0091-7613(1992)020<0561:ECOSSF>2.3.CO;2.

Jones, A.G., Craven, J.A., McNeice, G.W., Ferguson, I.J., Boyce, T., Farquarson, C., and Ellis, R.G. 1993a. North-American Central Plains conductivity anomaly within The Trans-Hudson Orogen in Northern Saskatchewan, Canada. Geology, **21**: 1027–1030. doi:10.1130/0091-7613(1993)021<1027:NACPCA>2.3.CO;2.

Jones, A.G., Groom, R.W., and Kurtz, R.D. 1993b. Decomposition and modelling of the BC87 dataset. Journal of Geomagnetism and Geoelectricity, **45**: 1127–1150. doi:10.5636/jgg.45.1127.

Jones, A.G., Bailey, R.C., and Mareschal, M. 1994. High-resolution electromagnetic images of conducting zones in an upthrust crustal block. Geophysical Research Letters, **21**: 1807–1810. doi:10.1029/94GL01106.

Jones, A.G., Katsube, T.J., and Schwann, P. 1997. The longest conductivity anomaly in the world explained: Sulphides in fold hinges causing very high electrical anisotropy. Journal of Geomagnetism and Geoelectricity, **49**: 1619–1629. doi:10.5636/jgg.49.1619.

Jones, A.G., Ferguson, I.J., Chave, A.D., Evans, R., and Spratt, J. 2001a. Slave electromagnetic studies. Pan-Lithoprobe Workshop III, Banff, Canada. pp. 50–53.

Jones, A.G., Ferguson, I.J., Chave, A.D., Evans, R.L., and McNeice, G.W. 2001b. The electric lithosphere of the Slave craton. Geology, **29**: 423–426. doi:10.1130/0091-7613(2001)029<0423:ELOTSC>2.0.CO;2.

Jones, A.G., Ferguson, I.J., Chave, A.D., Evans, R.L., and McNeice, G.W. 2001c. Electric lithosphere of the Slave craton. Geology, **29**: 423–426. doi:10.1130/0091-7613(2001)029<0423:ELOTSC>2.0.CO;2.

Jones, A.G., Snyder, D., Hanmer, S., Asudeh, I., White, D., Eaton, D., and Clarke, G. 2002a. Magnetotelluric and teleseismic study across the Snowbird Tectonic Zone, Canadian Shield: A Neoarchean mantle suture? Geophysical Research Letters, **29**(17): 1829. doi:10.1029/2002GL015359.

Jones, A.G., Spratt, J., and Evans, S. 2002b. CBEX: Central Baffin electromagnetic experiment. Geological Survey of Canada. pp. 5 pages.

Jones, A.G., Lezaeta, P., Ferguson, I.J., Chave, A.D., Evans, R.L., Garcia, X., and Spratt, J. 2003. The electrical structure of the Slave craton. Lithos, **71**: 505–527. doi:10.1016/j.lithos.2003.08.001.

Jones, A.G., Ledo, J., and Ferguson, I.J. 2005a. Electromagnetic images of the Trans-Hudson Orogen: The North American Central Plains anomaly revealed. Canadian Journal of Earth Sciences, **42**(4): 457–478. doi:10.1139/e05-018.

Jones, A.G., Ledo, J., Ferguson, I.J., Farquharson, C., Garcia, X., Grant, N., McNeice, G., Roberts, B., Spratt, J., Wennberg, G., Wolynec, L., and Wu, X.H. 2005b. The electrical resistivity structure of Archean to Tertiary lithosphere along 3200 km of SNORCLE profiles, northwestern Canada. Canadian Journal of Earth Sciences, **42**(6): 1257–1275. doi:10.1139/e05-080.

Jones, A.G., Evans, R.L., and Eaton, D.W. 2009. Velocity-conductivity relationships for mantle mineral assemblages in Archean cratonic lithosphere based on a review of laboratory data and Hashin-Shtrikman extremal bounds. Lithos, **109**(1–2): 131–143. doi:10.1016/j.lithos.2008.10.014.

Jones, A.G., Plomerova, J., Korja, T., Sodoudi, F., and Spakman, W. 2010. Europe from the bottom up: A statistical examination of the central and northern European lithosphere-asthenosphere boundary from comparing seismological and electromagnetic observations. Lithos, **120**: 14–29. doi:10.1016/j.lithos.2010.07.013.

Jones, A.G., Fullea, J., Evans, R.L., and Muller, M.R. 2012. Calibrating laboratory-determined models of electrical conductivity of mantle minerals using geophysical and petrological observations. Geochemistry, Geophysics, Geosystems, **13**: Q06010. doi:10.1029/2012GC004055.

Jones, A.G., Fishwick, S., Evans, R.L., Muller, M.R., and Fullea, J. 2013. Velocity-conductivity relations for cratonic lithosphere and their application: Example of Southern Africa. Geochemistry, Geophysics, Geosystems, **14**(4): 806–827. doi:10.1002/ggge.20075.

Jones, A.G., Afonso, J.C., Fullea, J., and Salajegheh, F. 2014. The lithosphere-asthenosphere system beneath Ireland from integrated geophysical-petrological modeling – I: Observations, 1D and 2D hypothesis testing and modeling. Lithos, **189**: 28–48. doi:10.1016/j.lithos.2013.10.033.

Jones, F.W., and Correia, A. 1992. Magneto-telluric soundings in the frequency range 0.01-130 Hz in northern Saskatchewan.

Jones, F.W., and Kalvey, A. 1993. Magnetotelluric measurements between 106o-107o W and 55.5o-55.75o N in northern Saskatchewan.

Jones, F.W., Munro, R.A., Craven, J.A., Boerner, D.E., Kurtz, R.D., and Sydora, R.D. 2002c. Regional geoelectrical complexity of the Western Canada Basin from magnetotelluric tensor invariants. Earth, Planets and Space, **54**: 899–905.

Kalvey, A.R. 1994. Magnetotelluric survey in west-central Alberta. Department of Physics. University of Alberta, Edmonton, Alberta, Canada.

Kalvey, A., and Jones, F.W. 1995. Magnetotelluric measurements in an area of west-central Alberta where deep electrical-conductivity and basin sediment geothermal anomalies coincide. Journal of Applied Geophysics, **34**: 35–40. doi:10.1016/0926-9851(94)00050-X.

Kang, S. 1995. Electromagnetic induction in the Nigeria region. Department of Physics. University of Victoria, Victoria, B.C., Canada.

Karato, S.I. 2006. Remote sensing of hydrogen in Earth's mantle. *In* Water in Nominally Anhydrous Minerals. *Edited by* H. Keppler and J.R. Smyth, pp. 343.

Katsube, T.J., and Mareschal, M. 1993. Petrophysical model of deep electrical conductors - graphite lining as a source and its disconnection due to uplift. Journal of Geophysical Research-Solid Earth, **98**: 8019–8030. doi:10.1029/92JB02864.

Kellett, R.L., Mareschal, M., and Kurtz, R.D. 1992. A model of lower crustal electrical anisotropy for the Pontiac subprovince of the Canadian Shield. Geophysical Journal International, **111**: 141–150. doi:10.1111/j.1365-246X.1992.tb00560.x.

Kellett, R.L., Barnes, A.E., and Rive, M. 1994. The deep-structure of the Grenville Front - A new perspective from western Quebec. Canadian Journal of Earth Sciences, **31**(2): 282–292. doi:10.1139/e94-027.

Kennedy, C.S., and Kennedy, G.C. 1976. Equilibrium boundary between graphite and diamond. Journal of Geophysical Research - Solid Earth, **81**: 2467–2470. doi:10.1029/JB081i014p02467.

Kind, R., Yuan, X.H., and Kumar, P. 2012. Seismic receiver functions and the lithosphere-asthenosphere boundary. Tectonophysics, **536–537**: 25–43. doi:10.1016/j.tecto.2012.03.005.

Kohlstedt, D.L., and Mackwell, S.J. 1998. Diffusion of hydrogen and intrinsic point defects in olivine. Zeitschrift fur Physikalische Chemie, **207**: 147–162. doi:10.1524/zpch.1998.207.Part_1_2.147.

Krivochieva, S. 1993. Étude du système aquifère de Santa Catarina, bassin de Mexico, par sondage électromagnétique. Ecole Polytechnique, Montreal, Quebec, Canada.

Krivochieva, S. 2002. Application des méthodes électromagnétiques transitoires à la prospection des aquifères profonds. Ecole Polytechnique, Montreal, Quebec, Canada.

Kumar, P., Yuan, X.H., Kumar, M.R., Kind, R., Li, X.Q., and Chadha, R.K. 2007. The rapid drift of the Indian tectonic plate. Nature, **449**: 894–897. doi:10.1038/nature06214. PMID:17943128.

Kurtz, R.D., and Gupta, J.C. 1992. Shallow and deep crustal conductivity studies in the Miramichi earthquake zone, New Brunswick. Canadian Journal of Earth Sciences, **29**(7): 1549–1564. doi:10.1139/e92-122.

Kurtz, R.D., Delaurier, J.M., and Gupta, J.C. 1986a. A magnetotelluric sounding across Vancouver Island detects the subducting Juan De Fuca plate. Nature, **321**: 596–599. doi:10.1038/321596a0.

Kurtz, R.D., Ostrowski, J.A., and Niblett, E.R. 1986b. A magnetotelluric survey over the East Bull Lake gabbro-anorthosite complex. Journal of Geophysical Research-Solid Earth and Planets, **91**: 7403–7416. doi:10.1029/JB091iB07 p07403.

Kurtz, R.D., Macnae, J.C., and West, G.F. 1989. A controlled-source, time-domain electromagnetic survey over an upthrust section of Archean crust in the Kapuskasing structural zone. Geophysical Journal International, **99**: 195–203. doi:10.1111/j.1365-246X.1989.tb02024.x.

Kurtz, R.D., Craven, J.A., Niblett, E.R., and Stevens, R.A. 1993. The conductivity of the crust and mantle beneath the Kapuskasing Uplift - Electrical anisotropy in the Upper Mantle. Geophysical Journal International, **113**: 483–498. doi:10.1111/j.1365-246X.1993.tb00901.x.

Lahti, I., Korja, T., Kaikkonen, P., Vaittinen, K., and BEAR-Working-Group. 2005. Decomposition analysis of the BEAR magnetotelluric data: implications for the upper mantle conductivity in the Fennoscandian Shield. Geophysical Journal International, **163**: 900–914. doi:10.1111/j.1365-246X.2005.02744.x.

Langlois, P., Chouteau, M.C., and Bolduc, L. 2000. Two years of magnetotelluric measurements in Abitibi, western Quebec, using a telephone line. Geophysical Journal International, **140**: 509–520. doi:10.1046/j.1365-246X.2000.00028.x.

Larson, K.M., Freymueller, J.T., and Philipsen, S. 1997. Global plate velocities from the Global Positioning System. Journal of Geophysical Research-Solid Earth, **102**: 9961–9981. doi:10.1029/97JB00514.

Ledo, J., and Jones, A.G. 2001. Regional electrical resistivity structure of the southern Canadian Cordillera and its physical interpretation. Journal of Geophysical Research-Solid Earth, **106**: 30755–30769. doi:10.1029/2001JB000358.

Ledo, J., and Jones, A.G. 2005. Upper mantle temperature determined from combining mineral composition, electrical conductivity laboratory studies and magnetotelluric field observations: Application to the intermontane belt, Northern Canadian Cordillera. Earth and Planetary Science Letters, **236**: 258–268. doi:10.1016/j.epsl.2005.01.044.

Ledo, J., Jones, A.G., Ferguson, I.J., and Wennberg, G. 2001. Electromagnetic images of the Tintina fault. No. Lithoprobe Report #79.

Ledo, J., Jones, A.G., and Ferguson, I.J. 2002. Electromagnetic images of a strike-slip fault: The Tintina Fault - Northern Canadian. Geophysical Research Letters, **29**(8): 66-1–66-4. doi:10.1029/2001GL013408.

Ledo, J., Jones, A.G., Ferguson, I.J., and Wolynec, L. 2004. Lithospheric structure of the Yukon, northern Canadian Cordillera, obtained from magnetotelluric data. Journal of Geophysical Research-Solid Earth, **109**, B04410. doi:10.1029/2003JB002516.

Legault, J. 2005. Geologically constrained inversion modeling of Titan magnetotelluric and induced polarization survey results at Kidd Creek mine. Ecole Polytechnique, Montreal, Quebec, Canada.

Lezaeta, P., Chave, A., Jones, A.G., and Evans, R. 2007. Source field effects in the auroral zone: Evidence from the Slave craton (NW Canada). Physics of the Earth and Planetary Interiors, **164**: 21–35. doi:10.1016/j.pepi.2007.05.002.

Lilley, F.E.M. 1993. Three-Dimensionality of the BC87 magnetotelluric data set studied using Mohr circles. Journal of Geomagnetism and Geoelectricity, **45**: 1107–1113. doi:10.5636/jgg.45.1107.

Livelybrooks, D., Mareschal, M., Blais, E., and Smith, J.T. 1996. Magnetotelluric delineation of the Trillabelle massive sulfide body in Sudbury, Ontario. Geophysics, **61**: 971–986. doi:10.1190/1.1444046.

Majorowicz, J.A., and Gough, D.I. 1991. Crustal structures from MT soundings in the Canadian Cordillera. Earth and Planetary Science Letters, **102**: 444–454. doi:10.1016/0012-821X(91)90034-F.

Majorowicz, J.A., and Gough, D.I. 1994. A model of crustal conductive structure in the Canadian Cordillera. Geophysical Journal International, **117**: 301–312. doi:10.1111/j.1365-246X.1994.tb03934.x.

Majorowicz, J.A., Gough, D.I., and Lewis, T.J. 1993a. Correlation between the depth to the lower-crustal high conductive layer and heat-flow in the Canadian Cordillera. Tectonophysics, **225**: 49–56. doi:10.1016/0040-1951(93)90247-H.

Majorowicz, J.A., Gough, D.I., and Lewis, T.J. 1993b. Electrical-conductivity and temperature in the Canadian Cordilleran crust. Earth and Planetary Science Letters, **115**: 57–64. doi:10.1016/0012-821X(93)90212-R.

Marchand, M. 2005. Restauration de signaux magnétotelluriques contaminés par un bruit harmonique. Ecole Polytechnique, Montreal, Quebec, Canada.

Mareschal, M., and Chouteau, M. 1990. A magnetotelluric investigation of the structural geology beneath Charlevoix crater, Quebec. Physics of the Earth and Planetary Interiors, **60**: 120–131. doi:10.1016/0031-9201(90)90254-U.

Mareschal, M., Kurtz, R.D., Chouteau, M., and Chakridi, R. 1991. A magnetotelluric survey on Manitoulin Island and Bruce Peninsula along GLIMPCE seismic line-J - Black shales mask the Grenville Front. Geophysical Journal International, **105**: 173–183. doi:10.1111/j.1365-246X.1991.tb03453.x.

Mareschal, M., Fyfe, W.S., Percival, J., and Chan, T. 1992. Grain-boundary graphite in Kapuskasing gneisses and implications for lower-crustal conductivity. Nature, **357**: 674–676. doi:10.1038/357674a0.

Mareschal, M., Kurtz, R.D., and Bailey, R.C. 1994. A review of electromagnetic investigations in the Kapuskasing Uplift and surrounding regions – electrical properties of key rocks. Canadian Journal of Earth Sciences, **31**: 1042–1051. doi:10.1139/e94-094.

Mareschal, M., Kellett, R.L., Kurtz, R.D., Ludden, J.N., Ji, S., and Bailey, R.C. 1995. Archean cratonic roots, mantle shear zones and deep electrical anisotropy. Nature, **375**: 134–137. doi:10.1038/375134a0.

Marquis, G. 1992. Geophysical studies of saline fluids in the deep crust. Earth and Ocean Sciences. University of Victoria, Victoria.

Marquis, G., and Hyndman, R.D. 1992. Geophysical support for aqueous fluids in the deep crust - seismic and electrical relationships. Geophysical Journal International, **110**: 91–105. doi:10.1111/j.1365-246X.1992.tb00716.x.

Marquis, G., Jones, A.G., and Hyndman, R.D. 1995. Coincident conductive and reflective middle and lower crust in southern British Columbia. Geophysical Journal International, **120**: 111–131. doi:10.1111/j.1365-246X.1995.tb05915.x.

McLeod, J. 2013. Assessment of electrical conductivity structure of the northwest Superior craton and adjacent Trans Hudson Orogen using the magnetotelluric method. University of Manitoba, Winnipeg, Canada.

McNeice, G.W. 1998. Magnetotelluric investigation of the Appalachians, Newfoundland, Canada. Department of Earth Sciences. Memorial University of Newfoundland, St. John's, Newfoundland, Canada.

McNeice, G.W., and Jones, A.G. 1996: Multisite, multifrequency tensor decomposition of magnetotelluric data. 66th Society of Exploration Geophysicists Annual General Meeting, Denver, Colorado.

McNeice, G., and Jones, A.G. 1998. Magnetotellurics in the frozen north: measurements on lake ice. 14th EM Induction Workshop, Sinaia, Romania.

McNeice, G., and Jones, A.G. 2001. Multisite, multifrequency tensor decomposition of magnetotelluric data. Geophysics, **66**: 158–173. doi:10.1190/1.1444891.

Miensopust, M.P., Jones, A.G., Muller, M.R., Garcia, X., and Evans, R.L. 2011. Lithospheric structures and Precambrian terrane boundaries in northeastern Botswana revealed through magnetotelluric profiling as part of the Southern African Magnetotelluric Experiment. Journal of Geophysical Research-Solid Earth, **116**: B02401. doi:10.1029/2010JB007740.

Mooney, W.D., Laske, G., and Masters, T.G. 1998. Crust 5.1: a global crustal model at 5°×5°. Journal of Geophysical Research, **103**: 727–747. doi:10.1029/97JB02122.

Moorkamp, M., Jones, A.G., and Eaton, D.W. 2007. Joint inversion of teleseismic receiver functions and magnetotelluric data using a genetic algorithm: Are seismic velocities and electrical conductivities compatible? Geophysical Research Letters, **34**: L16311. doi:10.1029/2007GL030519.

Moorkamp, M., Jones, A.G., and Fishwick, S. 2010. Joint inversion of receiver functions, surface wave dispersion, and magnetotelluric data. Journal of Geophysical Research-Solid Earth, **115**: B04318. doi:10.1029/2009JB006369.

Narod, B.B., and Bennest, J.R. 1990. Ring-core fluxgate magnetometers for use as observatory variometers. Physics of the Earth and Planetary Interiors, **59**: 23–28. doi:10.1016/0031-9201(90)90205-C.

Niblett, E.R., and Sayn Wittgenstein, C. 1960. Variation of the electrical conductivity with depth by the magnetotelluric method. Geophysics, **25**: 998–1008. doi:10.1190/1.1438799.

Nieuwenhuis, G., Unsworth, M.J., Pana, D., and Craven, J.A. 2013. Three dimensional resistivity structure of Southern Alberta, Canada: Implications for Pre-Cambrian tectonics. Geophysical Journal International, doi:10.1093/gji/ggu068.

Norton, M. 2000. Detailed study of eastern Manitoba using the magnetotelluric method. University of Manitoba, Winnipeg, Canada.

Orellana, M. 2006. An evaluation of the conductivity structure of the Northwest Superior Province, Canadian Shield, using the magnetotelluric and audiomagnetotelluric methods Geosciences. Manitoba, Winnipeg.

Osterwald, F.W., Osterwald, O.B., Long, J.S., and Wilson, W.H. 1959. Mineral resources of Wyoming. Geological Survey of Wyoming.

Padilha, A.L., Vitorello, I., Padua, M.B., and Bologna, M.S. 2006. Lithospheric and sublithospheric anisotropy beneath central-southeastern Brazil constrained by long period magnetotelluric data. Physics of the Earth and Planetary Interiors, **158**: 190–209. doi:10.1016/j.pepi.2006.05.006.

Perry, C., Rosieanu, C., Mareschal, J.C., and Jaupart, C. 2010. Thermal regime of the lithosphere in the Canadian Shield. Canadian Journal of Earth Sciences, **47**(4): 389–408. doi:10.1139/E09-059.

Peslier, A.H., Woodland, A.B., Bell, D.R., and Lazarov, M. 2010. Olivine water contents in the continental lithosphere and the longevity of cratons. Nature, **467**: 78–81. doi:10.1038/nature09317. PMID:20811455.

Poe, B.T., Romano, C., Nestola, F., and Smyth, J.R. 2010. Electrical conductivity anisotropy of dry and hydrous olivine at 8 GPa. Physics of the Earth and Planetary Interiors, **181**: 103–111. doi:10.1016/j.pepi.2010.05.003.

Poll, H. 1994. Automatic forward modelling of two-dimensional problems in electromagnetic induction. Earth and Ocean Sciences. University of Victoria, Victoria, B.C., Canada.

Prawirodirdjo, L., and Bock, Y. 2004. Instantaneous global plate motion model from 12 years of continuous GPS observations. Journal of Geophysical Research-Solid Earth, **109**: B08405. doi:10.1029/2003JB002944.

Pu, X.-H. 1994. Three-dimensional numerical modelling of geo-electromagnetic induction phenomena Department of Physics. University of Victoria, Victoria, B.C., Canada.

Queralt, P., Jones, A.G., and Ledo, J. 2007. Electromagnetic imaging of a complex ore body: 3D forward modeling, sensitivity tests, and down-mine measurements. Geophysics, **72**: F85–F95. doi:10.1190/1.2437105.

Rankin, D., and Reddy, I.K. 1973. Crustal conductivity anomaly under the Black-Hills - a magnetotelluric study. Earth and Planetary Science Letters, **20**: 275–279. doi:10.1016/0012-821X(73)90167-2.

Reinecker, J., Heidbach, O., Tingay, M., Sperner, B., and Müller, B. 2005. The release 2005 of the World Stress Map. Available online at www.world-stress-map.org.

Reitzel, J.S., Gough, D.I., Porath, H., and Anderson, C.W. 1970. Geomagnetic deep spunding and upper mantle structure in western United States. Geophysical Journal of the Royal Astronomical Society, **19**: 213. doi:10.1111/j.1365-246X.1970.tb06044.x.

Rippe, D., Unsworth, M.J., and Currie, C.A. 2013. Magnetotelluric constraints on the fluid content in the upper mantle beneath the southern Canadian Cordillera: Implications for rheology. Journal of Geophysical Research. American Geophysical Union. **118**: 5601–5624. doi:10.1002/jgrb.50255.

Ritter, P., and Ritter, O. 1997. The BC87 dataset: Application of hypothetical event analysis on distorted GDS response functions and some thin sheet modelling studies of the deep crustal conductor. Journal of Geomagnetism and Geoelectricity, **49**: 757–766. doi:10.5636/jgg.49.757.

Roux, E., Moorkamp, M., Jones, A.G., Bischoff, M., Endrun, B., Lebedev, S., and Meier, T. 2011. Joint inversion of long-period magnetotelluric data and surface-wave dispersion curves for anisotropic structure: Application to data from Central Germany. Geophysical Research Letters, **38**: L05304. doi:10.1029/2010GL046358.

Rychert, C.A., and Shearer, P.M. 2009. A global view of the Lithosphere-Asthenosphere Boundary. Science, **324**: 495–498. doi:10.1126/science.1169754. PMID:19390041.

Saruwatari, K., Ji, S.C., Long, C.X., and Salisbury, M.H. 2001. Seismic anisotropy of mantle xenoliths and constraints on upper mantle structure beneath the southern Canadian Cordillera. Tectonophysics, **339**: 403–426. doi:10.1016/S0040-1951(01)00136-6.

Schultz, A., Kurtz, R.D., Chave, A.D., and Jones, A.G. 1993. Conductivity discontinuities in the upper mantle beneath a stable craton. Geophysical Research Letters, **20**: 2941–2944. doi:10.1029/93GL02833.

Senechal, G., Mareschal, M., Hubert, C., Calvert, A.J., Grandjean, G., and Ludden, J. 1996a. Integrated geophysical interpretation of crustal structures in the northern Abitibi belt: Constraints from seismic amplitude analysis. Canadian Journal of Earth Sciences, **33**(9): 1343–1362. doi:10.1139/e96-101.

Senechal, G., Rondenay, S., Mareschal, M., Guilbert, J., and Poupinet, G. 1996b. Seismic and electrical anisotropies in the lithosphere across the Grenville Front, Canada. Geophysical Research Letters, **23**: 2255–2258. doi:10.1029/96GL01410.

Shi, L., Francis, D., Ludden, J., Frederiksen, A., and Bostock, M. 1998. Xenolith evidence for lithospheric melting above anomalously hot mantle under the northern Canadian Cordillera. Contrib. Mineral. Petrol., **131**: 39–53. doi:10.1007/s004100050377.

Shragge, J., Bostock, M.G., Bank, C.G., and Ellis, R.M. 2002. Integrated teleseismic studies of the southern Alberta upper mantle. Canadian Journal of Earth Sciences, **39**(3): 399–411. doi:10.1139/e01-084.

Simpson, F. 2001. Resistance to mantle flow inferred from the electromagnetic strike of the Australian upper mantle. Nature, **412**: 632–635. doi:10.1038/35088051. PMID:11493919.

Simpson, F. 2002. Intensity and direction of lattice-preferred orientation of olivine: are electrical and seismic anisotropies of the Australian mantle reconcilable? Earth and Planetary Science Letters, **203**: 535–547. doi:10.1016/S0012-821X(02)00862-2.

Simpson, F., and Tommasi, A. 2006. Hydrogen diffusivity and electrical anisotropy of a peridotite mantle. Geophysical Journal International, **160**: 1092–1102. doi:10.1111/j.1365-246X.2005.02563.x.

Snyder, D. 2003. Teleseismic investigations of the lithosphere beneath central Baffin Island, Nunavut.

Snyder, D., and Bruneton, M. 2007. Seismic anisotropy of the Slave craton, NW Canada, from joint interpretation of SKS and Rayleigh waves. Geophysical Journal International, **169**: 170–188. doi:10.1111/j.1365-246X.2006.03287.x.

Snyder, D.B., and Grütter, H. 2010. Lithoprobe's impact on the Canadian diamond-exploration industry. Canadian Journal of Earth Sciences, **47**(5): 783–800. doi:10.1139/E09-055.

Snyder, D.B., Berman, R.G., Kendall, J.M., and Sanborn-Barrie, M. 2013. Seismic anisotropy and mantle structure of the Rae craton, central Canada, from joint interpretation of SKS splitting and receiver functions. Precambrian Research, **232**: 189–208. doi:10.1016/j.precamres.2012.03.003.

Soudarin, L., and Cretaux, J.F. 2006. A model of present-day tectonic plate motions from 12 years of DORIS measurements. Journal of Geodesy, **80**: 609–624. doi:10.1007/s00190-006-0090-4.

Soyer, W., and Unsworth, M. 2006. Deep electrical structure of the northern Cascadia (British Columbia, Canada) subduction zone: Implications for the distribution of fluids. Geology, **34**: 53–56. doi:10.1130/G21951.1.

Spratt, J. 2003. Magnetotelluric investigation across the Yarlung-Zangbo suture zone, Southern Tibet. Department of Geological Sciences. Syracuse University, Syracuse, N.Y., U.S.A.

Spratt, J., and Craven, J. 2011. Near-surface and crustal-scale images of the Nechako basin, British Columbia, Canada, from magnetotelluric investigations. Canadian Journal of Earth Sciences, **48**(6): 987–999. doi:10.1139/e10-098.

Spratt, J.E., Jones, A.G., Jackson, V., Collins, L., and Avdeeva, A. 2009. Lithospheric geometry of the Wopmay Orogen from a Slave Craton to Bear Province Magnetotelluric Transect. Journal of Geophysical Research: Solid Earth, **114**, B01101. doi:10.1029/2007JB005326.

Spratt, J., Snyder, D., and Craven, J.A. 2011. A magnetotelluric survey across the Committee Bay Belt and the Rae Craton in the Churchill Province of Nunavut. Geological Survey of Canada, Ottawa, Canada. pp. 31.

Spratt, J., Jones, A.G., Corrigan, D., and Hogg, C. 2013a. Lithospheric geometry revealed by deep-probing magnetotelluric surverying, Melville Peninsula, Nunavut. Geological Survey of Canada. pp. 18.

Spratt, J.E., Roberts, B., Kiyan, D., and Jones, A.G. 2013b. Magnetotelluric soundings from the Central Rae Domain of the Churchill Province, Nunavut. Pp. 34. Open File. Geological Survey of Canada, Ottawa, Canada.

Stevens, K. 1999. The interpretation of magnetotelluric measurements from the Glennie Domain to the Flin Flon Belt, eastern Saskatchewan: part of the Lithoprobe Trans-Hudson Orogen transect. Geosciences. Manitoba, Winnipeg.

Stevens, K.L., and Ferguson, I.J. 1997. 1D interpretation of high frequency magnetotelluric data across the Glennie Domain of the Trans Hudson Orogen Transect. *In* LITHOPROBE Trans Hudson Orogen Transect Workshop, Saskatoon, Canada. *Edited by* R.M. Clowes. pp. 197–205.

Stevens, K.M., and McNeice, G.W. 1998. On the detection of Ni-Cu Ore hosting structures in the Sudbury Igneous Complex using the Magnetotelluric Method. SEG Technical Program Expanded Abstracts 17, pp. 751–755.

Takasugi, S., Sato, T., and Honkura, Y. 1993. 2-dimensional forward modeling for the COPROD2 mt data. Journal of Geomagnetism and Geoelectricity, **45**: 957–962. doi:10.5636/jgg.45.957.

Tournerie, B., and Chouteau, M. 1998. Deep conductivity structure in Abitibi, Canada, using long dipole magnetotelluric measurements. Geophysical Research Letters, **25**: 2317–2320. doi:10.1029/98GL51690.

Tournerie, B., and Chouteau, M. 2002. Analysis of magnetotelluric data along the Lithoprobe seismic line 21 in the Blake River Group, Abitibi, Canada. Earth Planets and Space, **54**: 575–589.

Tournerie, B., Gibert, D., and Virieux, J. 1995. Inversion of the COPROD2 magnetotelluric data using a diffusive-to-propagative mapping (DPM). Geophysical Research Letters, **22**: 2187–2190. doi:10.1029/95GL02016.

Tuncer, V. 2007. Exploration for unconformity type uranium deposits with audio-magnetotelluric data: a case study from the McArthur River mine, Saskatchewan, Canada. Department of Physics. University of Alberta, Edmonton, Alberta, Canada.

Tuncer, V., Unsworth, M.J., Siripunvaraporn, W., and Craven, J.A. 2006. Exploration for unconformity-type uranium deposits with audiomagnetotelluric data: A case study from the McArthur River mine, Saskatchewan, Canada. Geophysics, **71**: B201–B209. doi:10.1190/1.2348780.

Turkoglu, E., Unsworth, M., and Pana, D. 2009. Deep electrical structure of northern Alberta (Canada): implications for diamond exploration. Canadian Journal of Earth Sciences, **46**(2): 139–154. doi:10.1139/E09-009.

Tycholiz, C. 2010. Investigation of the electrical resistivity structure of the crust and upper mantle at Lake Nipigon, Ontario using the magnetotelluric method. University of Manitoba, Winnipeg, Canada.

Uchida, T. 1993. Inversion of COPROD2 magnetotelluric data by use of ABIC minimization method. Journal of Geomagnetism and Geoelectricity, **45**: 1063–1071. doi:10.5636/jgg.45.1063.

Vieira, F.P., and Hamza, V.M. 2010. Global heat loss: New estimates using digital geophysical maps and GIS techniques. IV Symposium of the Brazilian Geophysical Society, Brasilia, Brazil. pp. 1–6.

Wang, D.J., Mookherjee, M., Xu, Y.S., and Karato, S.I. 2006. The effect of water on the electrical conductivity of olivine. Nature, **443**: 977–980. doi:10.1038/nature05256. PMID:17066032.

Wannamaker, P.E. 2000. Comment on "The petrologic case for a dry lower crust" by Bruce W.D. Yardley and John W. Valley. Journal of Geophysical Research-Solid Earth, **105**(B3): 6057–6064. doi:10.1029/1999JB900324.

Wannamaker, P.E. 2005. Anisotropy versus heterogeneity in continental solid earth electromagnetic studies: Fundamental response characteristics and implications for physicochemical state. Surveys in Geophysics, **26**: 733–765. doi:10.1007/s10712-005-1832-1.

Watts, M.D., and Balch, S.J. 2000. AEM-constrained 2D inversion of AMT data over the Voisey's Bay massive sulfide body, Labrador. SEG Technical Program Expanded Abstracts 19, pp. 1119–1121.

Weidelt, P. 1985. Construction of conductance bounds from magnetotelluric impedances. Journal of Geophysics-Zeitschrift für Geophysik, **57**: 191–206.

Wennberg, G. 1999. Investigation of the Western Superior Province in Manitoba using the magnetotelluric method. University of Manitoba, Winnipeg, Canada.

Wennberg, G. 2003. Magnetotelluric response of the Northern Cordillera: interpretation of the lithospheric structure of the SNORCLE transect, line 2a and connector line. Department of Geosciences. University of Manitoba, Winnipeg, Manitoba, Canada.

Wessel, P., and Smith, W.H.F. 1991. Free software help map and display data. EOS Transactions AGU, **72**: 441–446. doi:10.1029/90EO00319.

Wessel, P., and Smith, W.H.F. 1998. New, improved version of the Generic Mapping Tools released. EOS Transactions AGU, **79**: 579. doi:10.1029/98EO00426.

White, D., Boerner, D., Wu, J.J., Lucas, S., Berrer, E., Hannila, J., and Somerville, R. 2000. Mineral exploration in the Thompson nickel belt, Manitoba, Canada, using seismic and controlled-source EM methods. Geophysics, **65**: 1871–1881. doi:10.1190/1.1444871.

White, D.J., Thomas, M.D., Jones, A.G., Hope, J., Nemeth, B., and Hajnal, Z. 2005. Geophysical transect across a Paleoproterozoic continent-continent collision

zone: The Trans-Hudson Orogen. Canadian Journal of Earth Sciences, **42**(4): 385–402. doi:10.1139/e05-002.

Wolynec, L.L. 2000. LITHOPROBE magnetotelluric crustal study of the Carcross Area, Yukon Territory. University of Manitoba, Winnipeg, Canada.

Wu, N., Booker, J.R., and Smith, J.T. 1993. Rapid 2-dimensional inversion of COPROD2 data. Journal of Geomagnetism and Geoelectricity, **45**: 1073–1087. doi:10.5636/jgg.45.1073.

Wu, X. 2001. Determination of near-surface, crustal and lithospheric structures in the Canadian Precambrian Shield using time-domain electromagnetic and magnetotelluric methods. Geosciences. Manitoba, Winnipeg.

Wu, X., Ferguson, I.J., and Jones, A.G. 2002. Magnetotelluric response and geoelectric structure of the Great Slave Lake shear zone. Earth and Planetary Science Letters, **196**: 35–50. doi:10.1016/S0012-821X(01)00594-5.

Wu, X., Ferguson, I.J., and Jones, A.G. 2005. Geoelectric structure of the Proterozoic Wopmay Orogen and adjacent terranes, Northwest Territories, Canada. Canadian Journal of Earth Sciences, **42**(6): 955–981. doi:10.1139/e05-042.

Xiao, W. 2004. Magnetotelluric exploration in the Rocky Mountain Foothills, Alberta. Department of Physics. University of Alberta, Edmonton, Alberta, Canada.

Xu, Y.S., Poe, B.T., Shankland, T.J., and Rubie, D.C. 1998. Electrical conductivity of olivine, wadsleyite, and ringwoodite under upper-mantle conditions. Science, **280**: 1415–1418. doi:10.1126/science.280.5368.1415. PMID:9603726.

Xu, Y.S., Shankland, T.J., and Poe, B.T. 2000. Laboratory-based electrical conductivity in the Earth's mantle. Journal of Geophysical Research-Solid Earth, **105**: 27865–27875. doi:10.1029/2000JB900299.

Yardley, B.W.D., and Valley, J.W. 1997. The petrologic case for a dry lower crust. Journal of Geophysical Research-Solid Earth, **102**: 12173–12185. doi:10.1029/97JB00508.

Yoshino, T., and Noritake, F. 2011. Unstable graphite films on grain boundaries in crustal rocks. Earth and Planetary Science Letters, **306**: 186–192. doi:10.1016/j.epsl.2011.04.003.

Yoshino, T., Matsuzaki, T., Yamashita, S., and Katsura, T. 2006. Hydrous olivine unable to account for conductivity anomaly at the top of the asthenosphere. Nature, **443**: 973–976. doi:10.1038/nature05223. PMID:17066031.

Yoshino, T., Matsuzaki, T., Shatskiy, A., and Katsura, T. 2009. The effect of water on the electrical conductivity of olivine aggregates and its implications for the electrical structure of the upper mantle. Earth and Planetary Science Letters, **288**: 291–300. doi:10.1016/j.epsl.2009.09.032.

Yoshino, T., McIsaac, E., Laumonier, M., and Katsura, T. 2012. Electrical conductivity of partial molten carbonate peridotite. Physics of the Earth and Planetary Interiors, **194**: 1–9. doi:10.1016/j.pepi.2012.01.005.

Yuan, X.H., Kind, R., Li, X.Q., and Wang, R.J. 2006. The S receiver functions: synthetics and data example. Geophysical Journal International, **165**: 555–564. doi:10.1111/j.1365-246X.2006.02885.x.

Zhang, P., and Chouteau, M. 1992. The use of magnetotellurics for mineral exploration - an experiment in the Chibougamau region of Quebec. Canadian Journal of Earth Sciences, **29**(4): 621–635. doi:10.1139/e92-054.

Zhang, P., Pedersen, L.B., Mareschal, M., and Chouteau, M. 1993. Channeling contribution to tipper vectors - a magnetic equivalent to electrical distortion. Geophysical Journal International, **113**: 693–700. doi:10.1111/j.1365-246X.1993.tb04661.x.

Zhang, P., Chouteau, M., Mareschal, M., Kurtz, R., and Hubert, C. 1995. High-frequency magnetotelluric investigation of crustal structure in north-central Abitibi, Quebec, Canada. Geophysical Journal International, **120**: 406–418. doi:10.1111/j.1365-246X.1995.tb01828.x.

Zhao, G.Z., Ji, T., and Yan, Z. 1993. 2-dimensional modeling by using COPROD2 magnetotelluric data. Journal of Geomagnetism and Geoelectricity, **45**: 963–968. doi:10.5636/jgg.45.963.